A REGULATORY ROLE FOR ATM IN SUPPRESSION OF MRE11-DEPENDENT DNA DEGRADATION AND MICROHOMOLOGY-MEDIATED END JOINING

by

Elias Adel Rahal

A Dissertation Submitted to the Faculty of the

DEPARTMENT OF MOLECULAR AND CELLULAR BIOLOGY

In Partial Fulfillment of the Requirements
For the Degree of

DOCTOR OF PHILOSOPHY

In the Graduate College

THE UNIVERSITY OF ARIZONA

2009

THE UNIVERSITY OF ARIZONA
GRADUATE COLLEGE

As members of the Dissertation Committee, we certify that we have read the dissertation prepared by Elias Adel Rahal
entitled A Regulatory Role for ATM in Suppression of Mre11-Dependent DNA Degradation and Microhomology-Mediated End Joining
and recommend that it be accepted as fulfilling the dissertation requirement for the Degree of Doctor of Philosophy

_____ Date: 04/14/2009
Dr. Kathleen Dixon

_____ Date: 04/14/2009
Dr. Ted Weinert

_____ Date: 04/14/2009
Dr. Giovanni Bosco

_____ Date: 04/14/2009
Dr. Joyce Schroeder

_____ Date: 04/14/2009
Dr. Daniela Zarnescu

Final approval and acceptance of this dissertation is contingent upon the candidate's submission of the final copies of the dissertation to the Graduate College.
I hereby certify that I have read this dissertation prepared under my direction and recommend that it be accepted as fulfilling the dissertation requirement.

_____ Date: 04/14/2009
Dissertation Director: Dr. Kathleen Dixon

STATEMENT BY AUTHOR

This dissertation has been submitted in partial fulfillment of requirements for an advanced degree at the University of Arizona and is deposited in the University Library to be made available to borrowers under rules of the Library.

Brief quotations from this dissertation are allowable without special permission, provided that accurate acknowledgment of source is made. Requests for permission for extended quotation from or reproduction of this manuscript in whole or in part may be granted by the head of the major department or the Dean of the Graduate College when in his or her judgment the proposed use of the material is in the interests of scholarship. In all other instances, however, permission must be obtained from the author.

SIGNED: Elias Adel Rahal

ACKNOWLEDGEMENTS

Despite their utility, mere words are not sufficient for me to express my gratitude to Dr. Kathleen Dixon. Being mentored by Kate has cultivated my character as a scientist and refined the cognitive processes inherent to my nature. In simpler terms, as a researcher prior to joining the Dixon lab, I was rather like some fuzzy DNA band on a 0.5% low-melting temperature agarose gel. Now, I feel more like a focused band on a denaturing sequencing gel. Kate has been supportive in all imaginable capacities and I will always be thankful that she created room for me to shape the science I undertook yet kept me grounded. She is an objective critic, a pragmatic skeptic and an ardent educator. The artist and person behind the scientist in Kate are no less admirable and I can only hope that some of those qualities have seeped into my personality by association. I am also forever indebted to Dr. Leigh Ann Henricksen; the concepts and applications I have learned from Leigh Ann are innumerable. The breadth of these concepts and applications is also immeasurable and varies from the molecular basis of primase function to the number of kids adopted by Angelina Jolie per day. Leigh Ann has always been the first person I turn to for discussing scientific ideas, experimental approaches, manuscripts, pop culture and personal problems. I'm absolutely sure she is the keenest listener on this planet and commensurately the best troubleshooter. Her advice has always been sound and on the spot. Much like a protein with separation of function alleles Leigh Ann has been a friend, a personal mentor and a supervisor. She is after all the person who helped me realize, much to my awe, that I inherently *am* a biochemist!

I am very fortunate to have had Drs. Ted Weinert, Giovanni Bosco, Joyce Schroeder and Daniela Zarnescu as committee members. Ted and Gio's enthusiasm for science is inspiring and their astute comments have helped me reorganize my thoughts countless times. Thank you for all the awesome discussions! Joyce and Daniela have always offered a new perspective and their remarks have many times led me to novel avenues in my research.

To all the past and current lab members especially Eric (aka Jesus of Austria), Lauren (aka Shanaynay), Jessica (aka Maria Lopita Gonzalez Lopez Alonso etc.), Danny (aka Cheekz with a Zee), Pablo (aka *!<,%$ Sanchez), Aneesha (aka Quickimart), Bryan (aka Frodo), Jen (aka Chopstick), Rosy (aka Frijolito's mom) and all the nicknameless members, thank you for making this a joyful ride! To Hope and Helen, thank you for the discussions, comments and sharing of ideas. To my lifetime buddies (in order of appearance in my life), Moose, Elie, Youmna, Daad, Rola, Nabiha, Youssef, Dima, Zeina, Aline, Christelle, Lori, Joumana, Marita and Hussam, your friendship has been one of the best gifts of life. I am so lucky to have encountered friends like you. And to that white board on the 5th floor in Life Sciences South, thank you for being the comic relief in my life and for laughing at my jokes even when they weren't funny! To the "cave" on that very same floor, thanks for bearing with me during preparations for my oral exam (those were trying times I am still attempting to forget) and for being as mute and as boring as usual in the depths of the night, now, as I write these concluding lines. You, dear "cave", I will not miss at all!

DEDICATION

To my Mom and Dad who have endured so much and sacrificed so much to see their children through the good times and the bad. To my sisters, Nadine and Claudine, who will always be my mentors and role models. And to Marianne, Michel, Michael, Anthony and Mia, you remain my beacons of light in this sea of tumultuous waters…

TABLE OF CONTENTS

LIST OF FIGURES

ABSTRACT

ATM is the defective kinase in the neurodegenerative disorder ataxia telangiectasia. This kinase is associated with DNA double-strand break (DSB) repair and cell cycle control. Our laboratory previously demonstrated elevated levels of deletions and error-prone double-strand break repair via microhomology-mediated end joining (MMEJ) in ATM-deficient (A-T) extracts when compared to controls (wtATM+). To assess the involvement of enhanced nuclease activities in A-T extracts we studied the stability of DNA duplex substrates in A-T and control nuclear extracts under DSB repair conditions. We observed a marked shift in detection from full-length products to shorter products in A-T extracts. Addition of purified ATM to A-T nuclear extracts restored full-length product detection. This repression of degradation by ATM was dependent on its kinase activities. These results demonstrated a role for ATM in suppressing the degradation of DNA ends possibly through inhibiting nucleases implicated in MMEJ such as Mre11. Therefore, we assessed DNA end-stability in Mre11-depleted nuclear extracts and in extracts treated with the Mre11 nuclease inhibitor, Mirin. This resulted in decreased DNA degradation in both control and A-T extracts. Knockdown of Mre11 levels also led to an enhancement of DNA end-stability in nuclear extracts. Examining MMEJ levels by employing an *in vivo* reporter assay system revealed a decline in this pathway in Mre11-knockdown cells and in those treated with Mirin. These results signify a role for the Mre11 nuclease in MMEJ in mammalian cells and indicate a regulatory function for ATM in the control of error-prone DSB repair and preservation of DNA end-stability at a break.

CHAPTER I: INTRODUCTION

Overview

Maintenance of genomic integrity is essential to the vitality of any organism. Multiple pathways have evolved that respond to genetic aberrations by activating protein networks involved in cell cycle control and DNA repair. Failure at either level is associated with disease processes characterized by abnormal development, genetic instability, cancer and neurodegeneration (1).

Of the various types of lesions that affect DNA integrity, a double-strand break (DSB) is thought to have the highest potential for genotoxicity and mutagenesis (2). While the repair of a single-strand break (SSB), an abasic site or a damaged base relies on the presence of an intact template, the complementary strand, in close proximity, an intact DNA homologue is not always available for DSB repair (3). A key component at the heart of the response to a DSB is the ataxia telangiectasia mutated (ATM) kinase. The activation of ATM after DSB formation results in the phosphorylation of a myriad of mediators that play a role in DSB repair and cell cycle regulation (4).

Although a role for ATM in DNA repair and cell cycle regulation is well documented, the particular defect in repair stemming from an ATM dysfunction is not well characterized. The work presented herein highlights a role for ATM in preserving the stability of DNA ends via suppressing nuclease-mediated degradation. We also show that the Mre11 nuclease is the major culprit behind error-prone DSB repair and DNA degradation in the absence of appropriate ATM function.

Review of the literature

Ataxia telangiectasia: the disorder

Ataxia telangiectasia (A-T) is an autosomal recessive disorder that typically becomes apparent in early childhood (5). Progressive neurological manifestations, the most prominent feature of the disease, are the result of cerebellar degeneration. Despite the loss of peripheral neurons, the most affected neurocytes are the Purkinje cells, which leads to significant thinning of the cerebellum (6). Ataxia, the loss of the ability to coordinate muscular movement, of both upper and lower limbs develops in early adolescence (7) and affected individuals are usually wheelchair-bound by their teenage years (8). The disorder is accompanied by dysarthria (speech impediments) (9) and telangiectasia (blood vessel dilation) (10). These dilated blood vessels are most apparent over the bulbar conjunctivae of the eye, do not occur internally and remain a poorly explained feature of the disease (11). A-T patients also suffer from immune defects particularly absent or low IgA, IgE, IgG_2 and IgG_4 levels in addition to cellular immune defects (6, 12-15).

Other features of this pleiotropic disease include sterility, elevated levels of serum α-fetoprotein, increased sensitivity to ionizing radiation, premature aging and a very high risk of developing cancer (16). While about one-third of A-T patients develop some form of neoplasia, 10-15% present with a malignancy of the lymphoreticular type such as leukemia or lymphoma during an early age (17). ATM mutations have also been associated with prostate cancer, and head and neck cancer (11). However, the most common cause of death in A-T is lower respiratory tract infections and pulmonary

diseases, which are probably the result of impaired mastication and swallowing leading to food aspiration (18, 19). ATM heterozygosity, on the other hand, has been attributed with predisposition to epithelial neoplasia particularly with breast cancer formation (20-22). Besides this small cancer cancer risk, heterozygotes are seemingly unaffected (23). The incidence of A-T is estimated to be 1:40,000-1:100,000 live births (24).

ATM gene and associated mutations

The ATM gene occupies 150 kb on chromosome 11q22–23. It includes 66 exons and encodes a 13 kb transcript. Multiple transcripts have been identified sharing the same 9.2 kb open reading frame but having various 5' and 3' untranslated regions (UTRs) formed by alternative splicing of the primary transcript (25-27).

The majority of A-T patients are compound heterozygotes with around 85% of ATM gene mutations being truncating or splice-site mutations resulting in a truncated form of the protein. It is believed that these truncated forms of ATM are highly unstable and are degraded. This is based on their being undetectable by conventional immunoblotting and by various immunoassays (28-30). Other mutations are of the missense type or are in-frame deletions and insertions. Mutations have been detected along the gene with no "hot spots" being identified (31-36).

The ATM protein

ATM is a 370 KDa protein composed of 3056 amino acids. It belongs to a family of kinases referred to as the phosphatidylinositol (PI) 3-kinase related kinases (PIKK) (Figure 1). Despite sharing homology at its carboxy-terminus with the PI3K family of

kinases, ATM is a protein kinase rather than a lipid kinase. Other members of the mammalian PIKK family are ATR (ATM-Rad3 related), DNA-PKcs (the catalytic subunit of the DNA-dependent protein kinase), FRAPP/mTOR (FKBP-12-rapamycin associated protein/mammalian target of rapamycin), SMG1 (suppressor with morphogenetic defects on genitalia 1) and TRRAP (transformation/transcription domain–associated protein) (37). Except for TRRAP, these proteins are serine/threonine kinases. TRRAP is the only member of this family that appears to be catalytically inactive (38).

ATM shares homology with members of the PIKK family in its PI3K-related catalytic site in addition to other similar domains. These include a FAT domain, so called because it was initially identified as a common motif in FRAPP/ATM/TRRAP, and also include a FATC domain which is a sequence of amino acids found at the carboxy-termini of this family of proteins (5).

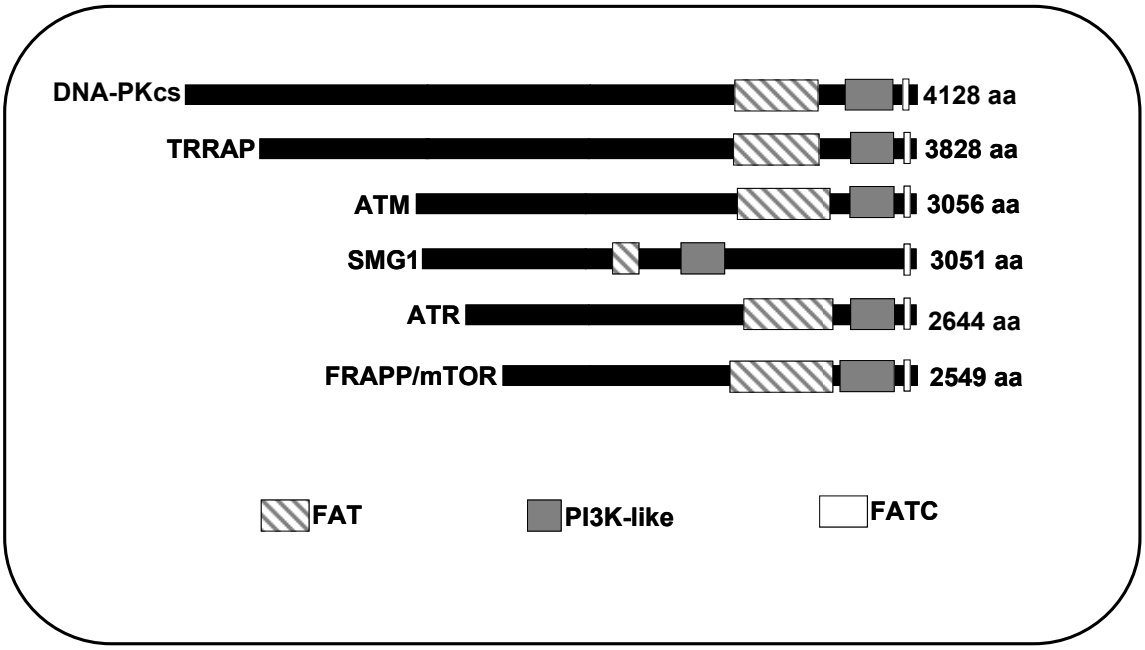

Figure 1. The PIKK superfamily of kinases. This family includes DNA-PKcs, TRRAP, ATM, SMG1, ATR and FRAPP/mTOR. The FATC, PI3K-like and FAT domains of homology are indicated. The PI3K-like kinase domain is believed to be catalytically active in all members of this family except for TRRAP.

ATM activation

In its inactive state, ATM is found in cells in the form of dimers or higher order multimers. It is postulated that in this type of arrangement the catalytic domain of one ATM molecule is blocked by the FAT domain of another. Upon activation, each molecule will phosphorylate the other on a serine residue at position 1981 in the FAT domain. This allows the molecules to release each other, monomerize and phosphorylate downstream effectors (39) .

Several other autophosphorylation sites are present on ATM, including serines at positions 367 and 1893. All three autophosphorylation sites appear critical to ATM function. A mutation in any of these three sites results in deficient ATM signaling and cellular phenotypes similar to those seen in A-T cells (40). Some debate exists in the field regarding the significance of these autophosphorylation sites since, unlike in human cells, a mutation in these conserved residues in mice does not abrogate ATM function *in vitro* and *in vivo* at the organismal level (41). ATM activation is also believed to be dependent on phosphatase activities. The protein phosphatase 5 (PP5) seems to have a role in ATM activation (42) whereas protein phosphatase 2A (PP2A) may play a negative regulatory role by dephosphorylation of catalytic-activity inducing sites (43). Other post-translational modifications, such as acetylation (44, 45) may also play a role in ATM activation. Chromatin remodeling and changes in chromatin architecture also contribute to ATM activation (46).

The primary activator of ATM is believed to be the formation a DNA double-strand break (DSB). Nevertheless, hypotonic stress is known to activate ATM in the absence of DSB generation (39); however, this activation is attributed to chromatin status changes that occur in response to hypotonicity (47, 48). The activation of ATM by a DSB is believed to be largely dependent on the upstream function of the MRN (Mre11-Rad50-Nbs1) complex (Figure 2). This is thought to occur through ATM's interaction with the Nbs1 component of the MRN complex (49, 50). This complex migrates rapidly to DSB sites (51) and recruits ATM which is then monomerized and activated consequently initializing a signaling cascade. Support for this model is drawn from several lines of evidence. On one hand, ATM is inefficiently activated when Nbs1 or Mre11 are not present (52, 53). Evidence from *in vitro* experiments has also shown that the MRN complex is retained at DNA ends, recruits ATM and is capable of monomerizing ATM dimers thus activating them to phosphorylate downstream mediators (54). Moreover, immunodepletion of Mre11 from Xenopus extracts inhibits ATM-dependent phosphorylation of downstream effectors in response to DSBs (55). Other mediators such as MDC1, 53BP1, and H2AX may contribute to enhancing ATM activation probably by increasing effective local concentrations and assembly of DSB repair factors at the break site (56, 57). Upon activation, ATM phosphorylates a myriad of mediators involved in DSB repair, cell cycle regulation and apoptosis. Some pertinent substrates are depicted in Figure 3.

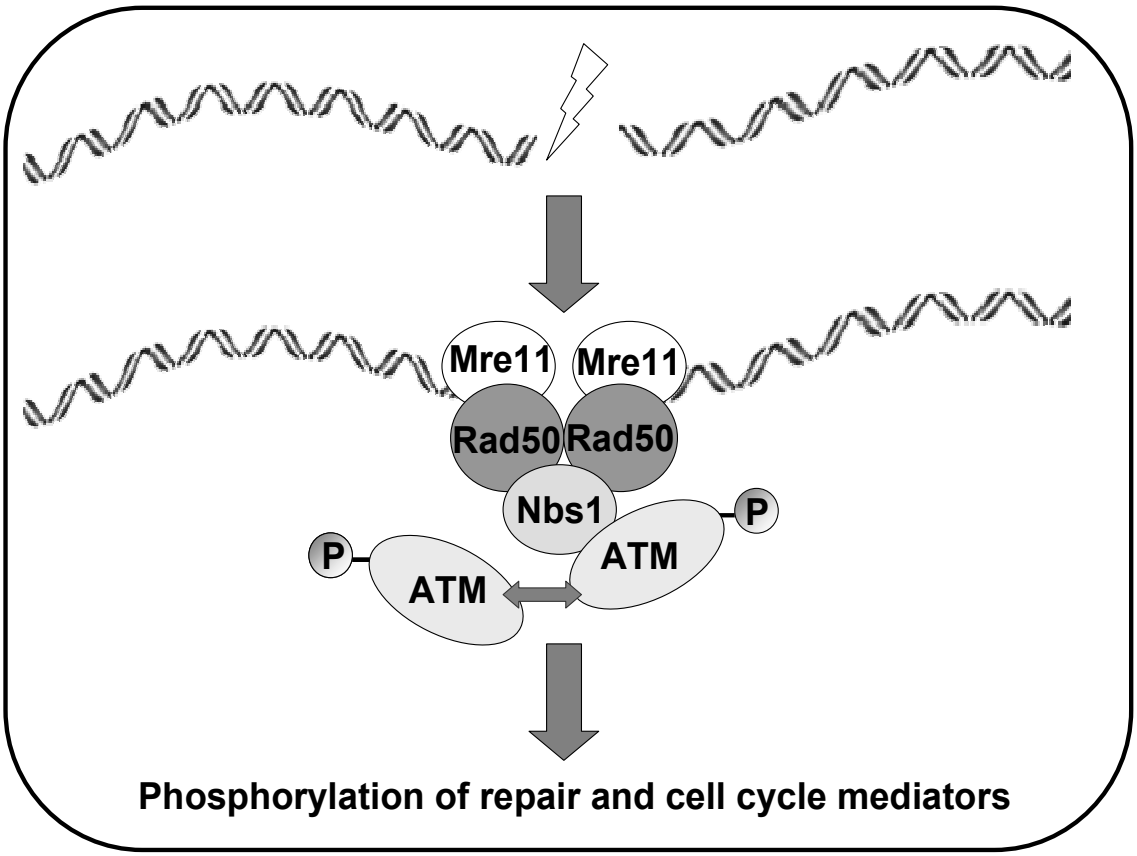

Figure 2. Activation of ATM after DNA double-strand break formation. The MRN complex is believed to be one of the earliest repair mediators to arrive at the break site and recruit ATM. Inactive ATM dimers or multimers are activated by interacting with MRN. This induces monomerization and transautophosphorylation of the ATM molecules. Active ATM can now mediate downstream phosphorylation events.

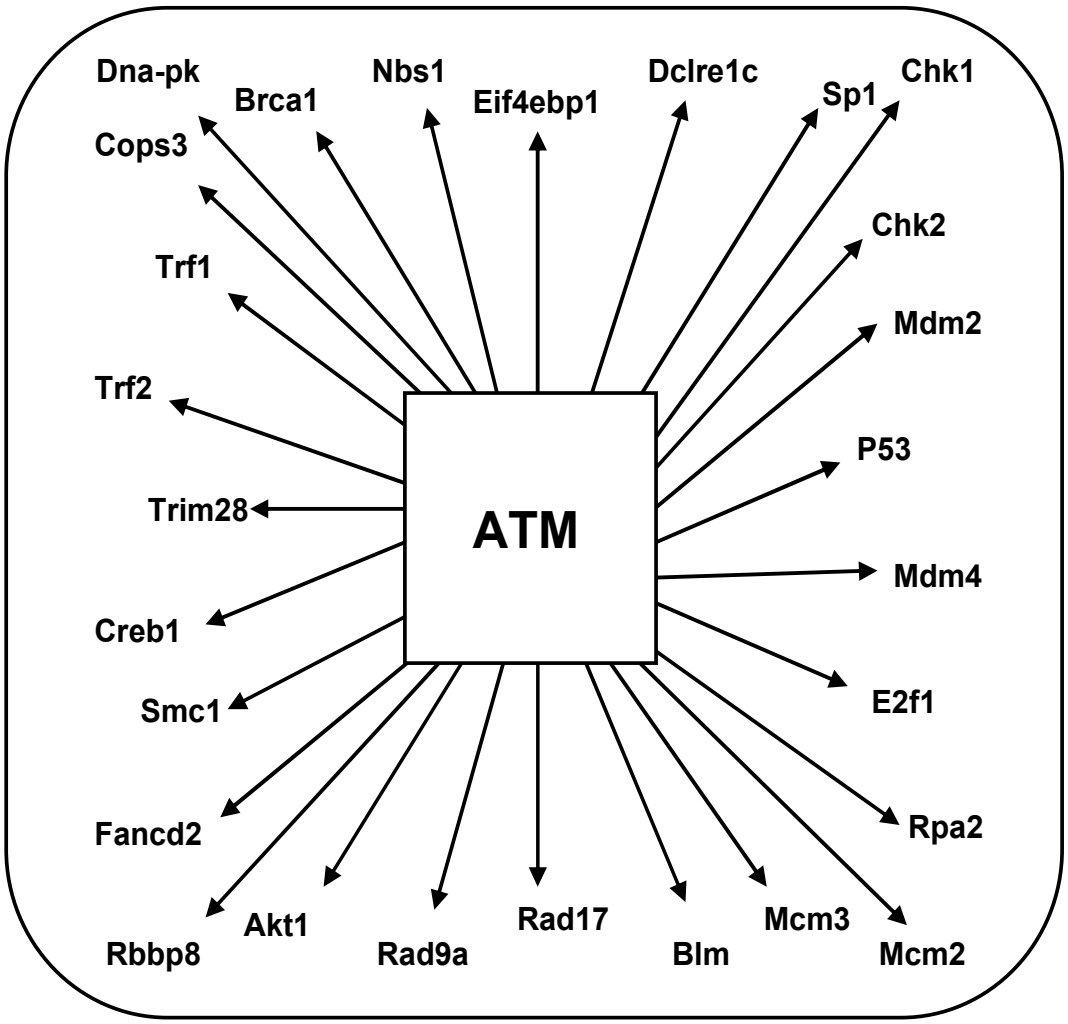

Figure 3. The range of ATM phosphorylation targets. Upon activation, ATM phosphorylates a wide range of substrates involved in DNA double-strand break repair, cell cycle regulation and apoptosis. Some of these substrates are depicted here.

The A-T cellular phenotype

Cells derived from A-T patients are commonly referred to as A-T cells. The hallmark feature of these cells is their pronounced radiosensitivity. They are highly sensitive to ionizing radiation and other radiomimetic drugs such as bleomycin and neocarzinostatin (58). A-T cells are also known to be sensitive to free radical production (59, 60). The sensitivity to other types of DNA damaging agents varies depending on the cell lines used and the conditions employed. Consequently, variable results regarding sensitivity to MMS, MNNG, ENU, EMS and other agents have been reported by different groups (58). The sensitivity of these cells to UV irradiation has also remained debatable with groups reporting responses similar to those obtained in control cells (61, 62) while others reporting enhanced cell-killing (63, 64). It remains possible that the damaging agents employed in some of these studies were used under conditions that generate DSBs, lesions that A-T cells would not be able to cope with. This would explain the variability obtained by different groups.

A-T cells are also characterized by spontaneous genetic instability resulting in chromosomal rearrangements. Commonly reported rearrangements involve chromosome bands 7p14, 7q34, 14q12 and 14q32 (58). Unsurprisingly, these are proximal to some immunoglobulin genes and can be explained by a presumed role for ATM in immunoglobulin gene rearrangement (65). These aberrations may be behind the immunodeficiency and lymphoid malignancies reported in A-T. An increased incidence of chromosomal breakage and aberrations following ionizing radiation treatment (66) or exposure to radiomimetic chemicals (67) has also been observed in A-T cells. Elevated

chromosomal aberrancies in response to UV irradiation have been reported in some A-T cell lines as well (68).

Lymphocytes from affected individuals and cell lines also show increased rates of chromosomal fusions and shortened telomere lengths in the presence of normal telomerase activity (69). This indicates a potential role for ATM in telomeric maintenance (70).

Along with increased cell-killing and chromosomal aberrancies in response to irradiation, A-T cells also display cell cycle checkpoint defects (71). A-T cells do not arrest in G_1 in response to irradiation and do not display a decrease in DNA synthesis upon exposure to ionizing radiation or radiomimetic chemicals like normal cells. This is termed radioresistant DNA synthesis (RDS). On the other hand, DNA synthesis inhibition in response to UV irradiation is comparable to normal cells (61). A G_2 delay in response to irradiation is also deficient in A-T cells (72). Therefore, the G_1/S, intra-S and G_2/M checkpoints are all defective in these cells. This can be explained at the molecular level by the role ATM plays in these checkpoints. Moreover, ATM has more recently been implicated in the spindle checkpoint in M-phase as well (73).

ATM defects result in outcomes reflective of its functions. Cells from homozygote or compound heterozygote A-T patients exhibit deficiencies in DSB repair and cell cycle checkpoints. The roles played by ATM in associated pathways are further elaborated below.

ATM and cell cycle regulation

A large number of ATM substrates consists of mediators that participate in cell cycle checkpoints that are activated after DSB formation (Figure 4). In response to damage, both ATM and its substrate, the Chk2 kinase, phosphorylate P53 (74). This latter is a key mediator in the G_1/S checkpoint. This results in efficient stabilization of the P53 protein. Although none of the ATM phosphorylation sites on P53 are essential for stabilization, they seem to contribute to the efficiency of this process (75). ATM also mediates direct and indirect phosphorylation events on Mdmx and Mdm2 thus relieving P53 suppression and degradation (76). Then, via its transactivational capabilities, P53 induces the expression of p21/WAF1, the cyclin-dependent kinase inhibitor (CKI) whose inhibition of cyclin-dependent kinases (Cdks) 4 and 6 represses the transcription of several genes needed for passage through the "restriction point" (R) in late G_1. Moreover, p21 is an inhibitor of Cdk2, the G_1/S and S-phase Cdk. Hence, ATM orchestrates a cascade that halts the cell cycle. This probably allows sufficient time for repair before DNA synthesis ensues. Alternatively, in the case of extensive damage, P53 induce Puma, Noxa and Bax consequently initiating caspase cascades and apoptosis (77).

ATM plays a no less significant role in the intra-S phase checkpoint. Two pathways are believed to control this checkpoint and ATM is an essential feature of both. In the first pathway ATM activates Chk2 by phosphorylation. Chk2 will in turn phosphorylate Cdc25A phosphatase resulting in promoting its ubiquitination and consequent degradation by the proteosome. A decline in Cdc25A levels leads to decreased dephosphorylation of Cdk2. This results in an inactive Cdk2 that is incapable

of promoting DNA synthesis and progression through S-phase (78). The other pathway controlled by ATM is less understood and depends on phosphorylation of BRCA1, FANCD22 and the Nbs1 component of the MRN complex. Phosphorylated Nbs1 is believed to act as an adaptor protein to mediate ATM-dependent SMC1 phosphorylation. This phosphorylation would then suppress the participation of SMC1 activities in replication (79).

The third checkpoint mediated by ATM is the G_2/M checkpoint. Activation of Chk2 by ATM results in phosphorylation of the Cdc25C phosphatase. This will promote binding of this phosphatase to the 14-3-3 family of proteins and its sequestration in the cytoplasm. This will prevent Cdc25c-mediated dephosphorylation of Cdk1 and therefore inhibits Cdk1-cyclin B from promoting entry into mitosis. Furthermore, stabilization of P53 protein after ATM-dependent phosphorylation is thought to contribute along with the retinoblastoma (Rb) protein to the G_2/M checkpoint by transcriptional downregulation of genes required for passage from G_2 to M such as Cdk1 and cyclin B (80).

ATM has also been implicated in a damage-dependent mitotic spindle checkpoint. Previous reports had suggested that an active form of the kinase was present in the cytoplasm of cells in mitosis (75). Moreover, active ATM has been observed at centrosomes (81) and some of its substrates, including Pin2/TRF1 and 53BP1, were detected at mitotic spindles (82, 83). More recently, ATM activation induced by DSB formation was reported to inhibit spindle assembly in Xenopus mitotic egg extracts and somatic cells therefore arresting cells in M-phase. ATM-mediated phosphorylation of the

centrosomal protein CEP63 was shown to result in the latter delocalizing from the centrosome and hence inhibiting spindle assembly (73).

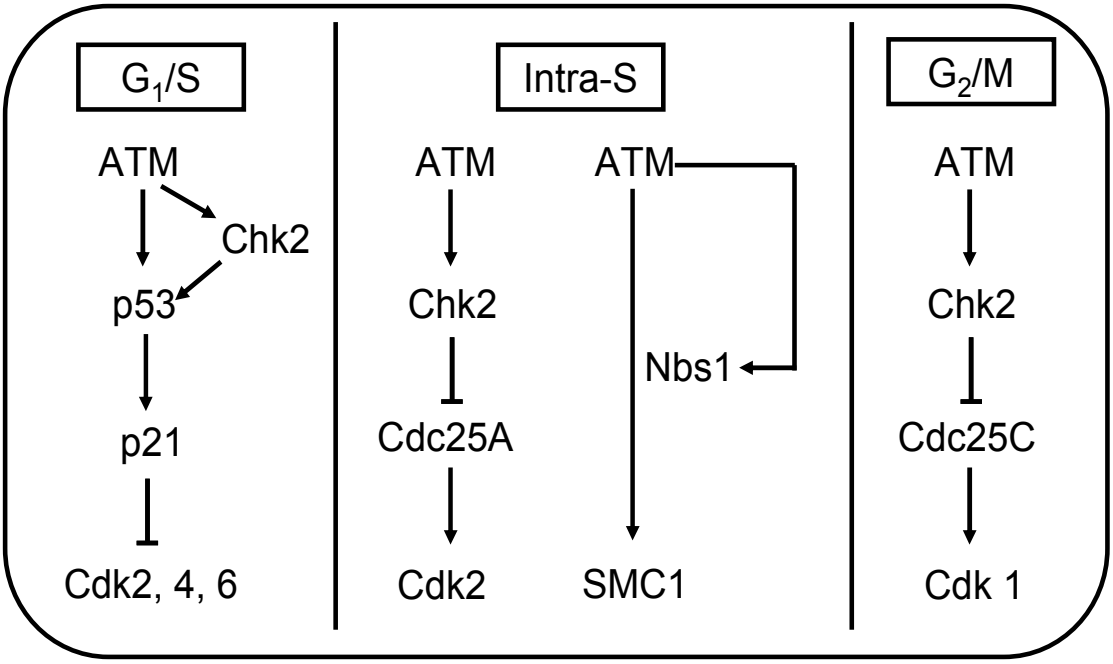

Figure 4. Cell cycle checkpoints mediated by ATM. Upon DSB formation, ATM activates multiple checkpoints involved in regulating cell cycle progression. A detailed description of these checkpoints can be found in the text.

ATM and DNA double-strand break repair

Alongside regulating the cell cycle in response to DSB formation, ATM phosphorylates mediators involved in repairing the break. The following is a brief overview of the pathways believed to repair a break and the mediators involved in them. The interactions of ATM with these mediators and the functions it may play in DSB repair pathways are also described.

A DSB may be caused by endogenous and exogenous mutagens as well as by normal physiologic processes. Such a break is necessary for initiation of normal meiotic recombination and for recombinogenic events that lead to antibody class switching and to T-cell receptor gene rearrangement. Ionizing radiation, such as γ- and x-rays, and free radicals are common non-physiologic causes of DSBs. Such a break may also occur during DNA replication if the process is compromised (3).

Several pathways have evolved to mediate DSB repair. These include recombination repair pathways (Figure 5), such as homologous recombination repair (the DSBR model of Szostak et al.), synthesis-dependent strand annealing (SDSA), break-induced replication (BIR) and single-strand annealing (SSA). The other major type of DSB repair is non-homologous end joining (NHEJ) (Figure 6). While recombination repair pathways rely on utilizing a sequence that shares high homology with the one harboring the DSB as a template for repair, NHEJ relies on ligation of DNA ends using little or no homology (84). Although the main focus of the literature has been on these two mechanisms through which a DSB is repaired, it has become evident in recent years that other “backup” or “alternative” pathways exist (85-90). These pathways are often

described as error-prone and will be dealt with herein. While NHEJ appears to be the prevalent DSB repair mechanism in mammalian cells during G0/G_1 and early S-phase of the cell cycle (91), recombination repair is favored during S/G_2 (92, 93). The way the cell cycle state affects alternative pathways of repair has not been examined. Other conditions that affect pathway choice are not fully understood but may include the nature of the lesion, availability of a ligatable end or a homologous template and the number of lesions. Pathway selection may also depend on the abundance or state of repair mediators. The following is an account of the mentioned repair mechanisms.

Mechanisms of recombination repair

The double-strand break repair model of Szostak et al.

In the revised DSBR model of Szostak et al. (Figure 5A) the DSB ends are resected by nucleases to form 3' single-stranded ends that can mediate the invasion of a homologous duplex. An invading 3' end will prime DNA synthesis on one strand of the intact DNA duplex leading to displacement of the other strand of the intact duplex and consequential formation of what is referred to as the D-loop. This D-loop will pair with the non-invading 3' end of the DSB in what is termed the second end capture. This allows the priming of DNA synthesis on that end. DNA synthesis and ligation lead to the formation of two tetrahedral structures called cross-strand exchanges or Holliday junctions. The double Holliday junction is eventually resolved by cutting and this resolution can result in crossing over or non-crossing over (94).

Synthesis-dependent strand annealing (SDSA)

Although the revised Szostak et al. model explains the outcome of meiotic recombination it does not adequately do so for mitotic recombination. Mitotic gene conversion events are infrequently associated with crossing over. This led to the development of the SDSA model (Figure 5B). In the standard version of this model a resected 3' end at the DSB mediates strand invasion and DNA synthesis in a manner similar to that explained in the Szostak et al. model. However, instead of ligation and formation of a Holliday junction, the newly synthesized regions are displaced and anneal via their complementary portions, then the gap is filled and hence the break is repaired without crossing over. Variations of this model exist (95).

Single-strand annealing (SSA)

If a break is flanked by direct repeats, an exonuclease can mediate end resection hence exposing complementary regions on both ends of the break (Figure 5C). Annealing of these regions will create flaps that can be digested by nucleases. Gap filling and ligation will seal the break. This process is considered to be mutagenic since it results in the loss of genetic information (96).

Break-induced replication (BIR)

The above-mentioned models may explain gene conversions in mitosis that involve short stretches of DNA. However, gene conversion events that involve long tracts have been documented as well. This especially occurs when one end of a DSB is presented for repair such as in the cases of broken chromosomes, certain types of collapsed replication

forks, exposed telomeres or if the other end of a break is unavailable for repair for any number of reasons. The single end produced can invade a homologous chromosome and undergo DNA synthesis up to the end of the template chromosome (Figure 5D) (96).

Proteins that mediate recombinogenic events

Initiation of recombination necessitates a DSB; such a break can be caused by damaging agents or by cellular enzymes. DSBs eliciting meiotic recombination in mammalian cells are catalyzed by Spo11 (97), a protein that is conserved across several species including yeast, fungi, flies, worms and plants (98).

Resecting a DSB end into a 3' single-stranded end that could carry out invasion is mediated by the MRN complex in mammalian cells (MRX in budding yeast). Nevertheless, it has been demonstrated in budding yeast that the nuclease function inherent to this complex and possessed by its Mre11 nuclease component is not required for this process (99). After all, resection predicts a 5' to 3' exonuclease - an activity not possessed by Mre11 *in vitro* – however, evidence indicates that the MRN complex indeed participates in this process (100, 101). Exo1, a 5' to 3' exonuclease, and CtIP (Sae2 in budding yeast), an endonuclease, are generally believed to cooperate with MRN in resection (99, 102-104). A role for the BLM helicase (Sgs1 in budding yeast) has been demonstrated as well (104, 105).

The single stranded DNA generated by resection is first bound by the replication protein A (RPA), a eukaryotic single stranded DNA binding protein. Then, RPA is displaced and replaced by Rad51, a recombinase that catalyzes invasion and pairing with the homologous strand. Displacement of RPA and Rad51 recruitment to the single

stranded DNA is mediated by Rad52. In mammalian cells Rad54 is a mediator of Rad51 DNA binding along with the Rad51 paralogs (XRCC2, XRCC3, Rad51B, Rad51C, Rad51D) (106), BRCA1 and BRCA2. This latter is thought to bind Rad51 in its inactive state in the absence of damage and to recruit it to the site of a DSB where it is released in its active state (107).

In budding yeast, deletion of *RAD52* results in severe defects in SSA, recombination between inverted repeats and in recombination pathways that result in gene conversion (DSBR, SDSA). Deletion of *RAD51*, on the other hand, does not affect SSA and results in a maximum 10-fold reduction in recombination between inverted repeats (96). In fact, RAD52 seems to be the only X-ray sensitivity gene required for SSA (108). Significant recombination rates are detectable in yeast *rad51* mutants. This is indicative of alternate recombination pathways that are probably RAD52-mediated. Support comes from experiments showing that human Rad52 can promote D-loop formation (109) and from yeast screens that identified the RAD59 gene. Mutants of either *rad51* or *rad59* displayed a minor defect in recombination between chromosomal inverted repeats. The *rad51 rad59* double mutant, however, was as defective as the *rad52* mutant. Data also indicates that RAD59 may play a role in the SSA pathway. RAD59 seems not to be required for interchromosomal recombination; nevertheless, events mediated by RAD59 appear dependent on RAD52. On the other hand, BIR also depends on RAD52 but not on RAD51, RAD54, RAD55, or RAD57 (94).

Until recently, the identification of a Holliday junction resolvase has been elusive. Genetic and biochemical lines of evidence attributed a resolvase function to several

eukaryotic proteins. These include budding yeast/human Mus81, yeast MMS4 and human Resolvase A (ResA). Some doubts have been raised about the function of MUS81 and MMS4 as Holliday junction resolvases; nevertheless, they could play a role in resolving other intermediates (96). The mammalian RecQ-like helicases, BLM and WRN, have been shown to promote Holliday junction migration *in vitro*; however, mutations in their genes lead to increased recombination frequencies. Therefore, these helicases are thought to play more of a role in processing stalled replication forks. The budding yeast BLM homologue, SGS1, may play a similar role (110). ResA, on the other hand, is capable of promoting branch migration. The activity of ResA was originally identified in a mammalian cell extract fraction; however, the protein was not isolated or characterized. More recently, GEN1 was identified as a mammalian classic Holliday junction resolvase and is believed to be identical to ResA. The budding yeast orthologue of GEN1 was found to be Yen1 (111).

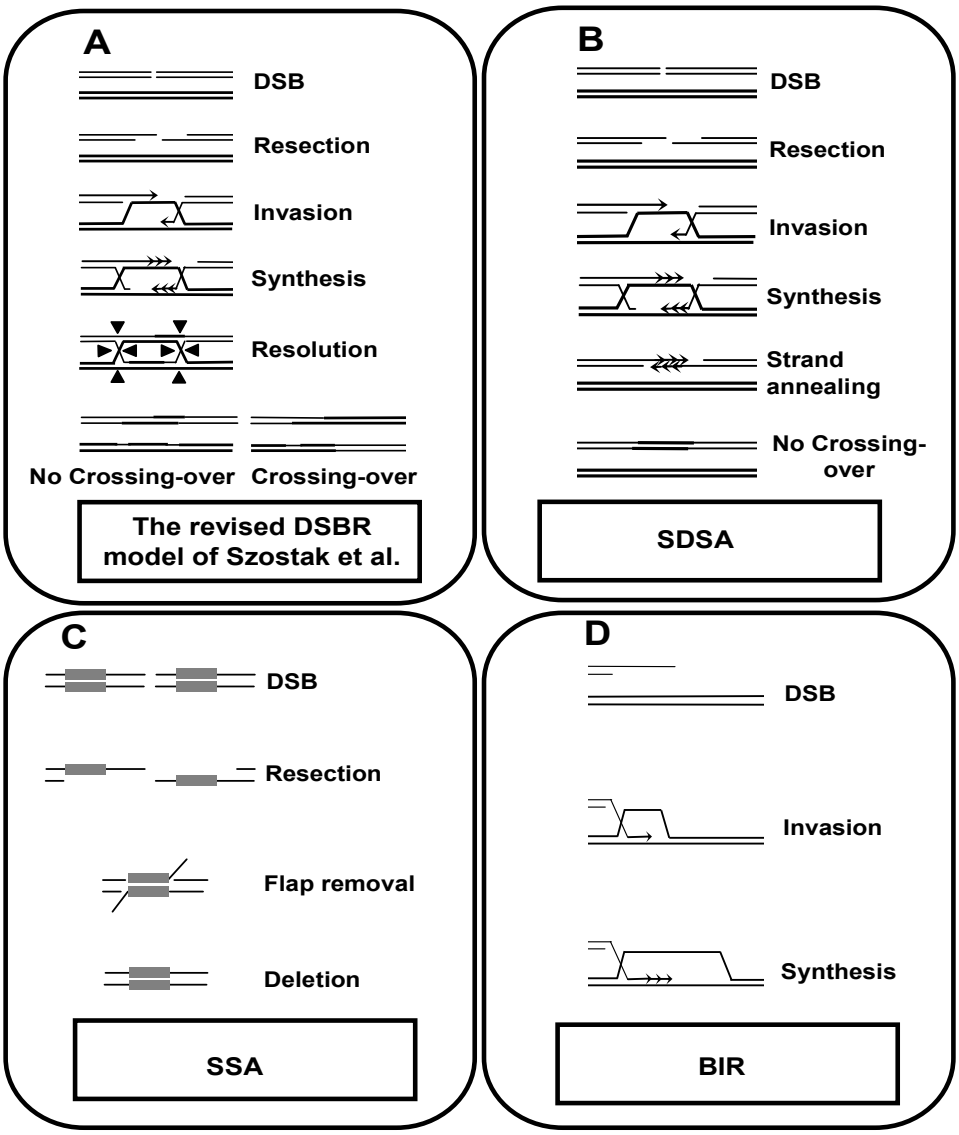

Figure 5. Pathways of recombination repair. (A) The revised double-strand break repair (DSBR) model of Szostak et al. (B) Synthesis-dependent strand annealing (SDSA) (C) Single strand annealing (SSA) (D) Break-induced replication (BIR).

Non-homologous end joining

In contrast to homologous recombination pathways, NHEJ uses little or no homology to ligate the ends of a DSB (Figure 6). In this pathway, the Ku70-Ku80 heterodimer binds to DNA ends at a DSB. The DNA protein kinase catalytic subunit (DNA-PKcs) is subsequently recruited in higher eukaryotes; a yeast DNA-PKcs has not been identified yet. The DNA ends are finally rejoined by mammalian XRCC4-DNA ligase IV (DNL4 in budding yeast) (84). DSBs that are not suitable for direct ligation may be processed by the MRN complex or Artemis, a nuclease that has a 5' to 3' exonucleolytic activity on single-stranded DNA and an endonucleolytic activity on 5' overhangs, 3' overhangs and hairpin loops (112). The process may also require gap filling by polymerases μ and λ (113).

Alternative DSB repair and microhomology-mediated end joining

Alternative DSB repair pathways are broadly defined as end-joining pathways that occur in the absence of classic NHEJ mediators such as Ku70, Ku80 and ligase IV. The number of such pathways and the mediators involved are not known.

The most commonly reported alternative pathway of end-joining is microhomology-mediated end joining (MMEJ) (Figure 7). Repair through this pathway relies on DNA degradation and rejoining at sequences of microhomology (1-10 bp direct repeats) that flank the break, resulting in deletion of the sequences between the two sites of microhomology as well as one microhomology site. Although MMEJ is often perceived as a subtype of NHEJ the genetic requirements of the two pathways are very

different. MMEJ is independent of the functions of the Ku proteins and XRCC4-DNA ligase IV. This pathway is also different from the SSA pathway which requires rejoining at direct repeat sequences of more than 30 bp that flank the break. The genetic requirements of SSA are also different since, unlike MMEJ, this pathway necessitates Rad52 function (114).

MMEJ is often described as a "back-up" mechanism, which may imply an insignificant role for the pathway when other DSB repair mediators are functional. Nevertheless, recent studies have demonstrated a substantial contribution of this pathway to DSB repair in V(DJ) recombination despite the presence of intact NHEJ factors. In V(DJ) recombination, diversity in T-cell receptors and antibody molecules is generated by a gene rearrangement reaction that involves break-formation and rejoining. Moreover, it was shown that MMEJ is even capable of partially rescuing V(D)J recombination end-joining defects in cells deficient in either DNA-PKcs or XRCC4 (115). Another physiologically relevant pathway shown to proceed via microhomology-directed repair in the absence of intact NHEJ is class switch recombination (CSR). This pathway takes place in B cells and involves DSB formation and rejoining to switch from the production of one antibody class to another (116). Taken together, the above mentioned studies indicate that MMEJ is a rather robust pathway of DSB repair and may be physiologically significant.

Little is known about the mediators involved in MMEJ or its regulation. Studies attempting to characterize the genetic requirement for MMEJ in yeast have revealed roles for the MRX complex, Exo1, Sae2, Tel1, Srs2, Dnl4, Rad1-Rad10, Pol4, Polη, Polζ , and

Pol32 (polδ subunit) (117, 118). These findings demonstrate an essential difference between pathway requirements in yeast and those in mammalian cells. Dnl4, which is the yeast homologue of the mammalian DNA ligase IV, was necessary for the pathway. This is in contrast to MMEJ in mammalian cells whereby the pathway is defined as being DNA ligase IV-independent. Mediators suggested to play a role in MMEJ in mammalian cells include the BLM helicase (119), PARP-1, XRCC1, DNA ligase III (120), the FEN1 endonuclease, DNA polymerase ε (121) and Exo1 (122).

Repair events via MMEJ have been linked to multiple diseases involving chromosomal translocations and cancers (123-127). Although our understanding of the regulation of alternative repair is lacking, some possibilities can be drawn from NHEJ-deficient mouse studies. The observation that Ku-deficient mice have a higher viability than XRCC4 or DNA ligase IV-deficient mice suggests that the Ku proteins may have a suppressive effect on error-prone repair. This may occur through DNA end-binding by Ku with consequent hindering of the alternative repair machinery (128). This possibility, however, requires further exploration.

The existence of other alternative end-joining pathways besides MMEJ has seldom been demonstrated. Nevertheless, evidence from human cells shows that a Ku and DNA-PKcs-independent end-joining mechanism can result in accurate end-joining with very rare deletions (85, 129, 130). Hence, unlike MMEJ this alternative pathway does not rely on microhomologies. Whether the microhomology-independent repair products reported in these studies are the result of repair through one alternative mechanism or more remains to be clarified.

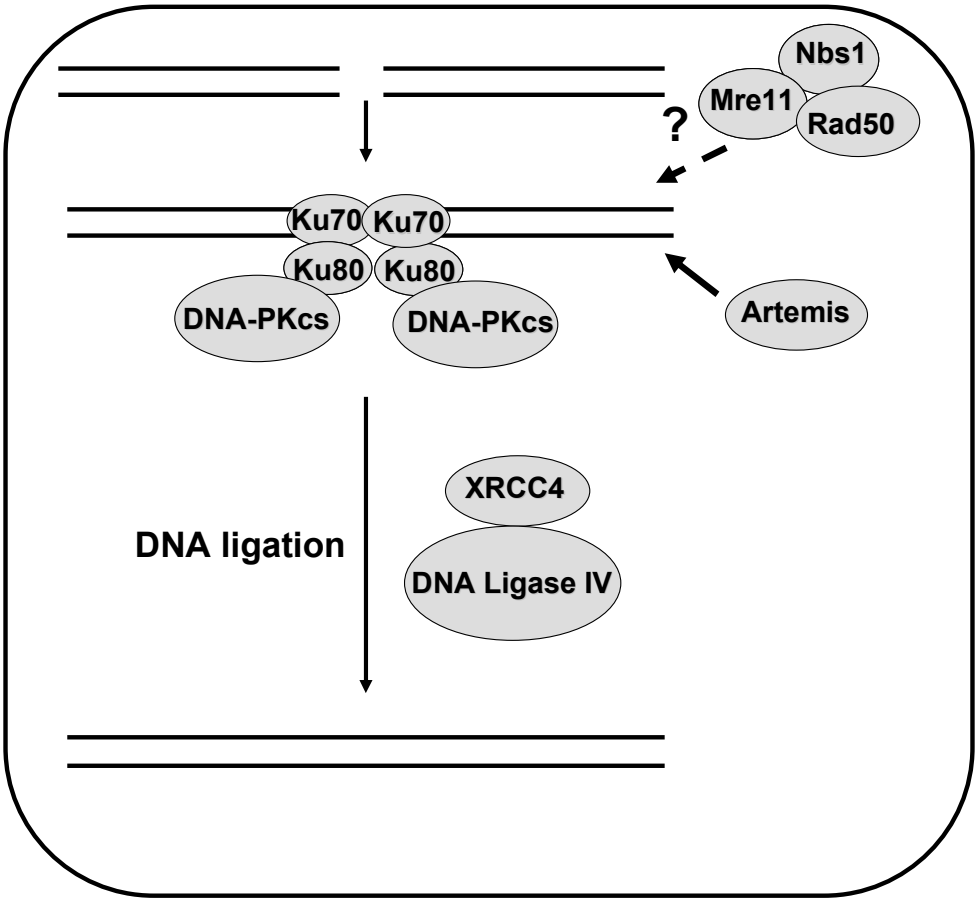

Figure 6. Non-homologous end joining. This pathway of DNA double-strand break repair involves recruitment of the Ku proteins and DNA-PKcs to the break site prior to ligase-mediated rejoining. The DNA ends may be processed prior to ligation by the Artemis nuclease. The role of the MRN complex in processing the break ends in mammalian cells is debatable.

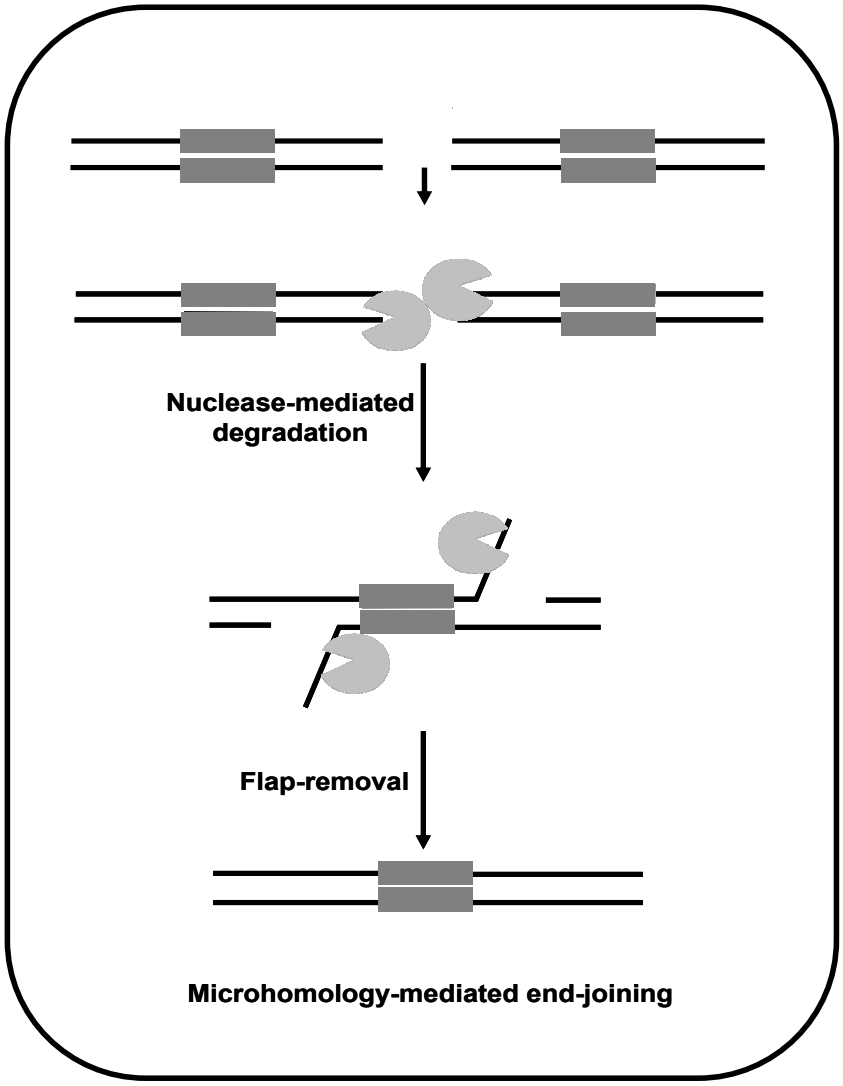

Figure 7. Speculative model for microhomology-mediated end joining (MMEJ). The error-prone double-strand break repair pathway is thought to be mediated by nuclease(s) that resect DNA thereby revealing short direct-repeat sequences flanking the break. These are complementary bases that can anneal. Any flaps that are created can then be removed. Therefore, this pathway results in loss of DNA sequences.

ATM and DSB repair mediators

The phosphorylation and recruitment of several NHEJ and recombination repair mediators upon a DSB event is thought to be ATM-dependent. Among ATM's substrates is the MRN complex. ATM was shown to phosphorylate Nbs1 in response to DNA damage (131, 132) and ATM-dependent phosphorylation of Mre11 (133) and Rad50 (134) has also been reported. The dependence of ATM activation on this complex after DSB formation was described in a previous section. Hence, the MRN complex has functions upstream and downstream of ATM activation. ATM-dependent phosphorylation of other recombination repair-associated proteins, such as BRCA1 (135) and Rad51 (136) has also been reported. The NHEJ nuclease, Artemis, is also phosphorylated by ATM (137) and ATM-dependent phosphorylation of DNA-PKcs has also been indicated (138). The significance of these phosphorylation activities is not known.

The deficiency in DSB repair in absence of intact ATM function

The initial observation that A-T patients were radiosensitive indicated a possible deficiency in DSB repair in these patients. Several groups have examined the efficiency and fidelity of DSB repair in A-T cells and their extracts employing various high and low resolution techniques. Results have been variable depending on the technique used. The current view is that repair efficiency is not affected by an ATM deficiency with very few, if any, residual unrepaired ends after DSB generation in A-T cells. Several reports

including ones from our laboratory indicate that the fidelity, rather than efficiency, of DSB repair is compromised in A-T cells.

A number of groups (139-142) employed sucrose gradients to analyze break rejoining after irradiation of A-T cells. This allows monitoring repair-associated formation of high molecular weight DNA products from lower molecular weight products after repair. Employing this technique, these groups reported no major differences between A-T and control cells. Using neutral filter elution, which is attributed with having a better resolution than sucrose gradient analysis, Van der Schans et al. (143) and Shiloh et al. (144) did not observe differences between A-T and control cell lines in the rejoining of DSBs whereas Coquerelle et al. (145), using the same technique, indicated that the kinetics of rejoining were slower in A-T cells. Using fluorometric analysis of DNA unwinding (FADU), Thierry et al. (146) reported no significant differences in DSB repair between A-T cells and controls. Using pulsed-field gel electrophoresis, which allows an estimate of DNA fragments remaining post-irradiation repair, variable results were obtained depending on the dose, dose rate, temperature at which irradiation is carried out and repair time allowed (147-149). Cytogenetic and cytologic studies monitoring chromosomal aberrations have also reported the existence of a higher number of unrepaired breaks after irradiation in A-T cells (150, 151). Applying immunofluorescent detection of γ-H2AX as a marker of repair foci in A-T cells and controls, Kühne et al. (152) reported a persistent number of foci in A-T cells which they presumed to be unrepaired DSBs. Results from all these studies are complicated by the variability in the experimental conditions employed. Moreover,

estimates of persistent breaks from most of these studies in A-T cells is in the 1-10% range, which does not account for the severity of radiosensitivity seen in both A-T patients and cells. A-T is after all believed to be the most radiosensitive disorder known (153).

Investigations into the fidelity of repairing restriction-linearized plasmids in A-T cells have also been performed. Plasmids were transfected, retrieved and the repair products were analyzed by Southern blotting. Probing for the plasmid has shown deletions, insertions and rearrangements in plasmids repaired in A-T cells (154, 155). Dar et al. (156), on the other hand, studied the repair of plasmids linearized by bleomycin-treatment, which is believed to induce ionizing radiation-like breaks. Plasmids were transfected, retrieved and then analyzed by sequencing. Deletions and base substitutions were seen at a higher frequency in A-T cells with very few insertions. This again supports the notion of compromised DSB repair fidelity in A-T cells.

Our laboratory has previously examined the efficiency and fidelity of repairing restriction-linearized plasmids *in vitro* in nuclear extracts from A-T cells (157). Rejoining efficiency was evaluated by bacterial transformation. Circular plasmid are estimated to have a 100X higher transformation efficiency than linear plasmids. Consequently, transformation efficiency is a direct measure of rejoining efficiency.

First, the rejoining of restriction-linearized pUC18 plasmids was examined in nuclear extracts from control and A-T cells. Transformation efficiencies, and therefore the rejoining potential, were similar from both types of extracts, indicating that ATM does not play a significant role in affecting the efficiency of plasmid rejoining. On the

other hand, the pUC18 plasmids were linearized within the *lacZα* gene thus disrupting its function. The mutation frequency upon rejoining was therefore quantified by classic blue-white screening. Mutation frequency was around 2-fold higher in extracts from A-T cells compared to controls. Some of these mutations were then characterized by DNA sequencing and all turned out to be deletions that spanned the break site. Furthermore, most of these deletions were rejoining events at microhomology sequences.

To further examine the MMEJ capacity of A-T nuclear extracts, repair of the *SupF22* plasmid was studied. This plasmid harbors the *SupF* gene, which encodes an amber suppressor tyrosyl-tRNA, interrupted by a multicloning site that is flanked by two 4 bp microhomologies. This renders the amber suppressor gene non-functional. Repair by MMEJ of a *SupF22* plasmid linearized within the multicloning site and utilizing the flanking microhomologies results in deletion of the intervening multicloning site along with one microhomology. This restores the functionality of the amber suppressor tRNA in the plasmid, which is then used to transform an indicator bacterial strain. This strain harbors an amber mutation within the *lacZ* gene. Reversion of the mutated *SupF* gene to a functional one by MMEJ is therefore scored as blue colony formation. The frequency of MMEJ observed after rejoining of the *SupF22* plasmid was up to 50-fold increased in A-T nuclear extracts compared to controls.

This increase in MMEJ in A-T nuclear extracts may indicate that the stability of DNA ends is compromised in these extracts. Therefore, ATM may be involved in regulation of nucleases that may be capable of mediating DNA end-degradation and MMEJ. One potential candidate for regulation by ATM is the MRN complex.

Interactions between this complex and ATM were described in the section on ATM activation. The following is a description of this complex and evidence implicating it in MMEJ.

The MRN complex and its potential role in MMEJ

The MRN complex is composed of Mre11, Rad50 and Nbs1. Mre11 preferentially acts as a 3' to 5' exonuclease on 3' recessed strands and it has endonuclease functions on single-stranded loops (158). Rad50 is an ATPase related to the structural maintenance of chromosomes (SMC) proteins (159) and distantly related to the ATP binding cassette (ABC) family of transporters (160). Nbs1, on the other hand, seems to mediate protein interactions. The three proteins that constitute the MRN complex appear to be essential in mammals (161-164).

Whereas the role of MRN in NHEJ remains debatable in mammalian cells, it is required for this pathway in budding yeast (96). Mre11 is required for homologous recombination in both yeast and mammalian cells (165) however its nuclease activity appears to be dispensable for the process (99). This nuclease function is nevertheless essential for the repair of DSBs generated by Spo11 during meiosis (166). Structural studies of the Mre11-Rad50 complex reveal that it is a heterotetramer composed of two Mre11 and two Rad50 subunits (167, 168). Rad50 possesses the Walker A and Walker B DNA binding motifs characteristic of SMC proteins. These motifs are separated by a long coiled coil that contains a hinge region. Dimerization via this hinge region results in an arrangement that can bring together different DNA molecules (169). Indeed, a DNA tethering activity has been described for the complex with a particular dependence on an

adenylate kinase activity of the Rad50 component (170). A DNA duplex unwinding activity has also been detected (171). A role for this complex as an early sensor of DSB formation and activator of ATM signaling has been described and is further delineated in the section on ATM activation above.

Studies in yeast indicate that the Mre11 exonuclease plays a major role in MMEJ (117, 118). Biochemical studies performed with purified recombinant human Mre11 corroborate the ability of this nuclease to mediate MMEJ *in vitro*; it has been demonstrated that the nuclease is capable of degrading DNA duplex substrates up to regions of microhomology (172). Moreover, recent biochemical evidence from crystal structure analysis implied that the conformation of the MRN complex may permit MMEJ (Figure 8) (173). Nevertheless, the role this complex may play in MMEJ in mammalian cells has not been deciphered. The information explained above coupled with our knowledge of ATM-mediated phosphorylation (131-134) of the MRN complex components place it at the heart of the MMEJ pathway and of regulation by ATM.

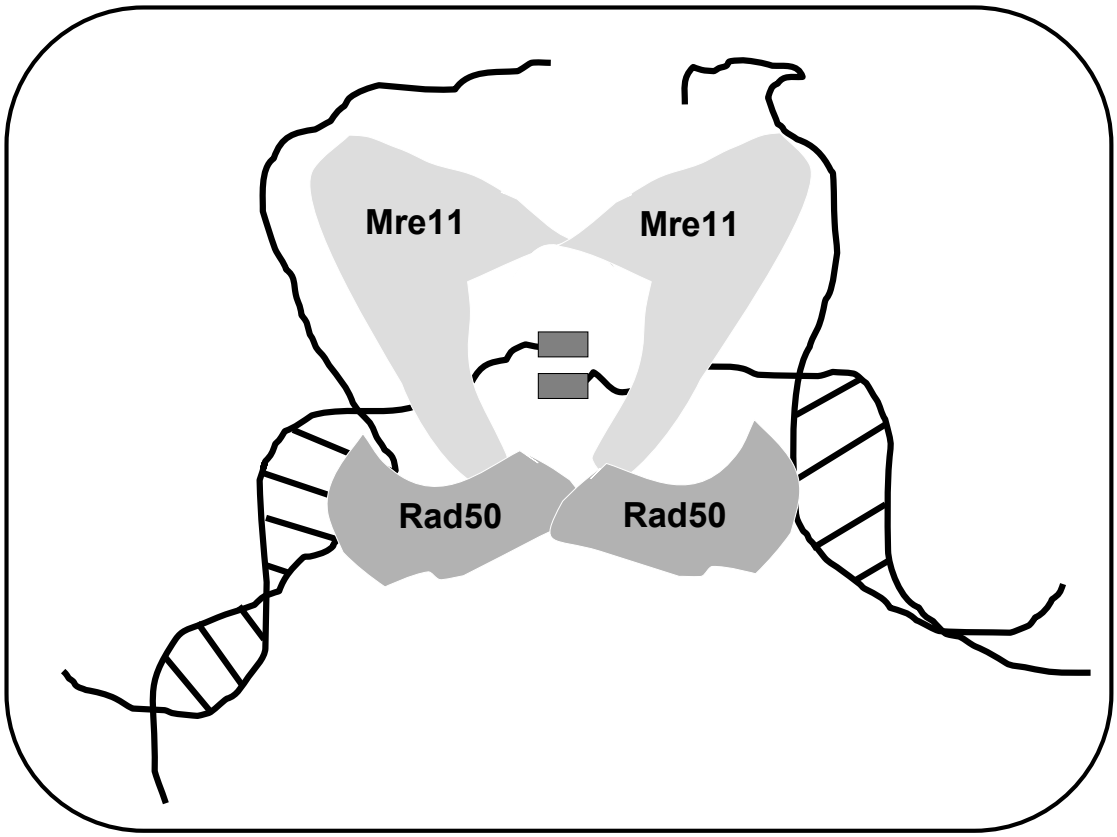

Figure 8. Speculative model for the mechanism by which the MRN complex mediates microhomology-mediated end joining. Structural studies revealed that the complex formed by the Mre11 and Rad50 proteins is a heterotetramer. An extrapolation from this structure is that the two Mre11 subunits can degrade the two different DNA strands at a break site up to regions of microhomology. These regions can then anneal within the nuclease complex hence stopping the degradation reaction.

Explanation of the dissertation format

This dissertation is comprised of two chapters: an introductory chapter that includes a survey of the literature pertinent to this work (Chapter I: Introduction) and a chapter summarizing and discussing novel findings in the dissertation (Chapter II: Present Study). These findings are appended in the form of two manuscripts (Appendices A and B). The studies presented in these two manuscripts were of my own design and were conducted and analyzed by me with guidance from my advisor Dr. Kathleen Dixon and contributions from Dr. Leigh Ann Henricksen and members of the Dixon laboratory. The purification of ATM employed in the series of experiments described in Appendix A was performed by Katherine S. Pawelczak in the laboratory of Dr. John J. Turchi at the Indiana University School of Medicine.

CHAPTER II: PRESENT STUDY

A detailed account of the methods and findings of the studies comprising this dissertation can be found in the appended manuscripts (Appendices A and B). The manuscripts also provide an elaborate discussion of these findings. The following represents a brief summary of these manuscripts in addition to a conclusions section that proposes potential avenues and experimental methods to tackle remaining questions.

ATM mediates repression of DNA end-degradation in an ATP-dependent manner (Appendix A)

Summary

A deficiency in ataxia telangiectasia mutated (ATM) function has been associated with defects in DNA double-strand break (DSB) repair and cell cycle misregulation. Although the role of ATM in cell cycle checkpoints is well studied, the defect in DSB repair that may occur in the absence of intact ATM remains debatable. Our laboratory has previously reported comparable linear plasmid rejoining efficiencies in nuclear extracts from both ATM deficient (A-T) and control (wtATM+) cells. Rejoined plasmids retrieved from the A-T nuclear extracts, however, contained deletions resulting from end-joining at sites of microhomology. This suggested a role for ATM in stabilizing DNA ends and suppressing error-prone DSB repair pathways that involve nuclease-mediated degradation of DNA ends at a break.

To assess the capability of ATM in enhancing DNA end-stability, we assessed the degradation of DNA duplex substrates in A-T and control nuclear extracts. The DNA oligonucleotides employed were designed to limit degradation to one end of the duplex substrate. DNA was extracted from the repair reactions after incubation with the extracts and its extent of degradation was analyzed. Two different methods were used to assess degradation. The first method of analysis involved testing product lengths in a primer extension assay using a Cy3-labeled primer. The second method made use of oligonucleotides that were Cy3-labeled and incorporated into the DNA duplexes incubated with the extracts. In both cases, products were run on sequencing gels and their intensities analyzed after gel-imaging.

A shift in signal intensity from full-length products to shorter products in A-T nuclear extracts was observed indicating an increase in DNA degradation in these extracts. The addition of purified ATM to A-T nuclear extracts restored full-length product detection. Suppression of degradation in the control extracts and in A-T extracts to which purified ATM was added was ATP-dependent. This suppression of degradation was also inhibited by addition of the PIKK inhibitors wortmannin and caffeine to the extracts. Addition of pre-phosphorylated ATM to an A-T nuclear extract in the presence of PIKK inhibitors was incapable of suppressing degradation. This indicated that kinase activities downstream of ATM transautophosphorylation are required. Taken together, these results denote a role for ATM in enhancing the stability of DNA ends potentially through inhibiting nucleases that play a role in microhomology-dependent repair.

ATM regulates Mre11-dependent DNA end-degradation and microhomology-mediated end joining (Appendix B)

Summary

Observations indicating an increase in DNA double-strand break (DSB) repair via microhomology-mediated end joining (MMEJ) in ATM-deficient (A-T) nuclear extracts signified a role for ATM in suppressing this pathway. Moreover, an increase in DNA end-degradation levels in A-T nuclear extracts suggested that ATM may suppress MMEJ by regulating the function of nucleases involved in this error-prone repair pathway. One potential candidate for suppression was the Mre11 nuclease. This nuclease is a member of the MRN complex that also includes Rad50 and Nbs1 and is involved in pathways of DNA metabolism and cell cycle signaling. The yeast homologue of this complex has been implicated in MMEJ and some biochemical evidence indicates that it is capable of performing MMEJ *in vitro*.

We assessed DNA substrate stability in extracts from kinase-dead-ATM (KD-ATM) expressing cells to examine whether its kinase activities were required for suppression of DNA degradation. We observed elevated degradation levels in extracts expressing this form of ATM. This indicated that phosphorylation reactions mediated by ATM were necessary for enhancing DNA end-stability. The role of the Mre11 nuclease in this process was examined by studying DNA end-stability in Mre11-depleted nuclear extracts and in extracts treated with the Mre11 nuclease inhibitor, Mirin. In both cases, we detected a decrease in DNA degradation levels in both control and A-T extracts. Knockdown of Mre11 levels also resulted in enhanced DNA end-stability in nuclear

extracts. To study MMEJ and explore the roles of ATM and Mre11 in this pathway, we used an *in vivo* reporter assay system. This system makes use of a mutant EGFP gene harboring an insertion comprised of an I-*Sce*I megaendonuclease recognition site flanked by two microhomologies. Repair of the linearized mutant EGFP gene by MMEJ results in EGFP expression that can be scored in tested cells by flow cytometry. Use of this system revealed increased MMEJ levels in A-T cells over controls. This is consistent with our previously reported data from *in vitro* assays performed in nuclear extracts. We also detected a decreased level of MMEJ repair in Mre11-knockdown cells and in those treated with Mirin. These results indicate that the Mre11 nuclease plays a role in MMEJ in mammalian cells and that ATM has a regulatory function in the control of error-prone DSB repair and preservation of DNA end-stability at a break.

Conclusions

The studies presented in this work denote a regulatory role for ATM in enhancing DNA end-stability and suppressing error-prone microhomology-mediated end joining (MMEJ). We observed an increase in DNA degradation in ATM-deficient extracts signifying that ATM is involved in inhibiting nucleases that mediate degradation. Then, we examined the role of the Mre11 nuclease in the degradation phenomenon seen in A-T extracts and found that it indeed mediates these reactions. Examining MMEJ *in vivo* revealed that ATM suppresses this pathway and that the Mre11 nuclease contributes a major role to error-prone repair via MMEJ.

Kinase activities mediated by ATM were required for suppression of DNA degradation. This indicates that phosphorylation events of downstream targets are necessary to enhance the stability of DNA ends. The MRN complex itself is a target of ATM phosphorylation. ATM is known to directly phosphorylate Nbs1 in response to DNA damage (131, 132) and ATM-dependent phosphorylation of Mre11 (133) and Rad50 (134) has also been described. It would be interesting to express mutated forms of the MRN complex whereby the phosphorylation sites specific to ATM are substituted with either a non-phosphorylatable residue (alanine) or a phosphomimic (aspartate). Nuclear extracts from cells expressing mutated MRN can then be analyzed for DNA substrate degradation. DNA end-degradation is expected to increase when expressing the form of MRN that cannot be phosphorylated by ATM if regulation of the Mre11 nuclease is by direct phosphorylation. On the other hand, expression of the phosphomimics would lead to a decrease in the extent of degradation. Cells expressing these mutated forms of MRN can also be analyzed for their MMEJ capacity using the reporter system described in this dissertation (Appendix B).

Other mediators that are downstream of ATM activation may be involved in this regulation; potential candidates include the Chk2 kinase. This kinase is typically activated by ATM and mediates downstream phosphorylation of DNA repair and cell cycle components. Therefore, studies examining the role of Chk2 in suppression of degradation would be useful. Other kinases that may be involved include Chk1, ATR and DNA-PKcs. Participants in repair that have DNA-binding activities and could also play a role include Ku70, Ku80 and BRCA1. Examining extracts deficient for these mediators

may help elaborate the model presented in this dissertation (Appendix B) for enhancing DNA end-stability and suppressing MMEJ.

On the other hand, the role of MRN and other nucleases in MMEJ requires further examination. We observed a decrease in degradation and MMEJ levels when Mre11 was deficient or when its nuclease activity was inhibited. This was true for both 5' and 3'-end degradation. Mre11 is primarily a 3' exonuclease on recessed strands and an endonuclease on hairpin loops. Therefore, the 5'-end degradation that we observed to be Mre11-dependent in our extracts may be carried out by Mre11 itself or by an accessory nuclease. A potential explanation for how Mre11 may degrade the 5'-ends is that this reaction proceeds via its endonuclease activity on secondary structures generated during incubation of the duplex substrates with the extracts. Other nucleases that may be involved include Exo1, Fen1, CtIP, Artemis and ERCC1-XPF. The roles played by these nucleases can be assessed using approaches similar to the ones we employed to study Mre11. Whether the degradation reaction proceeds in an exonucleolytic or endonucleolytic manner on the different strands in our extracts could not be deduced from the degradation products obtained. Patterns of degradation-product separation imply that more than a single type of activity is involved. It would be interesting to examine whether the initiating event proceeds in a particular manner. This can be tested by employing phosphorothioate linkages to the nuclease-susceptible ends examined in this dissertation. Therefore by blocking, one at a time, the 3' and the 5'-ends from nuclease-mediated degradation, we can probably learn more about the initiating event. If degradation starts in an exonucleolytic manner then it will not ensue if the required end is

blocked. On the other hand, endonucleolytic activities that occur beyond the blocked end should go unperturbed.

The dependence on microhomologies in the degradation phenomenon detected in the A-T extracts is another aspect that can be further explored. The degradation of labeled DNA substrates in the presence of a none-labeled competitor harboring short sequences homologous to sequences in the labeled substrate (i.e. microhomologies) can be tested. The effects of the sequence nature and the lengths of these microhomologies on degradation can then be tested. Very little is known about the mechanistic basis of MMEJ and consequently such studies would be very useful.

Another facet of MMEJ that requires further investigation is the effect of the cell cycle on its regulation. NHEJ is known to predominate during G0/G_1 (91), while recombination repair is believed to prevail during G2/S (92, 93). No comparable studies have been conducted for MMEJ and it would be interesting to monitor MMEJ levels in cells that are synchronized to particular stages of the cell cycle. Furthermore, the role of ATM in repressing this pathway across these various stages is also of interest.

To conclude, ataxia telangiectasia is first and foremost a neurodegenerative disorder; however, the molecular basis of this degeneration remains elusive. The uncontrolled error-prone repair that ensues in the absence of intact ATM and discussed herein may be one of the underlying pathobiological mechanisms resulting in neuronal cell loss in A-T. Neurons are non-dividing cells and consequently the fidelity of repair processes may be particularly important in these cells. Multiple lines of evidence indicate that the cerebellar Purkinje cells, the neurons lost in A-T, are highly susceptible to

oxidative stress (174-176). Oxidative DNA damage is known to include DSBs and this may explain the absolute requirement for intact ATM function in these cells. Applying the experimental approaches used in this dissertation to neuronal cells would probably bring us closer to understanding the mechanisms behind neurodegeneration in A-T as well as in other neurodegenerative disorders.

REFERENCES

[1] Peterson CL and Cote J. Cellular machineries for chromosomal DNA repair, Genes Dev. 18 (2004) 602-616.

[2] Riches LC, Lynch AMGooderham NJ. Early events in the mammalian response to DNA double-strand breaks, Mutagenesis. 23 (2008) 331-339.

[3] van Gent DC, Hoeijmakers JHKanaar R. Chromosomal stability and the DNA double-stranded break connection, Nat Rev Genet. 2 (2001) 196-206.

[4] Lavin MF, Delia DChessa L. ATM and the DNA damage response. Workshop on ataxia-telangiectasia and related syndromes, EMBO Rep. 7 (2006) 154-160.

[5] McKinnon PJ. ATM and ataxia telangiectasia, EMBO Rep. 5 (2004) 772-776.

[6] Meyn MS. Ataxia-telangiectasia, cancer and the pathobiology of the ATM gene, Clin Genet. 55 (1999) 289-304.

[7] Boder E and Sedgwick RP. Ataxia-telangiectasia. (Clinical and immunological aspects), Psychiatr Neurol Med Psychol Beih. 13-14 (1970) 8-16.

[8] Taylor AM and Byrd PJ. Molecular pathology of ataxia telangiectasia, J Clin Pathol. 58 (2005) 1009-1015.

[9] Crawford TO. Ataxia telangiectasia, Semin Pediatr Neurol. 5 (1998) 287-294.

[10] Boder E and Sedgwick RP. Ataxia-telangiectasia; a familial syndrome of progressive cerebellar ataxia, oculocutaneous telangiectasia and frequent pulmonary infection, Pediatrics. 21 (1958) 526-554.

[11] Gatti RA, Becker-Catania S, Chun HH, Sun X, Mitui M, Lai CH, Khanlou N, Babaei M, Cheng R, Clark C, Huo Y, Udar NCIyer RK. The pathogenesis of ataxia-telangiectasia. Learning from a Rosetta Stone, Clin Rev Allergy Immunol. 20 (2001) 87-108.

[12] Ammann AJ, Cain WA, Ishizaka K, Hong RGood RA. Immunoglobulin E deficiency in ataxia-telangiectasia, N Engl J Med. 281 (1969) 469-472.

[13] Oxelius VA, Berkel AIHanson LA. IgG2 deficiency in ataxia-telangiectasia, N Engl J Med. 306 (1982) 515-517.

[14] Rivat-Peran L, Buriot D, Salier JP, Rivat C, Dumitresco SMGriscelli C. Immunoglobulins in ataxia-telangiectasia: evidence for IgG4 and IgA2 subclass deficiencies, Clin Immunol Immunopathol. 20 (1981) 99-110.

[15] Gatti RA, Bick M, Tam CF, Medici MA, Oxelius VA, Holland M, Goldstein ALBoder E. Ataxia-Telangiectasia: a multiparameter analysis of eight families, Clin Immunol Immunopathol. 23 (1982) 501-516.

[16] Frappart PO and McKinnon PJ. Ataxia-telangiectasia and related diseases, Neuromolecular Med. 8 (2006) 495-511.

[17] Gumy-Pause F, Wacker PSappino AP. ATM gene and lymphoid malignancies, Leukemia. 18 (2004) 238-242.

[18] Lefton-Greif MA, Crawford TO, Winkelstein JA, Loughlin GM, Koerner CB, Zahurak MLederman HM. Oropharyngeal dysphagia and aspiration in patients with ataxia-telangiectasia, J Pediatr. 136 (2000) 225-231.

[19] Nowak-Wegrzyn A, Crawford TO, Winkelstein JA, Carson KALederman HM. Immunodeficiency and infections in ataxia-telangiectasia, J Pediatr. 144 (2004) 505-511.

[20] Swift M, Morrell D, Massey RBChase CL. Incidence of cancer in 161 families affected by ataxia-telangiectasia, N Engl J Med. 325 (1991) 1831-1836.

[21] Olsen JH, Hahnemann JM, Borresen-Dale AL, Brondum-Nielsen K, Hammarstrom L, Kleinerman R, Kaariainen H, Lonnqvist T, Sankila R, Seersholm N, Tretli S, Yuen J, Boice JD, Jr.Tucker M. Cancer in patients with ataxia-telangiectasia and in their relatives in the nordic countries, J Natl Cancer Inst. 93 (2001) 121-127.

[22] Geoffroy-Perez B, Janin N, Ossian K, Lauge A, Stoppa-Lyonnet DAndrieu N. Variation in breast cancer risk of heterozygotes for ataxia-telangiectasia according to environmental factors, Int J Cancer. 99 (2002) 619-623.

[23] Concannon P. ATM heterozygosity and cancer risk, Nat Genet. 32 (2002) 89-90.

[24] Swift M, Morrell D, Cromartie E, Chamberlin AR, Skolnick MHBishop DT. The incidence and gene frequency of ataxia-telangiectasia in the United States, Am J Hum Genet. 39 (1986) 573-583.

[25] Platzer M, Rotman G, Bauer D, Uziel T, Savitsky K, Bar-Shira A, Gilad S, Shiloh YRosenthal A. Ataxia-telangiectasia locus: sequence analysis of 184 kb of human genomic DNA containing the entire ATM gene, Genome Res. 7 (1997) 592-605.

[26] Savitsky K, Platzer M, Uziel T, Gilad S, Sartiel A, Rosenthal A, Elroy-Stein O, Shiloh YRotman G. Ataxia-telangiectasia: structural diversity of untranslated sequences suggests complex post-transcriptional regulation of ATM gene expression, Nucleic Acids Res. 25 (1997) 1678-1684.

[27] Uziel T, Savitsky K, Platzer M, Ziv Y, Helbitz T, Nehls M, Boehm T, Rosenthal A, Shiloh YRotman G. Genomic Organization of the ATM gene, Genomics. 33 (1996) 317-320.

[28] Lakin ND, Weber P, Stankovic T, Rottinghaus ST, Taylor AMJackson SP. Analysis of the ATM protein in wild-type and ataxia telangiectasia cells, Oncogene. 13 (1996) 2707-2716.

[29] Butch AW, Chun HH, Nahas SAGatti RA. Immunoassay to measure ataxia-telangiectasia mutated protein in cellular lysates, Clin Chem. 50 (2004) 2302-2308.

[30] Chun HH, Sun X, Nahas SA, Teraoka S, Lai CH, Concannon PGatti RA. Improved diagnostic testing for ataxia-telangiectasia by immunoblotting of nuclear lysates for ATM protein expression, Mol Genet Metab. 80 (2003) 437-443.

[31] Stankovic T, Kidd AM, Sutcliffe A, McGuire GM, Robinson P, Weber P, Bedenham T, Bradwell AR, Easton DF, Lennox GG, Haites N, Byrd PJTaylor AM. ATM mutations and phenotypes in ataxia-telangiectasia families in the British Isles: expression of mutant ATM and the risk of leukemia, lymphoma, and breast cancer, Am J Hum Genet. 62 (1998) 334-345.

[32] Telatar M, Wang S, Castellvi-Bel S, Tai LQ, Sheikhavandi S, Regueiro JR, Porras OGatti RA. A model for ATM heterozygote identification in a large population: four founder-effect ATM mutations identify most of Costa Rican patients with ataxia telangiectasia, Mol Genet Metab. 64 (1998) 36-43.

[33] Li A and Swift M. Mutations at the ataxia-telangiectasia locus and clinical phenotypes of A-T patients, Am J Med Genet. 92 (2000) 170-177.

[34] Buzin CH, Gatti RA, Nguyen VQ, Wen CY, Mitui M, Sanal O, Chen JS, Nozari G, Mengos A, Li X, Fujimura FSommer SS. Comprehensive scanning of the ATM gene with DOVAM-S, Hum Mutat. 21 (2003) 123-131.

[35] Telatar M, Wang Z, Udar N, Liang T, Bernatowska-Matuszkiewicz E, Lavin M, Shiloh Y, Concannon P, Good RAGatti RA. Ataxia-telangiectasia: mutations in ATM cDNA detected by protein-truncation screening, Am J Hum Genet. 59 (1996) 40-44.

[36] Sandoval N, Platzer M, Rosenthal A, Dork T, Bendix R, Skawran B, Stuhrmann M, Wegner RD, Sperling K, Banin S, Shiloh Y, Baumer A, Bernthaler U, Sennefelder H,

Brohm M, Weber BHSchindler D. Characterization of ATM gene mutations in 66 ataxia telangiectasia families, Hum Mol Genet. 8 (1999) 69-79.

[37] Shiloh Y. ATM and related protein kinases: safeguarding genome integrity, Nat Rev Cancer. 3 (2003) 155-168.

[38] McMahon SB, Van Buskirk HA, Dugan KA, Copeland TDCole MD. The novel ATM-related protein TRRAP is an essential cofactor for the c-Myc and E2F oncoproteins, Cell. 94 (1998) 363-374.

[39] Bakkenist CJ and Kastan MB. DNA damage activates ATM through intermolecular autophosphorylation and dimer dissociation, Nature. 421 (2003) 499-506.

[40] Kozlov SV, Graham ME, Peng C, Chen P, Robinson PJLavin MF. Involvement of novel autophosphorylation sites in ATM activation, Embo J. 25 (2006) 3504-3514.

[41] Daniel JA, Pellegrini M, Lee JH, Paull TT, Feigenbaum LNussenzweig A. Multiple autophosphorylation sites are dispensable for murine ATM activation in vivo, J Cell Biol. 183 (2008) 777-783.

[42] Ali A, Zhang J, Bao S, Liu I, Otterness D, Dean NM, Abraham RTWang XF. Requirement of protein phosphatase 5 in DNA-damage-induced ATM activation, Genes Dev. 18 (2004) 249-254.

[43] Goodarzi AA, Jonnalagadda JC, Douglas P, Young D, Ye R, Moorhead GB, Lees-Miller SPKhanna KK. Autophosphorylation of ataxia-telangiectasia mutated is regulated by protein phosphatase 2A, Embo J. 23 (2004) 4451-4461.

[44] Sun Y, Xu Y, Roy KPrice BD. DNA damage-induced acetylation of lysine 3016 of ATM activates ATM kinase activity, Mol Cell Biol. 27 (2007) 8502-8509.

[45] Sun Y, Jiang X, Chen S, Fernandes NPrice BD. A role for the Tip60 histone acetyltransferase in the acetylation and activation of ATM, Proc Natl Acad Sci U S A. 102 (2005) 13182-13187.

[46] Kim YC, Gerlitz G, Furusawa T, Catez F, Nussenzweig A, Oh KS, Kraemer KH, Shiloh YBustin M. Activation of ATM depends on chromatin interactions occurring before induction of DNA damage, Nat Cell Biol. 11 (2009) 92-96.

[47] Earnshaw WC and Laemmli UK. Architecture of metaphase chromosomes and chromosome scaffolds, J Cell Biol. 96 (1983) 84-93.

[48] Jeppesen P, Mitchell A, Turner BPerry P. Antibodies to defined histone epitopes reveal variations in chromatin conformation and underacetylation of centric heterochromatin in human metaphase chromosomes, Chromosoma. 101 (1992) 322-332.

[49] Falck J, Coates JJackson SP. Conserved modes of recruitment of ATM, ATR and DNA-PKcs to sites of DNA damage, Nature. 434 (2005) 605-611.

[50] Cerosaletti K, Wright JConcannon P. Active role for nibrin in the kinetics of atm activation, Mol Cell Biol. 26 (2006) 1691-1699.

[51] Nelms BE, Maser RS, MacKay JF, Lagally MGPetrini JH. In situ visualization of DNA double-strand break repair in human fibroblasts, Science. 280 (1998) 590-592.

[52] Uziel T, Lerenthal Y, Moyal L, Andegeko Y, Mittelman LShiloh Y. Requirement of the MRN complex for ATM activation by DNA damage, Embo J. 22 (2003) 5612-5621.

[53] Cerosaletti K and Concannon P. Independent roles for nibrin and Mre11-Rad50 in the activation and function of Atm, J Biol Chem. 279 (2004) 38813-38819.

[54] Lee JH and Paull TT. ATM activation by DNA double-strand breaks through the Mre11-Rad50-Nbs1 complex, Science. 308 (2005) 551-554.

[55] Costanzo V, Paull T, Gottesman MGautier J. Mre11 assembles linear DNA fragments into DNA damage signaling complexes, PLoS Biol. 2 (2004) E110.

[56] Petrini JH and Stracker TH. The cellular response to DNA double-strand breaks: defining the sensors and mediators, Trends Cell Biol. 13 (2003) 458-462.

[57] Kim JE, Minter-Dykhouse KChen J. Signaling networks controlled by the MRN complex and MDC1 during early DNA damage responses, Mol Carcinog. 45 (2006) 403-408.

[58] McKinnon PJ. Ataxia-telangiectasia: an inherited disorder of ionizing-radiation sensitivity in man. Progress in the elucidation of the underlying biochemical defect, Hum Genet. 75 (1987) 197-208.

[59] Shiloh Y, Tabor EBecker Y. Abnormal response of ataxia-telangiectasia cells to agents that break the deoxyribose moiety of DNA via a targeted free radical mechanism, Carcinogenesis. 4 (1983) 1317-1322.

[60] Shiloh Y, Tabor EBecker Y. Cells from patients with ataxia telangiectasia are abnormally sensitive to the cytotoxic effect of a tumor promoter, phorbol-12-myristate-13-acetate, Mutat Res. 149 (1985) 283-286.

[61] de Wit J, Jaspers NGBootsma D. The rate of DNA synthesis in normal human and ataxia telangiectasia cells after exposure to X-irradiation, Mutat Res. 80 (1981) 221-226.

[62] Lehmann AR, Kirk-Bell S, Arlett CF, Harcourt SA, de Weerd-Kastelein EA, Keijzer WHall-Smith P. Repair of ultraviolet light damage in a variety of human fibroblast cell strains, Cancer Res. 37 (1977) 904-910.

[63] Keyse SM, McAleer MA, Davies DJMoss SH. The response of normal and ataxia-telangiectasia human fibroblasts to the lethal effects of far, mid and near ultraviolet radiations, Int J Radiat Biol Relat Stud Phys Chem Med. 48 (1985) 975-985.

[64] Smith PJ and Paterson MC. Abnormal responses to mid-ultraviolet light of cultured fibroblasts from patients with disorders featuring sunlight sensitivity, Cancer Res. 41 (1981) 511-518.

[65] Bredemeyer AL, Sharma GG, Huang CY, Helmink BA, Walker LM, Khor KC, Nuskey B, Sullivan KE, Pandita TK, Bassing CHSleckman BP. ATM stabilizes DNA double-strand-break complexes during V(D)J recombination, Nature. 442 (2006) 466-470.

[66] Higurashi M and Conen PE. In vitro chromosomal radiosensitivity in patients and in carriers with abnormal non-Down's syndrome karyotypes, Pediatr Res. 6 (1972) 514-520.

[67] Cohen MM and Simpson SJ. Increased clastogenicity and decreased inhibition of DNA synthesis by neocarzinostatin and tallysomycin in ataxia telangiectasia lymphoid cells, Mutat Res. 112 (1983) 119-128.

[68] Kaufmann WK and Wilson SJ. G1 arrest and cell-cycle-dependent clastogenesis in UV-irradiated human fibroblasts, Mutat Res. 314 (1994) 67-76.

[69] Vaziri H, West MD, Allsopp RC, Davison TS, Wu YS, Arrowsmith CH, Poirier GGBenchimol S. ATM-dependent telomere loss in aging human diploid fibroblasts and DNA damage lead to the post-translational activation of p53 protein involving poly(ADP-ribose) polymerase, Embo J. 16 (1997) 6018-6033.

[70] Wu Y, Xiao SZhu XD. MRE11-RAD50-NBS1 and ATM function as co-mediators of TRF1 in telomere length control, Nat Struct Mol Biol. 14 (2007) 832-840.

[71] Rotman G and Shiloh Y. ATM: from gene to function, Hum Mol Genet. 7 (1998) 1555-1563.

[72] Beamish H, Williams R, Chen PLavin MF. Defect in multiple cell cycle checkpoints in ataxia-telangiectasia postirradiation, J Biol Chem. 271 (1996) 20486-20493.

[73] Smith E, Dejsuphong D, Balestrini A, Hampel M, Lenz C, Takeda S, Vindigni ACostanzo V. An ATM- and ATR-dependent checkpoint inactivates spindle assembly by targeting CEP63, Nat Cell Biol. 11 (2009) 278-285.

[74] Abraham RT. Cell cycle checkpoint signaling through the ATM and ATR kinases, Genes Dev. 15 (2001) 2177-2196.

[75] Lavin MF and Kozlov S. ATM activation and DNA damage response, Cell Cycle. 6 (2007) 931-942.

[76] Meulmeester E, Pereg Y, Shiloh YJochemsen AG. ATM-mediated phosphorylations inhibit Mdmx/Mdm2 stabilization by HAUSP in favor of p53 activation, Cell Cycle. 4 (2005) 1166-1170.

[77] Israels ED and Israels LG. The cell cycle, Stem Cells. 19 (2001) 88-91.

[78] Falck J, Mailand N, Syljuasen RG, Bartek JLukas J. The ATM-Chk2-Cdc25A checkpoint pathway guards against radioresistant DNA synthesis, Nature. 410 (2001) 842-847.

[79] Kitagawa R, Bakkenist CJ, McKinnon PJKastan MB. Phosphorylation of SMC1 is a critical downstream event in the ATM-NBS1-BRCA1 pathway, Genes Dev. 18 (2004) 1423-1438.

[80] Stark GR and Taylor WR. Control of the G2/M transition, Mol Biotechnol. 32 (2006) 227-248.

[81] Oricchio E, Saladino C, Iacovelli S, Soddu SCundari E. ATM is activated by default in mitosis, localizes at centrosomes and monitors mitotic spindle integrity, Cell Cycle. 5 (2006) 88-92.

[82] Nakamura M, Zhou XZ, Kishi S, Kosugi I, Tsutsui YLu KP. A specific interaction between the telomeric protein Pin2/TRF1 and the mitotic spindle, Curr Biol. 11 (2001) 1512-1516.

[83] Jullien D, Vagnarelli P, Earnshaw WCAdachi Y. Kinetochore localisation of the DNA damage response component 53BP1 during mitosis, J Cell Sci. 115 (2002) 71-79.

[84] Fleck O and Nielsen O. DNA repair, J Cell Sci. 117 (2004) 515-517.

[85] DiBiase SJ, Zeng ZC, Chen R, Hyslop T, Curran WJ, Jr.Iliakis G. DNA-dependent protein kinase stimulates an independently active, nonhomologous, end-joining apparatus, Cancer Res. 60 (2000) 1245-1253.

[86] Feldmann E, Schmiemann V, Goedecke W, Reichenberger SPfeiffer P. DNA double-strand break repair in cell-free extracts from Ku80-deficient cells: implications for Ku serving as an alignment factor in non-homologous DNA end joining, Nucleic Acids Res. 28 (2000) 2585-2596.

[87] Guirouilh-Barbat J, Huck S, Bertrand P, Pirzio L, Desmaze C, Sabatier LLopez BS. Impact of the KU80 pathway on NHEJ-induced genome rearrangements in mammalian cells, Mol Cell. 14 (2004) 611-623.

[88] Liang F and Jasin M. Ku80-deficient cells exhibit excess degradation of extrachromosomal DNA, J Biol Chem. 271 (1996) 14405-14411.

[89] Wu W, Wang M, Wu W, Singh SK, Mussfeldt TIliakis G. Repair of radiation induced DNA double strand breaks by backup NHEJ is enhanced in G2, DNA Repair (Amst). 7 (2008) 329-338.

[90] Zhu C, Mills KD, Ferguson DO, Lee C, Manis J, Fleming J, Gao Y, Morton CCAlt FW. Unrepaired DNA breaks in p53-deficient cells lead to oncogenic gene amplification subsequent to translocations, Cell. 109 (2002) 811-821.

[91] Takata M, Sasaki MS, Sonoda E, Morrison C, Hashimoto M, Utsumi H, Yamaguchi-Iwai Y, Shinohara ATakeda S. Homologous recombination and non-homologous end-joining pathways of DNA double-strand break repair have overlapping roles in the maintenance of chromosomal integrity in vertebrate cells, Embo J. 17 (1998) 5497-5508.

[92] Wyman C, Warmerdam DOKanaar R. From DNA end chemistry to cell-cycle response: the importance of structure, even when it's broken, Mol Cell. 30 (2008) 5-6.

[93] Saleh-Gohari N and Helleday T. Conservative homologous recombination preferentially repairs DNA double-strand breaks in the S phase of the cell cycle in human cells, Nucleic Acids Res. 32 (2004) 3683-3688.

[94] Paques F and Haber JE. Multiple pathways of recombination induced by double-strand breaks in Saccharomyces cerevisiae, Microbiol Mol Biol Rev. 63 (1999) 349-404.

[95] Paques F, Leung WYHaber JE. Expansions and contractions in a tandem repeat induced by double-strand break repair, Mol Cell Biol. 18 (1998) 2045-2054.

[96] Krogh BO and Symington LS. Recombination proteins in yeast, Annu Rev Genet. 38 (2004) 233-271.

[97] Keeney S, Giroux CNKleckner N. Meiosis-specific DNA double-strand breaks are catalyzed by Spo11, a member of a widely conserved protein family, Cell. 88 (1997) 375-384.

[98] Keeney S. Mechanism and control of meiotic recombination initiation, Curr Top Dev Biol. 52 (2001) 1-53.

[99] Llorente B and Symington LS. The Mre11 nuclease is not required for 5' to 3' resection at multiple HO-induced double-strand breaks, Mol Cell Biol. 24 (2004) 9682-9694.

[100] Ivanov EL, Sugawara N, White CI, Fabre FHaber JE. Mutations in XRS2 and RAD50 delay but do not prevent mating-type switching in Saccharomyces cerevisiae, Mol Cell Biol. 14 (1994) 3414-3425.

[101] Tsubouchi H and Ogawa H. A novel mre11 mutation impairs processing of double-strand breaks of DNA during both mitosis and meiosis, Mol Cell Biol. 18 (1998) 260-268.

[102] Lengsfeld BM, Rattray AJ, Bhaskara V, Ghirlando RPaull TT. Sae2 is an endonuclease that processes hairpin DNA cooperatively with the Mre11/Rad50/Xrs2 complex, Mol Cell. 28 (2007) 638-651.

[103] Sartori AA, Lukas C, Coates J, Mistrik M, Fu S, Bartek J, Baer R, Lukas JJackson SP. Human CtIP promotes DNA end resection, Nature. 450 (2007) 509-514.

[104] Nimonkar AV, Ozsoy AZ, Genschel J, Modrich PKowalczykowski SC. Human exonuclease 1 and BLM helicase interact to resect DNA and initiate DNA repair, Proc Natl Acad Sci U S A. 105 (2008) 16906-16911.

[105] Gravel S, Chapman JR, Magill CJackson SP. DNA helicases Sgs1 and BLM promote DNA double-strand break resection, Genes Dev. 22 (2008) 2767-2772.

[106] Yamada NA, Hinz JM, Kopf VL, Segalle KDThompson LH. XRCC3 ATPase activity is required for normal XRCC3-Rad51C complex dynamics and homologous recombination, J Biol Chem. 279 (2004) 23250-23254.

[107] Venkitaraman AR. Functions of BRCA1 and BRCA2 in the biological response to DNA damage, J Cell Sci. 114 (2001) 3591-3598.

[108] Sugawara N and Haber JE. Characterization of double-strand break-induced recombination: homology requirements and single-stranded DNA formation, Mol Cell Biol. 12 (1992) 563-575.

[109] Kagawa W, Kurumizaka H, Ikawa S, Yokoyama SShibata T. Homologous pairing promoted by the human Rad52 protein, J Biol Chem. 276 (2001) 35201-35208.

[110] Enomoto T. Functions of RecQ family helicases: possible involvement of Bloom's and Werner's syndrome gene products in guarding genome integrity during DNA replication, J Biochem. 129 (2001) 501-507.

[111] Ip SC, Rass U, Blanco MG, Flynn HR, Skehel JMWest SC. Identification of Holliday junction resolvases from humans and yeast, Nature. 456 (2008) 357-361.

[112] Ma Y, Pannicke U, Schwarz KLieber MR. Hairpin opening and overhang processing by an Artemis/DNA-dependent protein kinase complex in nonhomologous end joining and V(D)J recombination, Cell. 108 (2002) 781-794.

[113] Lieber MR. The mechanism of human nonhomologous DNA end joining, J Biol Chem. 283 (2008) 1-5.

[114] McVey M and Lee SE. MMEJ repair of double-strand breaks (director's cut): deleted sequences and alternative endings, Trends Genet. 24 (2008) 529-538.

[115] Corneo B, Wendland RL, Deriano L, Cui X, Klein IA, Wong SY, Arnal S, Holub AJ, Weller GR, Pancake BA, Shah S, Brandt VL, Meek KRoth DB. Rag mutations reveal robust alternative end joining, Nature. 449 (2007) 483-486.

[116] Yan CT, Boboila C, Souza EK, Franco S, Hickernell TR, Murphy M, Gumaste S, Geyer M, Zarrin AA, Manis JP, Rajewsky KAlt FW. IgH class switching and translocations use a robust non-classical end-joining pathway, Nature. 449 (2007) 478-482.

[117] Ma JL, Kim EM, Haber JELee SE. Yeast Mre11 and Rad1 proteins define a Ku-independent mechanism to repair double-strand breaks lacking overlapping end sequences, Mol Cell Biol. 23 (2003) 8820-8828.

[118] Lee K and Lee SE. Saccharomyces cerevisiae Sae2- and Tel1-dependent single-strand DNA formation at DNA break promotes microhomology-mediated end joining, Genetics. 176 (2007) 2003-2014.

[119] Langland G, Elliott J, Li Y, Creaney J, Dixon KGroden J. The BLM helicase is necessary for normal DNA double-strand break repair, Cancer Res. 62 (2002) 2766-2770.

[120] Audebert M, Salles BCalsou P. Involvement of poly(ADP-ribose) polymerase-1 and XRCC1/DNA ligase III in an alternative route for DNA double-strand breaks rejoining, J Biol Chem. 279 (2004) 55117-55126.

[121] Gottlich B, Reichenberger S, Feldmann EPfeiffer P. Rejoining of DNA double-strand breaks in vitro by single-strand annealing, Eur J Biochem. 258 (1998) 387-395.

[122] Decottignies A. Microhomology-mediated end joining in fission yeast is repressed by pku70 and relies on genes involved in homologous recombination, Genetics. 176 (2007) 1403-1415.

[123] Weinstock DM, Elliott BJasin M. A model of oncogenic rearrangements: differences between chromosomal translocation mechanisms and simple double-strand break repair, Blood. 107 (2006) 777-780.

[124] Bentley J, Diggle CP, Harnden P, Knowles MAKiltie AE. DNA double strand break repair in human bladder cancer is error prone and involves microhomology-associated end-joining, Nucleic Acids Res. 32 (2004) 5249-5259.

[125] Yoshimoto M, Joshua AM, Chilton-Macneill S, Bayani J, Selvarajah S, Evans AJ, Zielenska MSquire JA. Three-color FISH analysis of TMPRSS2/ERG fusions in prostate cancer indicates that genomic microdeletion of chromosome 21 is associated with rearrangement, Neoplasia. 8 (2006) 465-469.

[126] Shin KH, Kang MK, Kim RH, Kameta A, Baluda MAPark NH. Abnormal DNA end-joining activity in human head and neck cancer, Int J Mol Med. 17 (2006) 917-924.

[127] Windhofer F, Krause S, Hader C, Schulz WAFlorl AR. Distinctive differences in DNA double-strand break repair between normal urothelial and urothelial carcinoma cells, Mutat Res. 638 (2008) 56-65.

[128] Haber JE. Alternative endings, Proc Natl Acad Sci U S A. 105 (2008) 405-406.

[129] Wang H, Perrault AR, Takeda Y, Qin W, Wang HIliakis G. Biochemical evidence for Ku-independent backup pathways of NHEJ, Nucleic Acids Res. 31 (2003) 5377-5388.

[130] Bennardo N, Cheng A, Huang NStark JM. Alternative-NHEJ is a mechanistically distinct pathway of mammalian chromosome break repair, PLoS Genet. 4 (2008) e1000110.

[131] Lim DS, Kim ST, Xu B, Maser RS, Lin J, Petrini JHKastan MB. ATM phosphorylates p95/nbs1 in an S-phase checkpoint pathway, Nature. 404 (2000) 613-617.

[132] Wu X, Ranganathan V, Weisman DS, Heine WF, Ciccone DN, O'Neill TB, Crick KE, Pierce KA, Lane WS, Rathbun G, Livingston DMWeaver DT. ATM phosphorylation of Nijmegen breakage syndrome protein is required in a DNA damage response, Nature. 405 (2000) 477-482.

[133] Yuan SS, Chang HL, Hou MF, Chan TF, Kao YH, Wu YCSu JH. Neocarzinostatin induces Mre11 phosphorylation and focus formation through an ATM- and NBS1-dependent mechanism, Toxicology. 177 (2002) 123-130.

[134] Linding R, Jensen LJ, Ostheimer GJ, van Vugt MA, Jorgensen C, Miron IM, Diella F, Colwill K, Taylor L, Elder K, Metalnikov P, Nguyen V, Pasculescu A, Jin J, Park JG, Samson LD, Woodgett JR, Russell RB, Bork P, Yaffe MBPawson T. Systematic discovery of in vivo phosphorylation networks, Cell. 129 (2007) 1415-1426.

[135] Gatei M, Scott SP, Filippovitch I, Soronika N, Lavin MF, Weber BKhanna KK. Role for ATM in DNA damage-induced phosphorylation of BRCA1, Cancer Res. 60 (2000) 3299-3304.

[136] Chen G, Yuan SS, Liu W, Xu Y, Trujillo K, Song B, Cong F, Goff SP, Wu Y, Arlinghaus R, Baltimore D, Gasser PJ, Park MS, Sung PLee EY. Radiation-induced assembly of Rad51 and Rad52 recombination complex requires ATM and c-Abl, J Biol Chem. 274 (1999) 12748-12752.

[137] Zhang X, Succi J, Feng Z, Prithivirajsingh S, Story MDLegerski RJ. Artemis is a phosphorylation target of ATM and ATR and is involved in the G2/M DNA damage checkpoint response, Mol Cell Biol. 24 (2004) 9207-9220.

[138] Chen BP, Uematsu N, Kobayashi J, Lerenthal Y, Krempler A, Yajima H, Lobrich M, Shiloh YChen DJ. Ataxia telangiectasia mutated (ATM) is essential for DNA-PKcs phosphorylations at the Thr-2609 cluster upon DNA double strand break, J Biol Chem. 282 (2007) 6582-6587.

[139] Taylor AM, Harnden DG, Arlett CF, Harcourt SA, Lehmann AR, Stevens SBridges BA. Ataxia telangiectasia: a human mutation with abnormal radiation sensitivity, Nature. 258 (1975) 427-429.

[140] Vincent RA, Jr., Sheridan RB, 3rdHuang PC. DNA strained breakage repair in ataxia telangiectasia fibroblast-like cells, Mutat Res. 33 (1975) 357-366.

[141] Paterson MC, Smith BP, Lohman PH, Anderson AKFishman L. Defective excision repair of gamma-ray-damaged DNA in human (ataxia telangiectasia) fibroblasts, Nature. 260 (1976) 444-447.

[142] Lehman AR and Stevens S. The production and repair of double strand breaks in cells from normal humans and from patients with ataxia telangiectasia, Biochim Biophys Acta. 474 (1977) 49-60.

[143] van der Schans GP, Paterson MCCross WG. DNA Strand Break and Rejoining in Cultured Human Fibroblasts Exposed to Fast Neutrons or Gamma Rays, International Journal of Radiation Biology. 44 (1983) 75-85.

[144] Shiloh Y, van der Schans GP, Lohman PHBecker Y. Induction and repair of DNA damage in normal and ataxia-telangiectasia skin fibroblasts treated with neocarzinostatin, Carcinogenesis. 4 (1983) 917-921.

[145] Coquerelle TM, Weibezahn KFLuÃ‚Â’ucke-Huhle C. Rejoining of Double Strand Breaks in Normal Human and Ataxia-telangiectasia Fibroblasts after Exposure to 60 Co γ-rays, 241 Am α-particles or Bleomycin, International Journal of Radiation Biology. 51 (1987) 209-218.

[146] Thierry D, Rigaud O, Duranton I, Moustacchi EMagdelenat H. Quantitative measurement of DNA strand breaks and repair in gamma-irradiated human leukocytes from normal and ataxia telangiectasia donors, Radiat Res. 102 (1985) 347-358.

[147] Foray N, Arlett CFMalaise EP. Dose-rate effect on induction and repair rate of radiation-induced DNA double-strand breaks in a normal and an ataxia telangiectasia human fibroblast cell line, Biochimie. 77 (1995) 900-905.

[148] Foray N, Priestley A, Alsbeih G, Badie C, Capulas EP, Arlett CFMalaise EP. Hypersensitivity of ataxia telangiectasia fibroblasts to ionizing radiation is associated with a repair deficiency of DNA double-strand breaks, Int J Radiat Biol. 72 (1997) 271-283.

[149] Blocher D, Sigut DHannan MA. Fibroblasts from ataxia telangiectasia (AT) and AT heterozygotes show an enhanced level of residual DNA double-strand breaks after low dose-rate gamma-irradiation as assayed by pulsed field gel electrophoresis, Int J Radiat Biol. 60 (1991) 791-802.

[150] Taylor AM. Unrepaired DNA strand breaks in irradiated ataxia telangiectasia lymphocytes suggested from cytogenetic observations, Mutat Res. 50 (1978) 407-418.

[151] Cornforth MN and Bedford JS. On the nature of a defect in cells from individuals with ataxia-telangiectasia, Science. 227 (1985) 1589-1591.

[152] Kuhne M, Riballo E, Rief N, Rothkamm K, Jeggo PALobrich M. A double-strand break repair defect in ATM-deficient cells contributes to radiosensitivity, Cancer Res. 64 (2004) 500-508.

[153] Jeggo PA and Lobrich M. Artemis links ATM to double strand break rejoining, Cell Cycle. 4 (2005) 359-362.

[154] Cox R, Debenham PG, Masson WKWebb MB. Ataxia-telangiectasia: a human mutation giving high-frequency misrepair of DNA double-stranded scissions, Mol Biol Med. 3 (1986) 229-244.

[155] Powell S, Whitaker S, Peacock JMcMillan T. Ataxia telangiectasia: an investigation of the repair defect in the cell line AT5BIVA by plasmid reconstitution, Mutat Res. 294 (1993) 9-20.

[156] Dar ME, Winters TAJorgensen TJ. Identification of defective illegitimate recombinational repair of oxidatively-induced DNA double-strand breaks in ataxia-telangiectasia cells, Mutat Res. 384 (1997) 169-179.

[157] Li Y, Carty MP, Oakley GG, Seidman MM, Medvedovic MDixon K. Expression of ATM in ataxia telangiectasia fibroblasts rescues defects in DNA double-strand break repair in nuclear extracts, Environ Mol Mutagen. 37 (2001) 128-140.

[158] Paull TT and Gellert M. The 3' to 5' exonuclease activity of Mre 11 facilitates repair of DNA double-strand breaks, Mol Cell. 1 (1998) 969-979.

[159] Abraham RT and Tibbetts RS. Cell biology. Guiding ATM to broken DNA, Science. 308 (2005) 510-511.

[160] Davidson AL. Structural biology. Not just another ABC transporter, Science. 296 (2002) 1038-1040.

[161] Yamaguchi-Iwai Y, Sonoda E, Sasaki MS, Morrison C, Haraguchi T, Hiraoka Y, Yamashita YM, Yagi T, Takata M, Price C, Kakazu NTakeda S. Mre11 is essential for the maintenance of chromosomal DNA in vertebrate cells, Embo J. 18 (1999) 6619-6629.

[162] Luo G, Yao MS, Bender CF, Mills M, Bladl AR, Bradley APetrini JH. Disruption of mRad50 causes embryonic stem cell lethality, abnormal embryonic development, and sensitivity to ionizing radiation, Proc Natl Acad Sci U S A. 96 (1999) 7376-7381.

[163] Xiao Y and Weaver DT. Conditional gene targeted deletion by Cre recombinase demonstrates the requirement for the double-strand break repair Mre11 protein in murine embryonic stem cells, Nucleic Acids Res. 25 (1997) 2985-2991.

[164] Stracker TH, Theunissen JW, Morales MPetrini JH. The Mre11 complex and the metabolism of chromosome breaks: the importance of communicating and holding things together, DNA Repair (Amst). 3 (2004) 845-854.

[165] Takeda S, Nakamura K, Taniguchi YPaull TT. Ctp1/CtIP and the MRN complex collaborate in the initial steps of homologous recombination, Mol Cell. 28 (2007) 351-352.

[166] Neale MJ, Pan JKeeney S. Endonucleolytic processing of covalent protein-linked DNA double-strand breaks, Nature. 436 (2005) 1053-1057.

[167] Hopfner KP, Karcher A, Craig L, Woo TT, Carney JPTainer JA. Structural biochemistry and interaction architecture of the DNA double-strand break repair Mre11 nuclease and Rad50-ATPase, Cell. 105 (2001) 473-485.

[168] Hopfner KP and Tainer JA. Rad50/SMC proteins and ABC transporters: unifying concepts from high-resolution structures, Curr Opin Struct Biol. 13 (2003) 249-255.

[169] Symington LS. Role of RAD52 epistasis group genes in homologous recombination and double-strand break repair, Microbiol Mol Biol Rev. 66 (2002) 630-670, table of contents.

[170] Bhaskara V, Dupre A, Lengsfeld B, Hopkins BB, Chan A, Lee JH, Zhang X, Gautier J, Zakian VPaull TT. Rad50 adenylate kinase activity regulates DNA tethering by Mre11/Rad50 complexes, Mol Cell. 25 (2007) 647-661.

[171] Paull TT and Gellert M. Nbs1 potentiates ATP-driven DNA unwinding and endonuclease cleavage by the Mre11/Rad50 complex, Genes Dev. 13 (1999) 1276-1288.

[172] Paull TT and Gellert M. A mechanistic basis for Mre11-directed DNA joining at microhomologies, Proc Natl Acad Sci U S A. 97 (2000) 6409-6414.

[173] Williams RS, Moncalian G, Williams JS, Yamada Y, Limbo O, Shin DS, Groocock LM, Cahill D, Hitomi C, Guenther G, Moiani D, Carney JP, Russell PTainer JA. Mre11 dimers coordinate DNA end bridging and nuclease processing in double-strand-break repair, Cell. 135 (2008) 97-109.

[174] Chen P, Peng C, Luff J, Spring K, Watters D, Bottle S, Furuya SLavin MF. Oxidative stress is responsible for deficient survival and dendritogenesis in purkinje neurons from ataxia-telangiectasia mutated mutant mice, J Neurosci. 23 (2003) 11453-11460.

[175] Reichenbach J, Schubert R, Schindler D, Muller K, Bohles HZielen S. Elevated oxidative stress in patients with ataxia telangiectasia, Antioxid Redox Signal. 4 (2002) 465-469.

[176] Rotman G and Shiloh Y. The ATM gene and protein: possible roles in genome surveillance, checkpoint controls and cellular defence against oxidative stress, Cancer Surv. 29 (1997) 285-304.

[177] You Z, Chahwan C, Bailis J, Hunter TRussell P. ATM activation and its recruitment to damaged DNA require binding to the C terminus of Nbs1, Mol Cell Biol. 25 (2005) 5363-5379.

[178] Rahal EA, Henricksen LA, Li Y, Turchi JJ, Pawelczak KSDixon K. ATM mediates repression of DNA end-degradation in an ATP-dependent manner, DNA Repair (Amst). 7 (2008) 464-475.

[179] Canman CE, Lim DS, Cimprich KA, Taya Y, Tamai K, Sakaguchi K, Appella E, Kastan MBSiliciano JD. Activation of the ATM kinase by ionizing radiation and phosphorylation of p53, Science. 281 (1998) 1677-1679.

[180] Lee JH and Paull TT. Direct activation of the ATM protein kinase by the Mre11/Rad50/Nbs1 complex, Science. 304 (2004) 93-96.

[181] van den Bosch M, Bree RTLowndes NF. The MRN complex: coordinating and mediating the response to broken chromosomes, EMBO Rep. 4 (2003) 844-849.

[182] Garner KM, Pletnev AAEastman A. Corrected structure of mirin, a small-molecule inhibitor of the Mre11-Rad50-Nbs1 complex, Nat Chem Biol. 5 (2009) 129-130; author reply 130.

[183] Dupre A, Boyer-Chatenet L, Sattler RM, Modi AP, Lee JH, Nicolette ML, Kopelovich L, Jasin M, Baer R, Paull TTGautier J. A forward chemical genetic screen reveals an inhibitor of the Mre11-Rad50-Nbs1 complex, Nat Chem Biol. 4 (2008) 119-125.

[184] Guirouilh-Barbat J, Rass E, Plo I, Bertrand PLopez BS. Defects in XRCC4 and KU80 differentially affect the joining of distal nonhomologous ends, Proc Natl Acad Sci U S A. 104 (2007) 20902-20907.

[185] Soulas-Sprauel P, Le Guyader G, Rivera-Munoz P, Abramowski V, Olivier-Martin C, Goujet-Zalc C, Charneau Pde Villartay JP. Role for DNA repair factor XRCC4 in immunoglobulin class switch recombination, J Exp Med. 204 (2007) 1717-1727.

APPENDIX A: ATM MEDIATES REPRESSION OF DNA END-DEGRADATION IN AN ATP-DEPENDENT MANNER

ATM Mediates Repression of DNA End-Degradation in an ATP-Dependent Manner

Elias A. Rahal[a], Leigh A. Henricksen[a], Yuling Li[b†], John J. Turchi[c,d], Katherine S. Pawelczak[d], and Kathleen Dixon[a,e*]

[a]*Department of Molecular & Cellular Biology ,University of Arizona, Tucson, AZ 85721, USA.*

[b]*Department of Environmental Health, University of Cincinnati College of Medicine, Cincinnati, OH 45267, USA.*

[c]*Department of Medicine, Indiana University School of Medicine, Indianapolis, IN 46202, USA.*

[d]*Department of Biochemistry and Molecular Biology, Indiana University School of Medicine, Indianapolis, IN 46202, USA.*

[e]*The Arizona Cancer Center, Tucson, AZ 85724, USA.*

* *Corresponding author*: Department of Molecular and Cellular Biology, University of Arizona, Life Sciences South 444A, P.O. Box 210106, Tucson, AZ 85721. Tel.: +1 520 621 7563; fax: +1 520 621 3709. E-mail address: dixonk@email.arizona.edu (K. Dixon).

† *Current address*: Humacyte Inc., Research Triangle Park, NC 27709, USA.

Abstract

Ataxia telangiectasia mutated (ATM) is a PI3-kinase-like kinase (PIKK) associated with DNA double-strand break (DSB) repair and cell cycle control. We have previously reported comparable efficiencies of DSB repair in nuclear extracts from both ATM deficient (A-T) and control (ATM+) cells; however, the repair products from the A-T nuclear extracts contained deletions encompassing longer stretches of DNA compared to controls. These deletions appeared to result from end-joining at sites of microhomology. These data suggest that ATM hinders error-prone repair pathways that depend on degradation of DNA ends at a break. Such degradation may account for the longer deletions we formerly observed in A-T cell extracts. To address this possibility we assessed the degradation of DNA duplex substrates in A-T and control nuclear extracts under DSB repair conditions. We observed a marked shift in signal intensity from full-length products to shorter products in A-T nuclear extracts, and addition of purified ATM to A-T nuclear extracts restored full-length product detection. This repression of degradation by ATM was both ATP-dependent and inhibited by the PIKK inhibitors wortmannin and caffeine. Addition of pre-phosphorylated ATM to an A-T nuclear extract in the presence of PIKK inhibitors was insufficient in repressing degradation, indicating that kinase activities are required. These results demonstrate a role for ATM in preventing the degradation of DNA ends possibly through repressing nucleases implicated in microhomology-mediated end-joining.

Key words: ATM; DNA degradation; Double-strand break repair; Microhomology-mediated end-joining; PI-3-kinase-like kinases.

1. Introduction

Preserving genomic integrity is critical to the vitality of an organism and the continuity of any species. The gravity of this task is perhaps best reflected in the number of pathways and mediators involved in maintaining the genetic code and the fidelity of its perpetuation. The repair of a DNA double-strand break (DSB) is one facet of the genomic maintenance tale with one key player being the ataxia telangiectasia mutated (ATM) protein. An ATM deficiency results in ataxia telangiectasia, a neurodegenerative disorder accompanied by immunological malfunctions and a propensity for cancer development. ATM, a PI3-kinase-like kinase (PIKK), is present in the nucleus in the form of inactive dimers and oligomers that undergo trans-autophosphorylation and dissociate upon DSB occurrence. Activated ATM then modulates the activity of a plethora of proteins involved in repair and cell cycle control (1, 2, 3). Although a role for ATM in DSB repair and cell cycle regulation is well documented, the particular defect in DNA repair emanating from an ATM dysfunction is not well characterized.

We have previously reported comparable DSB repair efficiencies in A-T and control nuclear extracts (4). The fidelity of repair, however, was defective in the A-T nuclear extracts. To demonstrate this we assessed the repair of a circular plasmid linearized with a restriction enzyme-induced DSB. Both A-T and control nuclear extracts had equivalent potentials of repairing a DSB and rejoining the plasmid. On the other hand, the mutation frequency was significantly higher in A-T nuclear extracts than in controls. A number of mutant plasmids generated from these experiments were sequenced and all revealed deletions spanning the repaired DSB site. Small sequences of

microhomology (1–6 nucleotide repeats) were involved in 95% of the deletion events. That is, rejoining occurred at sequences of microhomology that flanked both ends of the break more often than random expectation. Deletion stretches were longer in A-T than in control extracts. The repair fidelity of blunt-end DSBs and those with short (<4 nt) overhangs was significantly less in A-T than in control nuclear extracts. Differences in the fidelity of repairing DSBs with 4 nt overhangs were not statistically significant. This data indicated a potential role for ATM in repressing degradation at DSB ends thereby preventing error-prone repair.

We report here a greater extent of degradation of DNA ends in A-T than in control nuclear extracts. Degradation levels declined when purified ATM was added into repair reactions with an A-T nuclear extract background. Prevention of DNA end-degradation was ATP-dependent and was inhibited by the PIKK inhibitors wortmannin and caffeine. Addition of pre-phosphorylated ATM in the presence of PIKK inhibitors did not repress DNA end-degradation in an A-T nuclear extract. This excessive DNA end-degradation in nuclear extracts from A-T cells probably accounts for the longer deletion mutations and repair defects we observed in our previous study.

2. Materials and methods

2.1 Cell Culture

Cell lines AT5BIVA, GM16666 and GM16667 were obtained from the Coriell Cell Repository (Coriell Institute of Medical Research, Camden, NJ). The WI-38VA13 cell line was obtained from ATCC (American Type Culture Collection, Manassas, VA). AT5BIVA is a SV40-transformed fibroblast cell line derived from a patient afflicted with ataxia telangiectasia. WI-38VA13 is a SV-40 transformed lung fibroblast line used as an ATM positive control for AT5BIVA. GM16666 and GM16667 are matched lines derived from the AT22IJE-T A-T cell line which was transfected with either an ATM expression construct (GM16667) or an empty vector (GM16666) and maintained under hygromycin selection to generate A-T-corrected and A-T stable cell lines (5).

All cells lines were grown at 37°C in 5% CO_2 in Dulbecco's Modified Eagle Medium (GIBCO, Invitrogen Corporation, Carlsbad, CA) supplemented with 10% fetal bovine serum (Hyclone, Logan, UT), 100 U/ml penicillin, and 100 μg/ml streptomycin (Penicillin-streptomycin-glutamine, GIBCO, Invitrogen Corporation, Carlsbad, CA). Medium for both GM16666 and GM16667 additionally contained 100 μg/ml hygromycin (Invitrogen Corporation, Carlsbad, CA) to maintain stable cell line selection.

2.2 Nuclear Extract Preparation

Cells grown to 80% confluency in 250 mm^2 tissue culture flasks were washed three times with 20 ml of ice cold hypotonic buffer (0.25 mM EDTA pH 7.4, 0.2 mM PMSF, 0.5 mM DTT), collected using a cell lifter (Fisher Scientific Co., NJ) and centrifuged at

1850 x *g* for 10 min. Cells were resuspended in five times the pellet volume of hypotonic buffer and incubated for 30 min at 4°C. Cells were then collected by centrifugation at 1850 x *g* for 30 min and intact nuclei were released using a Dounce homogenizer using a loose fitting (Type B) pestle. Following concentration by centrifugation at 3300 x *g* for 30 min, nuclei were resuspended in one-half the packed nuclear volume of resuspension buffer (20 mM HEPES pH 7.9, 25% glycerol, 1.5 mM $MgCl_2$, 0.02M KCl, 0.2 mM EDTA, 0.2 mM PMSF, 0.5 mM DTT). Nuclear lysis buffer (resuspension buffer with a final concentration of 1.2 M KCl) equivalent to one-half the packed nuclear volume was then added. Nuclei were incubated for 30 min at 4°C and subjected to three cycles of snap-freezing in liquid nitrogen and rapid thawing at 37°C. After lysis by Dounce homogenization, nuclear lysates were centrifuged at 25,000 x *g* for 30 min and the supernatant was dialyzed for 18 hr at 4°C against dialysis buffer (50 mM Tris-Cl pH 7.5, 0.1 mM EDTA, 10 mM 2-mercaptoethanol, 0.1 mM PMSF, 10% glycerol). Aliquots of the samples were snap-frozen in liquid nitrogen and stored at -80°C. The protein concentration of the nuclear extracts was determined by the Bradford protein assay using the Bradford reagent (Sigma, St. Louis, MO) and BSA as a standard.

2.3 Purification of ATM

The purification of ATM was based on the procedure of Goodarzi and Lees-Miller (6). HeLa cells (6 L) were grown to log phase (4 x 10^5 cells/ml) and collected by sedimentation at 10,000 x g for 15 min at 4°C. The resulting cell pellet was washed twice with 10 ml low salt buffer (10 mM HEPES pH 7.4, 25 mM KCl, 10 mM NaCl, 1

mM $MgCl_2$, and 0.1 mM EDTA). The cells were collected and resuspended in 7 ml of high salt buffer (50 mM Tris-Cl pH 8.0, 5% glycerol, 1 mM EDTA, 10 mM $MgCl_2$, 400 mM KCl). This buffer and all subsequent buffers were supplemented with the protease inhibitors PMSF (0.1 mM), leupeptin (1 μg/ml) and pepstatin (1 μg/ml). After disruption using a Dounce homogenizer; the lysate was centrifuged at 10,000 x g for 30 min and the supernatant (S1) was saved. The pellet was extracted with 3 ml of high salt buffer and centrifuged generating a second supernatant (S2). S1 and S2 were combined (termed P10) and immediately diluted with TB buffer (50 mM Tris, 5% glycerol, 0.2 mM EDTA, 1 mM DTT) to a final conductivity equal to 75 mM KCl.

P10 (170 mg) was applied onto a 10 ml DEAE-Sepharose fast flow (GE Healthcare, Princeton, NJ) column equilibrated in TB-75 mM KCl at a rate of 2 ml/min. After the column was washed with 10 column volumes of TB-75 mM KCl, bound protein including ATM was eluted with 5 column volumes of TB-200 mM KCl. The eluted protein (32 mg) was pooled, immediately diluted to a conductivity equal to 75 mM KCl, and applied to a 5 ml SP-Sepharose fast flow column (Amersham Pharmacia Biotech, Piscataway, NJ). Again the column was washed with 10 column volumes of TB-75 mM KCl, and eluted with 5 column volumes of TB-200 mM KCl. The eluted protein (3.5 mg) containing ATM was diluted in TB buffer to a conductivity equal to 125 mM KCl and applied onto a 0.5 ml single-strand DNA-cellulose column (Sigma, St. Louis, MO) at 0.2 ml/min.

The flow-through fraction (2 mg), containing the majority of the ATM protein, was collected, diluted with TB buffer to a conductivity equal to 100 mM KCl and loaded

onto a 2 ml Macroprep-Q column (Bio-Rad Laboratories, Hercules, CA) equilibrated in TB-100 mM KCl. Protein was eluted with a 15 ml linear salt gradient from 0.1 to 1 M KCl at 0.5 ml/min. Fractions containing ATM were pooled (0.3 mg) and stored at -80°C. Fractions containing ATM were identified by SDS-PAGE. Protein concentration was determined by the Bradford assay using BSA as a standard.

2.4 Western Immunoblotting

Samples (20 μg of nuclear extract or 1 μg of the purified ATM preparation) were incubated at 100°C for 5 min in Laemmli sample buffer and then electrophoresed on 6% (for DNA-PK_{cs}, ATR and ATM) or 12% (for Ku80, Mre11, Ku70 and RPA2) denaturing-polyacrylamide gels. Proteins were transferred to Trans-Blot Medium nitrocellulose membranes (Bio-Rad Laboratories, Hercules, CA), probed and then visualized with the SuperSignal West Dura Extended Duration Substrate (Pierce Biotechnology, Inc., Milwaukee, WI). The FluorChem system (Alpha Innotech Corporation, San Leandro, CA) was used for gel documentation. The DNA-PK_{cs} (1:10,000), ATM (1:1000), Ku80 (1:10,000), Ku70 (1:10,000) and Mre11 (1:40,000) primary antibodies were obtained from Abcam, Inc. (Cambridge, MA). The ATR (1:10,000) primary antibody was from Novus Biologicals, Inc. (Littleton, CO) while the RPA2 (1:10,000) primary antibody was from Bethyl, Inc. (Montgomery, TX).

2.5 Autophosphorylation of ATM

To pre-phosphorylate ATM, 0.34 pmol of purified ATM were incubated with 0.83 pmol of ATP or [γ-^{32}P]ATP in 15 µl phosphorylation buffer (20 mM Tris-Cl pH 7.5, 20 mM $MgCl_2$, 10 mM $MnCl_2$, 1µM fostriecin).

2.6 Duplex Oligonucleotide Substrates

A series of duplex DNA oligonuleotide substrates (Integrated DNA Technologies, Inc., IA) were generated and used to measure degradation of DNA ends in different cellular extracts (Table 1). A 71 nt oligonucleotide (Template/ 5'Cy3 Template) was hybridized to a Top Strand of variable lengths resulting in substrates with different 5'-end overhangs or a blunt end. Alternatively, where indicated, a 45 nt Template was hybridized to a 50 nt 3'Cy3Sp Top Strand. Template (0.9 nmol) and Top Strand (0.9 nmol) oligonucleotides were incubated in 100 µl of hybridization buffer (10 mM Tris-Cl pH 7.9, 50 mM NaCl and 10 mM $MgCl_2$) for 10 min at 100°C and then slowly cooled to 25°C. The resulting substrates had either a blunt end or 5'-end overhang corresponding to 5'AATTC, 5'TAGC, 5'CGCG, 5'TAT, or 5'CG. Assays were designed to examine degradation at the overhang end of the duplexes; therefore, the final 6 bases at the 3'-end of each Top Strand were linked with phosphorothioate linkages to prevent nuclease digestion. Similarly, the first 6 nucleotides at the 5'-end of the Template were linked by phosphorothioate linkages for the same purpose. In addition, a 5'Cy3-labeled 71 nt Template protected from nuclease digestion by phosphorothioate linkages at its 5'-end

was used to measure the 3'-end degradation of the non-overhang presenting strand in the duplex.

2.7 DNA End Processing Assay

Measurement of DNA end protection was accomplished by incubating the oligonucleotide substrates defined above in control or A-T extracts, followed by DNA extraction and primer extension to detect the length of DNA products. The *in vitro* assay conditions simulated those used for DNA double-strand break repair. Reactions (50 µl) containing 50 µg of nuclear extract and 90 pmoles of a DNA duplex in reaction buffer (65.5 mM Tris-Cl pH 7.5, 10 mM $MgSO_4$, 10mM $MnSO_4$, 91 nM EDTA, 9.1% glycerol) were assembled on ice and then incubated for 10 min at 30°C. Reaction buffer was supplemented with Complete, Mini, EDTA-free Protease Inhibitor Cocktail (Roche Diagnostics GmbH, Mannheim, Germany) used according to the manufacturer's instructions. Reactions were stopped by adding 50 µl of phenol. Where indicated in the text, ATP (1 mM), the phosphatase inhibitor fostriecin (1 µM) and the PIKK inhibitors wortmannin (13 nM) and caffeine (71.85 µM) were included in the assay. When used, purified ATM or pre-phosphorylated purified ATM was incorporated into reactions containing A-T nuclear extracts as indicated in the text. The DNA duplex was recovered from the assay reactions by phenol phase separation and subsequent ethanol precipitation with 120 µg of glycogen (Fermentas, Hanover, MD) and 10 µl of 3 M sodium acetate pH 5.2.

2.8 Primer Extension Assay

The lengths of the Top Strands of DNA duplexes retrieved from the end processing reactions were determined by a primer extension assay using a 5'Cy3-labeled extension primer (Table 1). This primer anneals to the 3'-end of Top Strands used to generate the DNA duplexes. Reactions (20 µl) contained total DNA extracted from the end processing reactions, 12.3 pmoles of the extension primer and 0.5 units of Taq DNA polymerase (Roche Diagnostics GmbH, Mannheim, Germany) in extension assay buffer (200 µM of each dNTP, 50 mM Tris-Cl pH8.3, 10 mM KCl, 5mM $(NH_4)_2SO_4$, and 2 mM $MgCl_2$). The population of Top Strands was amplified by PCR in an Eppendorf Mastercycler Gradient (Eppendorf AG, Hamburg, Germany) thermocycler. Following an initial denaturation step at 94°C for 20 min, reactions were incubated for 5 cycles of 1 min at 94°C, 1 min at 58°C and 1 min at 72°C with a final extension at 72°C for 10 min. The 20 µl extension reactions were stopped by addition of 5 µl formamide buffer (95% formamide, 10 mM EDTA pH 7.6, 0.1% xylene cyanol, 0.1% bromophenol blue), heated to 95°C for 10 min and then brought down to room temperature prior to product analysis.

2.9 Product Analysis

Products from primer extension reactions and from end-processing assays employing a 5'Cy3-labeled Template were separated on 12% acrylamide/7 M urea sequencing gels (Sequagel Sequencing System reagents, National Diagnostics, Atlanta, GA). Reaction products were visualized using a Typhoon 9410 Variable Mode Imager (GE Healthcare, Princeton, NJ) and analyzed using ImageQuant v5.2 software (Molecular Dynamics,

Amersham Biosciences, Princeton, NJ). Product intensities were determined, corrected for background and then converted into percent intensities where percent intensity = (product intensity/ total lane intensity) x 100.

3. Results

We have previously reported a decrease in the fidelity of DSB repair in A-T nuclear extracts when compared to controls (4). The most prominent type of mutations observed were deletion events associated with sites of microhomology flanking a break. The deletions encompassed one of the two sites of microhomology in addition to the region between the two sites. To assess whether these events were the result of DNA end-degradation, we employed an *in vitro* system that simulates DSB repair conditions (Fig. 1). This system was used to assess the role of ATM in repressing degradation at DSB ends.

3.1 Increased levels of DNA end-degradation in A-T nuclear extracts

We used DNA duplex substrates with a single nuclease-susceptible end in an *in vitro* DSB repair reaction. Substrates were designed to limit degradation to the 5' end of the overhang-presenting strand and the 3' end of the 3'-recessed strand, here forth referred to as the Top Strand and the Template respectively. DNA was extracted from the repair reactions after incubation with the extracts and subjected to a primer extension assay that allowed examination of degradation levels of the Top Strand (Fig. 1A). The extension assay employed a 5'Cy3-labeled primer that annealed to the 3' end of the Top Strand. The inclusion of phosphorothioate linkages at the blunt end of the duplex prevented nuclease-mediated degradation of the primer annealing site on the Top Strand.

The potential role of ATM in repressing DNA end-degradation was tested using a substrate harboring a 5'AATTC overhang. The 5'AATTC substrate was incubated with

A-T or control nuclear extracts under *in vitro* DSB repair conditions. The AT5BIVA and GM16666 cell lines were used as sources of A-T nuclear extracts whereas the WI-38VA13 and GM16667 cell lines were used as their respective controls (Fig. 2A). The expected length of the product obtained from a fully extended non-degraded strand was 76 nt. Extension products were clustered into four groups for quantification purposes: full-length, long, medium-sized, short and un-extended primer. Product intensities were determined, corrected for background and then converted into percent intensities where percent intensity = (product intensity/total lane intensity) x 100. Intensities of the full-length product from the WI-38VA13 and GM16667 control nuclear extracts were 22% and 13% respectively. In comparison, the intensities of the full-length product retrieved from the AT5BIVA and GM16666 A-T nuclear extracts were both 1% (Table 2A). Hence, an elevated level of degradation of DNA ends is detected in both types of A-T nuclear extracts; this is strongly indicated by an approximate 10-fold decrease in full-length product intensities. The shift in intensity from the full-length product in the A-T extracts was mostly towards the un-extended primer.

In parallel with the reactions described above, the duplex and the labeled primer were incubated under repair reaction conditions in absence of nuclear extract, subjected to DNA extraction and then the primer extension assay (Fig. 2A Lanes 5 and 6). This was performed to ensure that the repair buffer, the DNA extraction and the primer extension procedures did not bias the results by affecting degradation or by adding background signal.

Since the chemistry of the primer extension assay only allows for examination of the Top Strand, a different strategy was employed to assess the degradation of the 3' end of the Template (Fig. 1B). Duplex substrates contained a Template labeled itself with a 5'Cy3 moiety. Following incubation with nuclear extracts, products were isolated, separated on a gel and then quantified.

A 5'AATTC substrate with a 5'Cy3-labeled Template was incubated with A-T and control extracts as described above for Fig 2A. Subsequent to incubation with WI-38VA13 and AT5BIVA nuclear extracts, the duplex was extracted, products were separated (Fig. 2B) and then quantified (Table 2B). In addition, the duplex substrate was incubated under repair reaction conditions in the absence of nuclear extract as a control (Fig. 2B Lane 3). Intensity of the full-length labeled Template retrieved from the control nuclear extract was 73% of the total intensity whereas it was 9% in the A-T nuclear extract. Hence, degradation of both strands in the duplex was elevated in A-T extracts.

To validate the primer extension assay described above and utilized in subsequent experiments, we assessed the degradation of a Top Strand labeled itself at the 3' end with a Cy3 moiety and incorporated into a 5'AATTC duplex (Figure 3A). This substrate was incubated under repair conditions in control and A-T nuclear extracts. Products were retrieved, gel-separated and then analyzed. As observed with the primer extension assay, an increase in Top Strand degradation in A-T nuclear extracts was observed over controls (Fig. 3B). Therefore, both assay systems revealed comparable results.

3.2 Repression of degradation of various types of DNA ends in control nuclear extracts

To examine whether the length and the sequence of the overhang affects degradation and protection activities, we used various duplex substrates in our *in vitro* repair system (Table 1). DNA duplexes tested had one blunt end protected from degradation by phosphorothioate linkages and a 5' overhang-presenting end. Overhang sequences assessed were 5'TAGC, 5'CGCG, 5'TAT, and 5'CG. We also tested a duplex with one blunt end vulnerable to degradation and another protected by phosphorothioate linkages.

These DNA substrates were incubated with control or A-T nuclear extracts under appropriate DSB repair conditions. DNA duplexes were then extracted and subjected to primer extension for the Top Strand population retrieved as described in the *Materials and Methods* section. Marked degradation in A-T nuclear extracts was observed for the different substrates tested (Fig. 4A). A decrease of around ten-fold in full-length product intensity was observed in A-T nuclear extracts when compared to controls (Fig. 4B). Average intensities of the full-length extension products for the substrates tested ranged from 12% to 19% in the control nuclear extracts. In comparison, their intensities in the A-T nuclear extracts were all less than 1%. The shift in intensity was again mostly towards the un-extended primer. Despite minor variability in the degradation trends observed for the various substrates, the data presented consistently demonstrate enhanced DNA end-protection in control extracts over A-T extracts (Compare Lanes 1, 3, 5, 7, 9 to Lanes 2, 4, 6, 8, 10 in Fig 4A). This protection is also independent of the nature of the DNA end.

Since we made extensive use of the WI-38VA13 (control) and AT5BIVA (A-T) nuclear extracts in this and all subsequent experiments, we ensured that levels of key DSB repair proteins, besides ATM, were relatively equivalent in both types of extracts (Fig. 4C). Western immunoblotting for DNA-PK_{cs}, ATR, Ku80, Mre11, Ku70 and RPA2 revealed comparable levels of these proteins in our nuclear extract preparations from both cell lines. We were unable to detect ATM in the AT5BIVA nuclear extracts.

3.3 ATP is required for prevention of end-degradation

To assess the ATP-requirement for the enhanced DNA end-stability phenomenon observed in the control extracts, we examined the degradation of the Top Strand in a duplex with a 5'AATTC overhang in the presence or absence of ATP (Fig. 5). In the presence of ATP, average intensities of the full-length product were 18% and 1% in WI-38VA13 (control) and in AT5BIVA (A-T) nuclear extracts, respectively (Table 3). Removing ATP from the repair reaction resulted in ablation of this difference; in ATP-deficient conditions both A-T and control extracts displayed a low intensity of the full-length product (<3%). Although we observed variations in the intensities of the long, medium-sized and short products generated by different control and A-T nuclear extract batches, the trend of elevated degradation in the A-T nuclear extracts was consistent. Moreover, ATP was required for hindering degradation in multiple independently prepared control nuclear extracts.

3.4 Addition of purified ATM to A-T nuclear extracts restores end protection

We examined if addition of purified ATM would restore DNA end-protection to A-T nuclear extracts. Purified ATM was added to AT5BIVA (A-T) nuclear extracts and DNA end-degradation of the Top Strand in a duplex with a 5'AATTC overhang was assessed (Fig. 6A). The intensity of the full-length product detected in the absence of purified ATM in an A-T nuclear extract was 1.82% (Fig. 6A Lane 14). Addition of increasing amounts of purified ATM (Fig. 6A Lane 11 (0.05 nM), Lane 12 (0.1 nM) and Lane 13 (0.2 nM)) increased the amount of full-length product intensity (to 2.01%, 10.78% and 28.45%, respectively). Full-length product intensity detected with 0.2 nM purified ATM was comparable to the 27.44% intensity detected in the WI-38VA13 (control) nuclear extract in this experiment (Fig. 6A Lane 15). Hence, a dose-response in protection from degradation was observed with increasing concentrations of ATM. The use of a reaction buffer lacking ATP eliminated the prevention of substrate degradation conferred by the purified ATM (Fig. 6A Lanes 5, 6 and 7). This again demonstrates the dependency on ATP for repressing degradation. To ensure that our purified ATM preparation did not contain other DSB-associated PIKKs that may affect restoration of DNA end-protection we used immunoblotting to assay for DNA-PK_{cs} and ATR (Fig. 6B); neither DNA-PK_{cs} nor ATR was detected in the ATM preparation.

3.5 Caffeine and wortmannin inhibit end protection

Prevention of end-degradation was ATP and ATM-dependent. With ATM being a PIKK kinase, we tested whether inhibition of its kinase activity would affect end-protection

(Fig. 7). The PIKK inhibitors caffeine and wortmannin were added to the end processing reactions at concentrations previously shown to inhibit the kinase activity of ATM (6). Both inhibitors were capable of abolishing the protective effects of 0.2 nM purified ATM (Fig. 7. Lanes 2 and 3) and of the control nuclear extract (Fig 7. Lanes 4 and 5) in the presence of ATP. This was evident by the sharp decline in the intensity of full-length products (Fig. 7).

3.6 ATM autophosphorylation is not sufficient for end-protection

The dependency on ATP to repress degradation and the inhibition of this repression by wortmannin or caffeine reflects the requirement for kinase activity for DNA end-protection. This requirement could reflect a dependence on ATM autophosphorylation alone; or it could indicate the need for phosphorylation of a downstream substrate by ATM or by another component of the system.

Hence, to examine whether an ATM autophosphorylation event was sufficient to confer protection to DNA ends without the need for subsequent kinase activities, we incubated pre-phosphorylated purified ATM with a duplex presenting a 5'AATTC overhang in an A-T nuclear extract along with wortmannin or caffeine (Fig. 8A). This was done in the presence of the phosphatase inhibitor fostriecin to ensure that ATM remained phosphorylated during the reaction. We used fostriecin at a concentration previously shown to inhibit ATM dephosphorylation by PP2A (7). The addition of fostriecin had no effect on end protection by purified ATM (Fig. 8A Lane 5) or by a control nuclear extract (Fig. 8A Lane 4). Pre-phosphorylated ATM was capable of

repressing DNA end-degradation. However, it was unable to do so in the presence of either wortmannin or caffeine as reflected by a sharp decline in detectable full-length product and an increase in intensities of shorter products (Compare Fig. 8A Lane 9 to Lanes 10 and 11). These data indicate that autophosphorylation of ATM is necessary but not sufficient and that downstream kinase activities are probably needed to prevent degradation of DNA ends. We ensured that ATM remained phosphorylated in the extract via parallel monitoring of ^{32}P-labeled ATM incubated with A-T nuclear extract, wortmannin, fostriecin and DNA duplex under typical repair reaction conditions (Fig. 8B).

4. Discussion

Non-homologous end-joining (NHEJ) is believed to be the major DNA double-strand break (DSB) repair mechanism in mammalian cells during G_0, G_1 and early S-phase of the cell cycle. Proteins involved in the NHEJ pathway include the Ku70/Ku80 heterodimer, DNA-PK_{cs}, XRCC4, DNA Ligase IV and Artemis. Microhomology-mediated NHEJ, on the other hand, may involve the MRN complex (discussed below). NHEJ-deficient cells fail to repair up to 60% of induced DSBs (8). On the other hand, cells with ATM deficiencies, or A-T cells, display levels of residual un-repaired DSBs that are similar to those detected in controls (9, 10, 11) or at most slightly elevated (12, 13). We have previously reported comparable efficiencies of DSB repair in A-T and control nuclear extracts; however, repair in the A-T extracts resulted in a higher level of mutations, mostly deletion events (4). These events involved rejoining at sequences of microhomology flanking a DSB. We report here increased levels of DNA end-degradation in A-T nuclear extracts. These data, along with our previous findings, support that the repair defect in A-T cells is based on the failure to protect DNA ends at a break from erroneous degradation. Such degradation probably leads to improper end-ligation and deletions which culminate in the genetic instability phenotype associated with defects in ATM. Our data is consistent with other studies indicating that the fidelity of repair rather than efficiency is primarily affected in A-T cells (4, 14, 15, 10, 16). These studies report an elevated level of deletions and rearrangements in the repair of plasmids harboring DSBs by A-T cells or their respective extracts.

In our former study (4), we used *Sup*F22 plasmids harboring endonuclease-induced DSBs to evaluate the repair of different types of ends at a break. Plasmids were subjected to DSB repair reactions in A-T and in control nuclear extracts; then they were isolated and used to transform competent bacterial cells. We observed an increased level of mutations in the repair of DSBs with short (< 3 nt) overhangs and blunt ends in A-T nuclear extracts. However, fidelity did not significantly vary from controls in the repair of DSBs with 4 nt overhangs. In the present study, we report an increased level of DNA end-degradation in A-T nuclear extracts for various types of DNA ends including those with 4 nt overhangs. Disparity in data regarding the repair of breaks with 4 nt overhangs is probably due to differences in the experimental systems utilized. It is conceivable that the use of a 5553 bp plasmid with cohesive 4 nt overhangs in our former study may have promoted intramolecular interactions resulting in plasmid circularization. This would have limited the duration of exposure of plasmid ends to nucleases in either type of extract hence resulting in greater end stability and higher repair fidelity.

In their 1993 paper, Powell et al. (10) concluded that nuclease-mediated degradation of DNA ends is probably not the sole repair defect in A-T cells. This was based on observing deletions and sequence-insertions affecting linearized plasmids at and around the break site in A-T cells. Moreover, they reported rearrangements involving multiple sites along an intact circular plasmid transfected into A-T cells. However, their analysis of the data did not include assessing whether a subset of those mutations was non-random or rather directed by the presence of microhomologies.

A possible link between loss of ATM function and illegitimate recombination may be deduced from the interaction between ATM and Mre11, a nuclease that has been implicated in microhomology-mediated end-joining and whose role in recombination is well documented. Mre11 is a member of the Mre11-Rad50-Nbs1 (MRN) complex that participates in end-resection at DNA DSBs. This process precedes the strand invasion step observed during meiotic recombination and homologous recombination repair. The role of Nbs1 has not been fully elucidated whereas resection seems to mostly depend on the Mre11-Rad50 complex. Rad50 is an ATPase related to the structural maintenance of chromosomes (SMC) proteins (2) and distantly related to the ATP binding cassette (ABC) family of transporters (17). Mre11, on the other hand, is a nuclease (18) whose role in NHEJ is under debate. Studies in budding yeast indicate that all three components of the complex are required for end-joining *in vivo* (19) and *in vitro* (20). On the other hand, while some *in vitro* studies in mammalian extracts support that the MRN complex is required for NHEJ (21, 22) others conclude that it is dispensable regardless of the type of DNA substrate (23). Insight into a possible role for this complex in a microhomolgy-dependent form of NHEJ comes from studies by Paull and Gellert (24, 25) demonstrating that recombinant human Mre11 can degrade duplex DNA substrates up to sequences of microhomology *in vitro*. End-degradation by Mre11 was stimulated by addition of DNA with nonhomologous ends but inhibited by ends capable of base pairing. Moreover, during degradation, the Mre11 nuclease activity stalled upon encountering cohesive sequences.

Mre11 is phosphorylated in an ATM-dependent manner in response to DNA damage (26). Whether this phosphorylation is direct by ATM (27) or indirect through a downstream kinase (28) remains debatable. Nbs1 is another member of the MRN complex that is phosphorylated by ATM (29, 30). These interactions provide the means through which ATM could regulate degradation at DNA ends. Hence, we envisage a model in which activated ATM is recruited to DNA ends by MRN which is then phosphorylated by ATM at sites that regulate its resection-related activities. We found ATP to be a requirement for prevention of substrate degradation in non-A-T control nuclear extracts. Moreover, this protection was inhibited by the PI-3 kinase-like kinase inhibitors caffeine and wortmannin. These pieces of evidence, although not conclusive, lend support to this model. Alternatively, ATM could be activating a downstream effector that in turn represses degradation. A myriad of proteins interacts with ATM and could play a role in enhancing DNA end-stability. The list of candidates includes multiple kinases (Chk1, Chk2, DNA-PK_{cs}, etc.) and repair-associated factors (BRCA1, MDC1, 53BP, etc.) The scope of protection mediated by ATM is probably not limited to Mre11 but also extends to other nucleases; however, our knowledge of the Mre11 nuclease and its activities places it as the primary candidate for microhomology-mediated end-joining. Worth noting is that the levels of non-full length products detectable in A-T nuclear extracts were slightly higher in reactions containing ATP than those lacking ATP. Although these differences are very subtle, they may signify an alternate, albeit less efficient, non-ATM dependant DNA end-protection mechanism.

When examining the repair of a plasmid with a bleomycin-induced DSB, Dar et al. (15) did not observe illegitimate recombinational repair in A-T extract, in contrast to predictions of the model delineated above. One possible explanation is that in the repair of ends generated by bleomycin in A-T cells, other pathways predominate over microhomology-mediated end-joining. Bleomycin induces oxidative damage and is believed to produce DSBs that resemble those induced by ionizing radiation (31). By virtue of their chemistry (3'-phosphoglycolate and 5'-phosphate termini), such ends may be resistant to the degradation process we observed in our assays.

To recapitulate, we have assessed the degradation of DNA substrates bearing various overhangs in A-T and control nuclear extracts. These substrates resemble DNA ends at a double- strand break and similar substrates were previously shown to activate ATM (32, 33, 34). We observed greater extents of degradation in A-T extracts, a phenomenon that was repressed by the addition of purified ATM. This repression of degradation was ATP-dependent and was inhibited by the PI3-kinase-like kinase inhibitors wortmannin and caffeine. Pre-phosphorylated ATM was incapable of hindering degradation in the presence of PI3-kinase-like kinase inhibitors. These pieces of data conform to a model in which ATM prevents the degradation of DNA ends via its kinase activity. Future exploration of this model will include assessing the actual involvement of the ATM kinase activity in the process and mediators, such as the MRN complex, it may be acting upon to repress degradation.

REFERENCES

[1] M.F. Lavin and S. Kozlov. ATM activation and DNA damage response, Cell Cycle. 6 (2007) 931-942.

[2] R.T. Abraham and R.S. Tibbetts. Guiding ATM to Broken DNA, Science. 308 (2005) 510-511.

[3] A.M.R. Taylor and P.J. Byrd. Molecular pathology of ataxia telangiectasia, J. Clin. Pathol. 58 (2005) 1009-1015.

[4] Y. Li, M.P. Carty, G.G. Oakley, M.M. Seidman, M. Medvedovic, K. Dixon. Expression of ATM in ataxia telangiectasia fibroblasts rescues defects in DNA double-strand break repair in nuclear extracts, Environ. Mol. Mutagen. 37 (2001) 128-140.

[5] Y. Ziv, A. Bar-Shira, I. Pecker, P. Russell, T.J. Jorgensen, I. Tsarfati, Y. Shiloh. Recombinant ATM protein complements the cellular A-T phenotype, Oncogene. 15 (1997) 159-167.

[6] A.A. Goodarzi and S.P. Lees-Miller. Biochemical characterization of the ataxia-telangiectasia mutated (ATM) protein from human cells, DNA Repair. 3 (2004) 753-767.

[7] A.A. Goodarzi, J.C. Jonnalagadda, P. Douglas, D. Young, R. Ye, G.B. Moorhead, S.P. Lees-Miller, K.K. Khanna. Autophosphorylation of ataxia-telangiectasia mutated is regulated by protein phosphatase 2A, EMBO J. 23 (2004) 4451-4461.

[8] P.A. Jeggo. DNA breakage and repair. In: J. C. Hall, J. C. Dunlap, T. Friedmann, and F. Gianelli (eds)., Advances in Genetics, Vol. 38, pp. 185–218.

[9] A.R. Lehmann and S. Stevens. The production and repair of double-strand breaks in cells from normal humans and from patients with ataxia-telangiectasia, Biochim. Biophys. Acta. 474 (1977) 49-60.

[10] S. Powell, S. Whitaker, J. Peacock, T. McMillan. Ataxia telangiectasia: an investigation of the repair defect in the cell line AT5BIVA by plasmid reconstitution, Mutation Res. 294(1993) 9-20.

[11] D. Thierry, O. Rigaud, I. Duranton, E. Moustacchi, H. Magdelenat. Quantitative measurement of DNA strand breaks and repair in gamma-irradiated human leukocytes from normal and ataxia telangiectasia donors, Radiation Res. 102 (1985) 347-358.

[12] N. Foray, C.F. Arlett, E.P. Malaise. Dose-rate effect on induction and repair rate of radiation-induced DNA double-strand breaks in a normal and an ataxia telangiectasia human fibroblast cell line, Biochimie. 77 (1995) 900 -905.

[13] N. Foray, A. Priestley, G. Alsbeih, C. Badie, E.P. Capulas, C.F. Arlett, E.P. Malaise. Hypersensitivity of ataxia telangiectasia fibroblasts to ionizing radiation is associated

with a repair deficiency of DNA double-strand breaks, Int. J. Radiat. Biol. 72 (1997) 271-283.

[14] R. Cox, P.G. Debenham, W.K. Masson, M.B. Webb. Ataxia-telangiectasia: a human mutation giving high-frequency misrepair of DNA double-stranded scissions, Mol. Biol. Med. 3 (1986) 229-244.

[15] M.E. Dar, T.A. Winters, T.J. Jorgensen. Identification of defective illegitimate recombinational repair of oxidatively-induced DNA double-strand breaks in ataxia-telangiectasia cells, Mutation Res. 384 (1997) 169-179.

[16] S.N. Powell, J. Mills, T.J. McMillan. Radiosensitive human tumour cell lines show misrepair of DNA termini, Br. J. Radiol. 71 (1998) 1178-1184.

[17] A.L. Davidson. Not just another ABC transporter, Science. 296 (2002) 1038-1040.

[18] L.S. Symington. Role of RAD52 epistasis group genes in homologous recombination and double-strand break repair, Microbiol. Mol. Biol. Rev. 66 (2002) 630- 670.

[19] J.K. Moore and J.E. Haber. Cell cycle and genetic requirements of two pathways of nonhomologous end-joining repair of double-strand breaks in *Saccharomyces cerevisiae*, Mol. Cell. Biol. 16 (1996) 2164–2173.

[20] S.J. Boulton and S.P. Jackson. Components of the Ku-dependent nonhomologous end-joining pathway are involved in telomeric length maintenance and telomeric silencing, EMBO J. 17 (1998) 1819-1828.

[21] J. Huang and W.S. Dynan. Reconstitution of the mammalian DNA double strand break end-joining reaction reveals a requirement for an Mre11/Rad50/NBS1-containing fraction, Nucleic Acids Res. 30 (2002) 667-674.

[22] Q. Zhong, T.G. Boyer, P.L. Chen, W.H. Lee. Deficient nonhomologous end- joining activity in cell-free extracts from Brca1-null fibroblasts, Cancer Res. 62 (2002) 3966-3970.

[23] M. Di Virgilio and J. Gautier. Repair of double-strand breaks by nonhomologous end joining in the absence of Mre11, J. Cell Biol. 171 (2005) 765-771.

[24] T.T. Paull and M. Gellert. The 3' to 5' exonuclease activity of Mre 11 facilitates repair of DNA double-strand breaks, Mol. Cell. 1 (1998) 969-979.

[25] T.T. Paull and M. Gellert. A mechanistic basis for Mre11-directed DNA joining at microhomologies, PNAS. 97 (2000) 6409-6414.

[26] S.S. Yuan, H.L. Chang, M.F. Hou, T.F. Chan, Y.H. Kuo, Y.C. Wu, J.H. Su. Neocarzinostatin induces Mre11 phosphorylation and focus formation through an ATM- and NBS1-dependent mechanism, Toxicology. 177 (2002) 123-130.

[27] S.T. Kim, D.S. Lim, C.S. Canman, M.B. Kastan. Substrate specificities and identification of putative substrates of ATM kinase family members, J. Biol. Chem. 274 (1999) 37538- 37543.

[28] S.T. Kim. Protein kinase CK2 interacts with Chk2 and phosphorylates Mre11 on serine 649, Biochem. Biophys. Res. Commun. 331 (2005) 247-252.

[29] X. Wu, V. Ranganathan, D.S. Weisman, W.F. Heine, D.N. Ciccone, T.B. O'Neill, K.E. Crick, K.A. Pierce, W.S. Lane, G. Rathbun, D.M. Livingston, and D.T. Weaver. ATM phosphorylation of Nijmegen breakage syndrome protein is required in a DNA damage response, Nature. 405 (2000) 477-482.

[30] D.S. Lim, S.T. Kim, B. Xu, R.S. Maser, J. Lin, J.H. Petrini and M.B. Kastan. ATM phosphorylates p95/nbs1 in an S-phase checkpoint pathway, Nature. 404 (2000) 613-617.

[31] N. Murugesan, C. Xu, G.M. Ehrenfeld, H. Sugiyama, R.E. Kilkuskie, L.O. Rodriguez, L.H. Chang, S.M. Hecht. Analysis of products formed during bleomycin-mediated DNA degradation. Biochemistry, 24 (1985) 5735-5744.

[32] Z You et al. ATM activation and its recruitment to damaged DNA require binding to the C terminus of Nbs1, Mol Cell Biol. 13 (2005) 5363-5379.

[33] J Lee et al. ATM Activation by DNA Double-Strand Breaks Through the Mre11 Rad50-Nbs1 Complex, Science. 308 (2005) 551 - 554.

[34] Z You et al. Rapid activation of ATM on DNA flanking double-strand breaks, Nat Cell Biol. 9 (2007) 1311-1318.

Table 1: Oligonucleotides used to assess DNA degradation.

Name	Overhang	Length (nt)	Sequence
Top Strand			
	5'AATTC	76	5'AATTCGAGCTCGGTACCCGGGGATCCTCTAGAGTCGACCTGCAGGCATGCAAGCTTGGCACTGGCCGTCG**TTTTAC**
	5'TAGC	75	5'TAGCGAGCTCGGTACCCGGGGATCCTCTAGAGTCGACCTGCAGGCATGCAAGCTTGGCACTGGCCGTCG**TTTTAC**
	5'CGCG	75	5'CGCGGAGCTCGGTACCCGGGGATCCTCTAGAGTCGACCTGCAGGCATGCAAGCTTGGCACTGGCCGTCG**TTTTAC**
	5'TAT	74	5'TATGAGCTCGGTACCCGGGGATCCTCTAGAGTCGACCTGCAGGCATGCAAGCTTGGCACTGGCCGTCG**TTTTAC**
	5'CG	73	5'CGGAGCTCGGTACCCGGGGATCCTCTAGAGTCGACCTGCAGGCATGCAAGCTTGGCACTGGCCGTCG**TTTTAC**
	Blunt	71	5'GAGCTCGGTACCCGGGGATCCTCTAGAGTCGACCTGCAGGCATGCAAGCTTGGCACTGGCCGTCG**TTTTAC**
Template		71	3'CTCGAGCCATGGGCCCCTAGGAGATCTCAGCTGGACGTCCGTACGTTCGAACCGTGACCGGCAGC**AAAATG**
Cy3 Template		71	3'CTCGAGCCATGGGCCCCTAGGAGATCTCAGCTGGACGTCCGTACGTTCGAACCGTGACCGGCAGC**AAAATG**/Cy3
Cy3Sp Top Strand	5'AATTC	50	5'AATTCAGTCGACCTGCAGGCATGCAAGCTTGGCACTGGCCGTCG**TTTTAC**/Cy3Sp
45 nt Template		45	3'TCAGCTGGACGTCCGTACGTTCGAACCGTGACCGGCAGC**AAAATG**
Extension Primer		20	3'CCGTGACCGGCAGCAAAATG/Cy3

Underlined nucleotides are unpaired in the final substrate. Bold nucleotides are linked by phosphorothioate bonds.

Table 2: Percent intensity of end-processing assay products using a 5'AATTC substrate.

A. Top Strand primer extension products

	Nuclear Extract					
	Control		A-T		Duplex	Primer
	WI-38VA13	GM16667	AT5BIVA	GM16666	only	only
Product						
Full-length	22	13	1	1	44	2
Long	6	8	0	2	5	5
Medium	6	13	13	0	0	0
Short	9	19	10	2	0	10
Un-extended Primer	57	47	76	95	51	83
Lane (Fig. 2A)	1	2	3	4	5	6

B. 5'Cy3 Template degradation products.

	Nuclear Extract		
	Control	A-T	Duplex
	WI-38VA13	AT5BIVA	only
Product			
Full-length	73	9	93
Long	12	42	7
Medium	15	38	0
Short	0	11	0
Lane (Fig. 2B)	1	2	3

Table 3. Percent intensity of primer extension products of the Top Strand in a 5'AATTC substrate in reactions with or without ATP.

	Nuclear Extract					
	Control WI-38VA13		A-T AT5BIVA		Duplex only	
ATP	-	+	-	+	-	+
Product						
Full-length	1±1	18±5	3±1	1±1	17±3	18±3
Long	3±2	5±4	3±3	4±4	6±1	6±2
Medium	4±4	2±3	0±3	3±3	4±1	4±3
Short	0±0	0±1	0±0	3±6	0±0	0±0
Un-extended Primer	92±5	75±5	94±1	89±5	73±4	72±7

FIGURE LEGENDS

Fig. 1- Assays used to measure degradation of DNA strands in a duplex incubated with control or A-T nuclear extracts under DNA double-strand break repair conditions. **(A)** PCR-based primer extension assay for measuring degradation of the overhang (Top) strand **(B)** Assay for measuring degradation of the 3'-recessed (Template) strand. Black diamonds (◆) represent nuclease-resistant phosphorothioate linkages while gray circles (●) a 5'Cy3 label. See text for details.

Fig. 2- A-T nuclear extracts show increased DNA end-degradation. **(A)** Top Strand primer extension products following gel separation. The 5'AATTC substrate was incubated with control (WI-38VA13, GM16667) or A-T (AT5BIVA, GM16666) nuclear extracts, isolated and then subjected to a primer extension assay as described in *Materials and Methods*. The duplex (Lane 5) and the 5'Cy3- labeled primer (Lane 6) were incubated in absence of nuclear extract as controls. **(B)** 5'Cy3-labeled Template degradation products following gel separation. The 5'AATTC substrate with a 5'Cy3-labeled Template strand was first incubated with WI-38VA13 (control) and AT5BIVA (A-T) nuclear extracts and then extracted from the reaction. Reactions with duplex only (Lane 3) in the absence of nuclear extract were included as controls.

Fig. 3- Validation of the primer extension assay used for assessment of Top Strand degradation. **(A)** Assay for measuring degradation of a 3'Cy3Sp-labeled Top Strand.

Black diamonds (◆) represent nuclease-resistant phosphorothioate linkages while gray circles (●) a 3'Cy3Sp label. **(B)** 3'Cy3Sp-labeled Top Strand degradation products following gel separation. A 5'AATTC substrate with a 3'Cy3Sp-labeled Top Strand was first incubated with WI-38VA13 (control) and AT5BIVA (A-T) nuclear extracts and then extracted from the reaction. Reactions with duplex only (Lane 3) in the absence of nuclear extract were included as controls.

Fig. 4- Increased DNA end-degradation in A-T nuclear extracts is independent of overhang sequence and length. **(A)** Extension products of Top Strands in various duplexes following gel separation. Substrates with different types of overhangs were first incubated with WI-38VA13 (C) or AT5BIVA (A) nuclear extracts, isolated and then subjected to a primer extension assay. **(B)** Full-length products were quantified for indicated overhangs and expressed as percent intensity (% intensity = (product intensity/total intensity) x 100). Data were generated from three independent experiments. **(C)** Western immunoblots for key double-strand break repair proteins in WI-38VA13 (C) and AT5BIVA (A) nuclear extracts. Nuclear extracts (20 μg) were separated by SDS-PAGE, transferred to PVDF membranes and incubated with various antibodies to detect indicated proteins as described in *Materials and Methods*.

Fig. 5- ATP is required for DNA end-protection. Top strand primer extension products following gel separation. The 5'AATTC substrate was first incubated with WI-38VA13 (C) or AT5BIVA (A) nuclear extracts in the presence or absence of ATP, isolated and

then subjected to a primer extension assay. The duplex (Lanes 5, 6) was also incubated with the reaction buffers (± ATP) in absence of nuclear extract as a control.

Fig. 6- Purified ATM restores DNA end-protection to A-T nuclear extracts. **(A)** Top strand primer extension products following gel separation. The 5'AATTC substrate was first incubated with WI-38VA13 (C) or AT5BIVA (A) nuclear extracts. Purified ATM was added to AT5BIVA extracts at 0.05, 0.1 and 0.2 nM (Lanes 5-7 and 11-13). The 5'Cy3-labeled primer (Lanes 1 and 2) and duplex (Lanes 3 and 4) were also incubated with the reaction buffers (± ATP) as controls. Products were isolated and then subjected to a primer extension assay. **(B)** Western immunoblots for the DNA repair-associated PI-3-kinase-like kinases DNA-PK_{cs}, ATR and ATM performed on the purified ATM preparation. WI-38VA13 (control) nuclear extract was used as a positive control. Purified protein (1 μg) and nuclear extract (20 μg) were separated by SDS-PAGE, transferred to PVDF membranes and incubated with various antibodies to detect indicated proteins as described in *Materials and Methods*.

Fig. 7- PI-3-kinase-like kinase inhibitors prevent DNA end-protection. Top strand primer extension products following gel separation. The 5'AATTC substrate was first incubated with WI-38VA13 (C) or AT5BIVA (A) nuclear extracts. Purified ATM (0.2 nM), wortmannin or caffeine were incorporated into the reaction where indicated. Products were isolated and then subjected to a primer extension assay.

Fig. 8- Autophosphorylation of ATM is insufficient for prevention of DNA end-degradation. **(A)** Top Strand primer extension products following gel separation. The 5'AATTC substrate was first incubated with WI-38VA13 (C) or AT5BIVA (A) nuclear extracts. Pre-phosphorylated ATM, wortmannin (W), caffeine (C) and the phosphatase inhibitor fostriecin were added where indicated. Products were isolated and then subjected to a primer extension assay. **(B)** Autoradiogram of ^{32}P-ATM incubated with AT5BIVA (A-T NE) nuclear extract, wortmannin and a duplex with a 5'AATTC overhang under repair reaction conditions with or without fostriecin. ^{32}P-ATM was monitored in parallel with reactions in 7A to ensure that pre-phosphorylated ATM remained phosphorylated in the reactions.

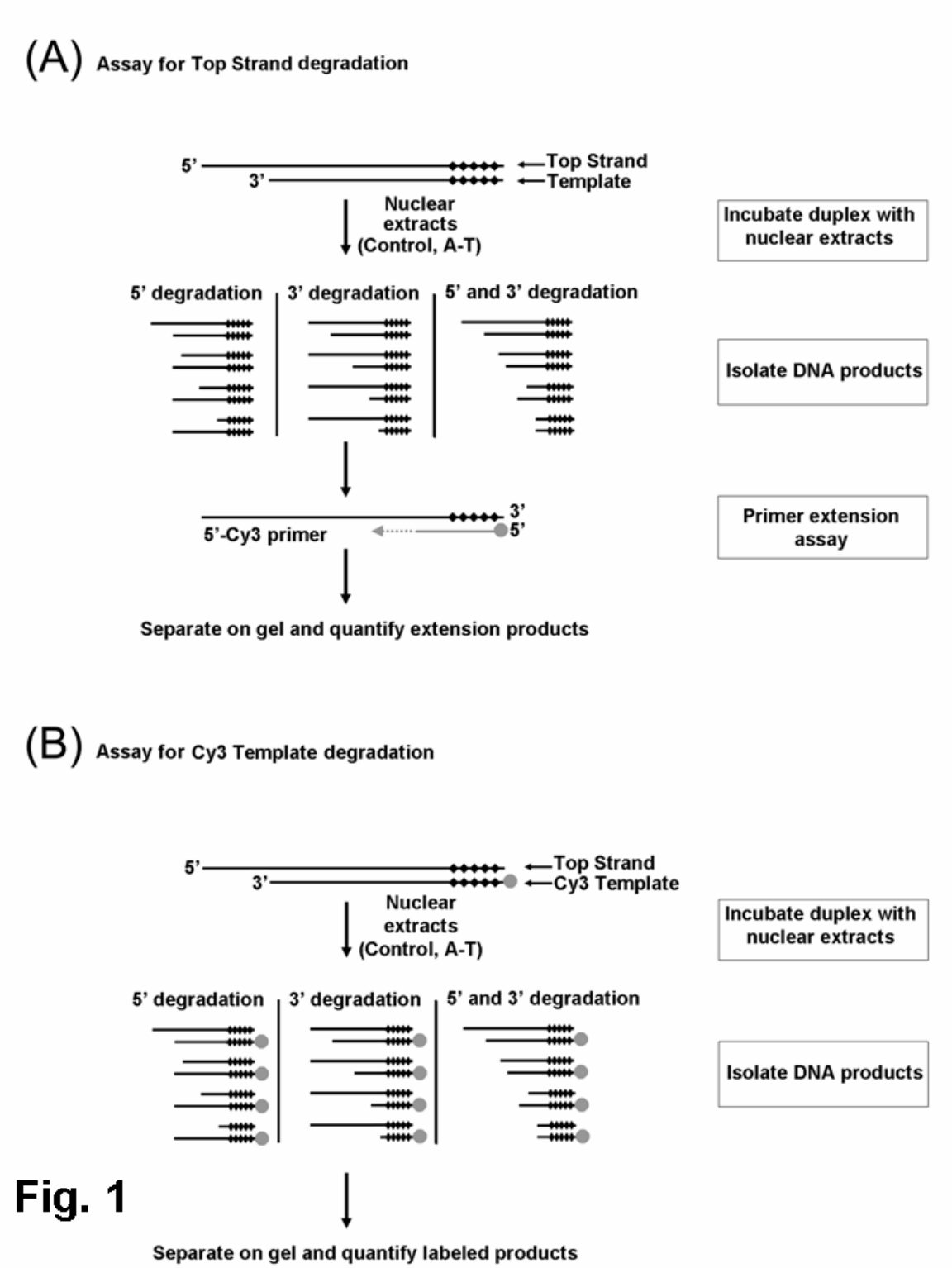
(A) Assay for Top Strand degradation
5'
3'
Top Strand
Template
Nuclear extracts (Control, A-T)
Incubate duplex with nuclear extracts
5' degradation
3' degradation
5' and 3' degradation
Isolate DNA products
3'
5'
5'-Cy3 primer
Primer extension assay
Separate on gel and quantify extension products
(B) Assay for Cy3 Template degradation
5'
3'
Top Strand
Cy3 Template
Nuclear extracts (Control, A-T)
Incubate duplex with nuclear extracts
5' degradation
3' degradation
5' and 3' degradation
Isolate DNA products
Separate on gel and quantify labeled products

Fig. 1

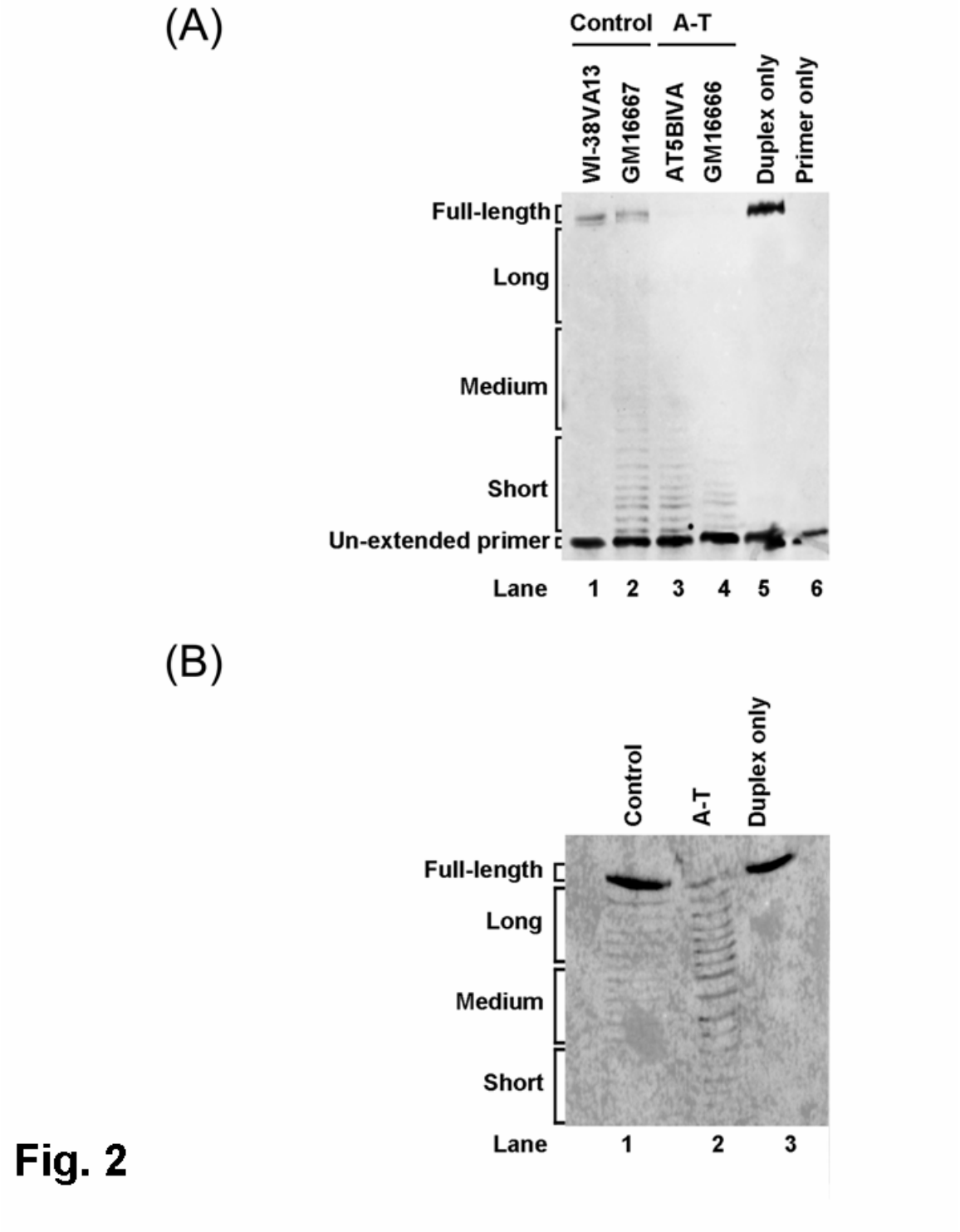
(A)
Control
A-T
WI-38VA13
GM16667
AT5BIVA
GM16666
Duplex only
Primer only
Full-length
Long
Medium
Short
Un-extended primer
Lane 1 2 3 4 5 6
(B)
Control
A-T
Duplex only
Full-length
Long
Medium
Short
Lane 1 2 3

Fig. 2

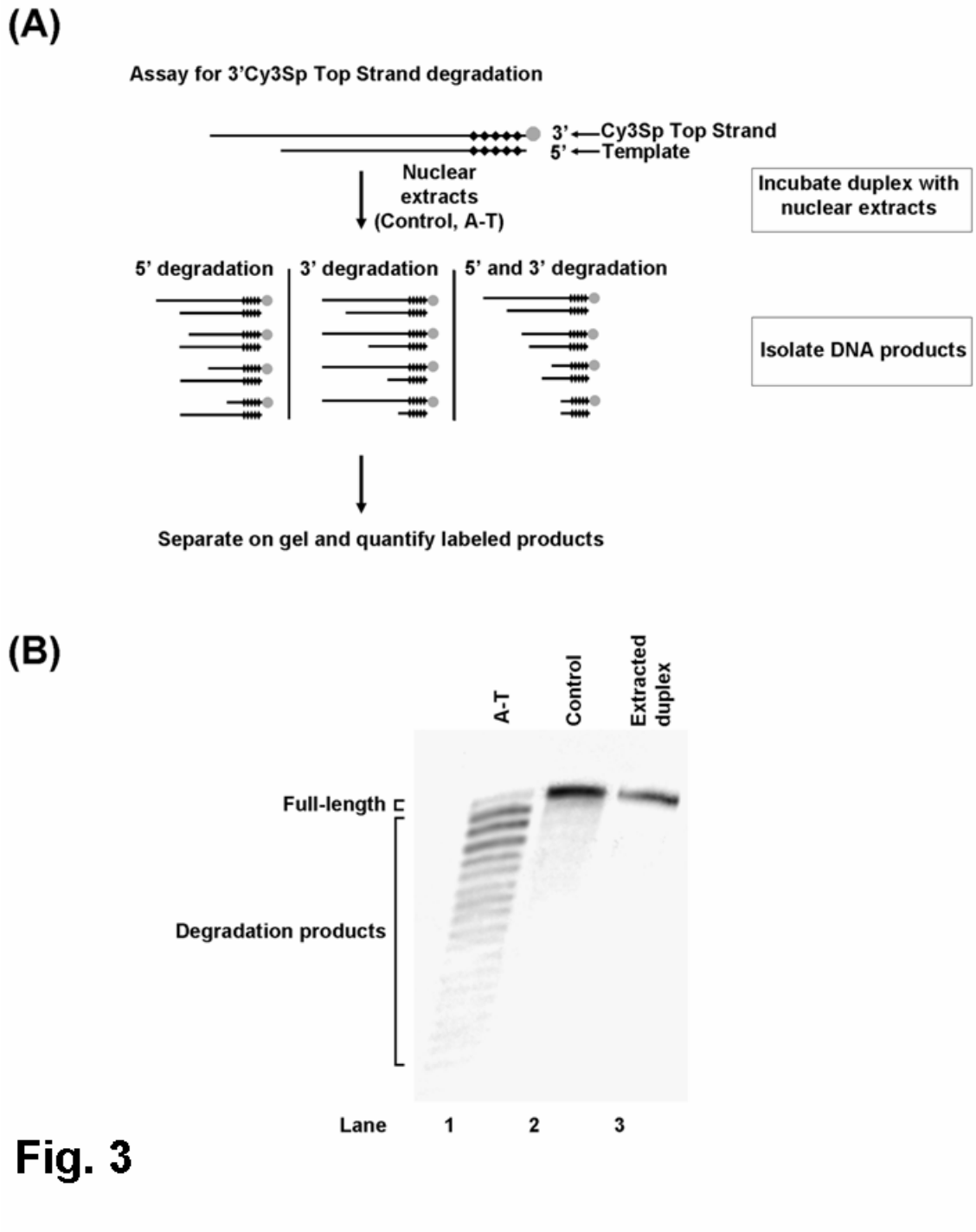
(A)
Assay for 3'Cy3Sp Top Strand degradation
3' ←Cy3Sp Top Strand
5' ←Template
Nuclear extracts (Control, A-T)
Incubate duplex with nuclear extracts
5' degradation
3' degradation
5' and 3' degradation
Isolate DNA products
Separate on gel and quantify labeled products
(B)
A-T
Control
Extracted duplex
Full-length
Degradation products
Lane 1 2 3

Fig. 3

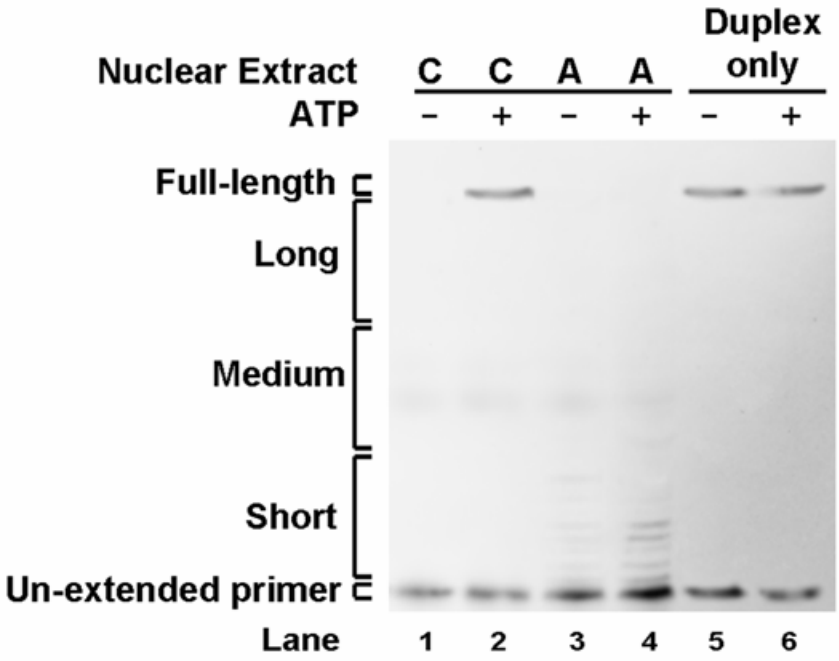
Nuclear Extract
C C A A Duplex only
ATP
– + – + – +
Full-length
Long
Medium
Short
Un-extended primer
Lane
1 2 3 4 5 6

Fig. 4

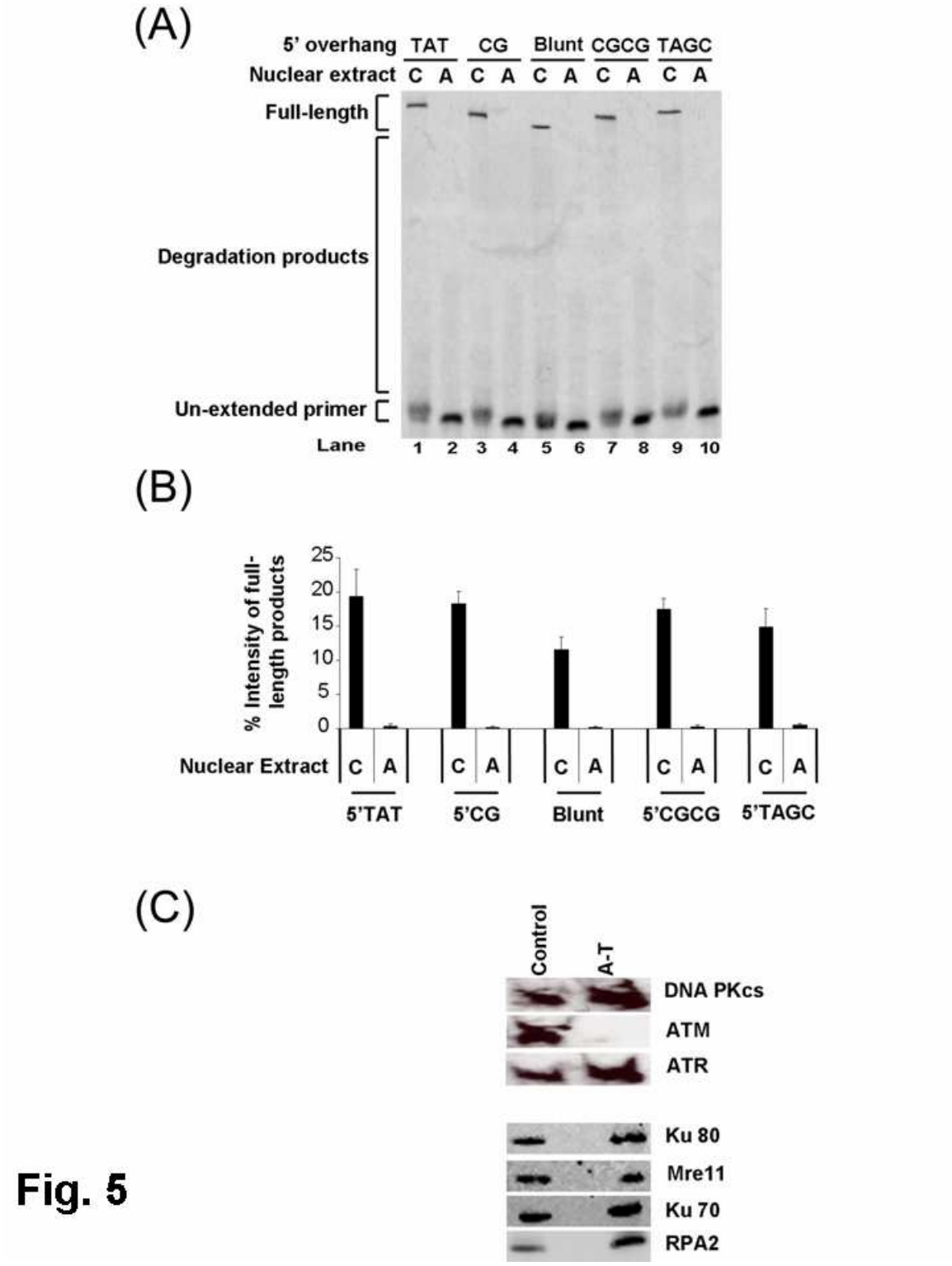
(A)
5' overhang
TAT
CG
Blunt
CGCG
TAGC
Nuclear extract
C A C A C A C A C A
Full-length
Degradation products
Un-extended primer
Lane
1 2 3 4 5 6 7 8 9 10
(B)
% Intensity of full-length products
25
20
15
10
5
0
Nuclear Extract
C A C A C A C A C A
5'TAT
5'CG
Blunt
5'CGCG
5'TAGC
(C)
Control
A-T
DNA PKcs
ATM
ATR
Ku 80
Mre11
Ku 70
RPA2

Fig. 5

(A)

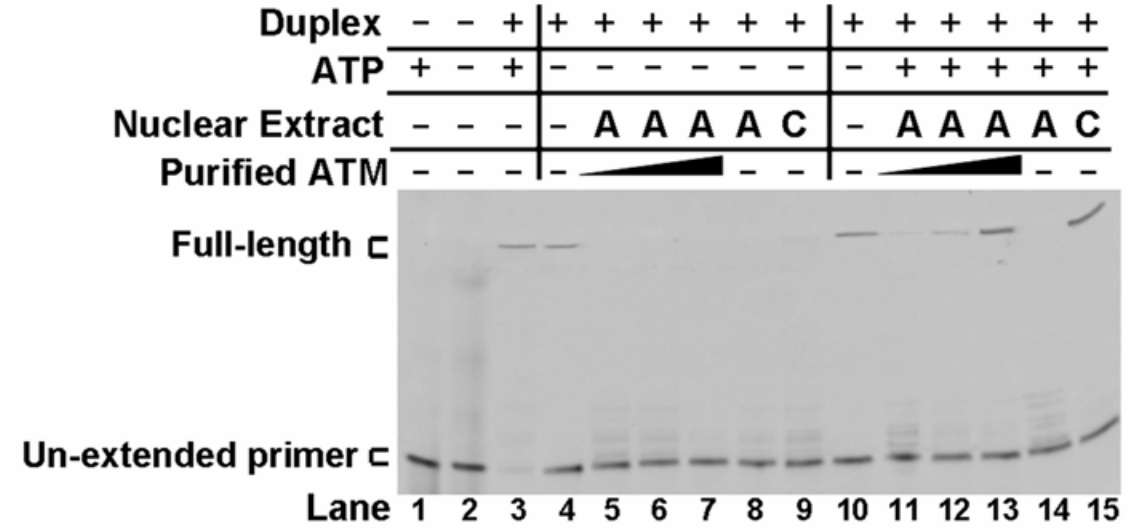
Duplex
ATP
Nuclear Extract
Purified ATM
Full-length
Un-extended primer
Lane
1 2 3 4 5 6 7 8 9 10 11 12 13 14 15

(B)

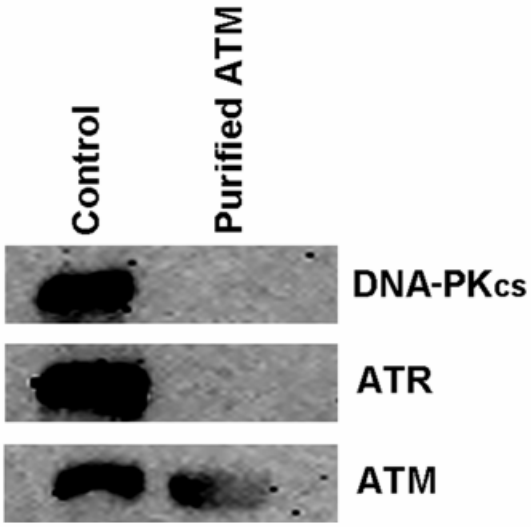
Control
Purified ATM
DNA-PKcs
ATR
ATM

Fig. 6

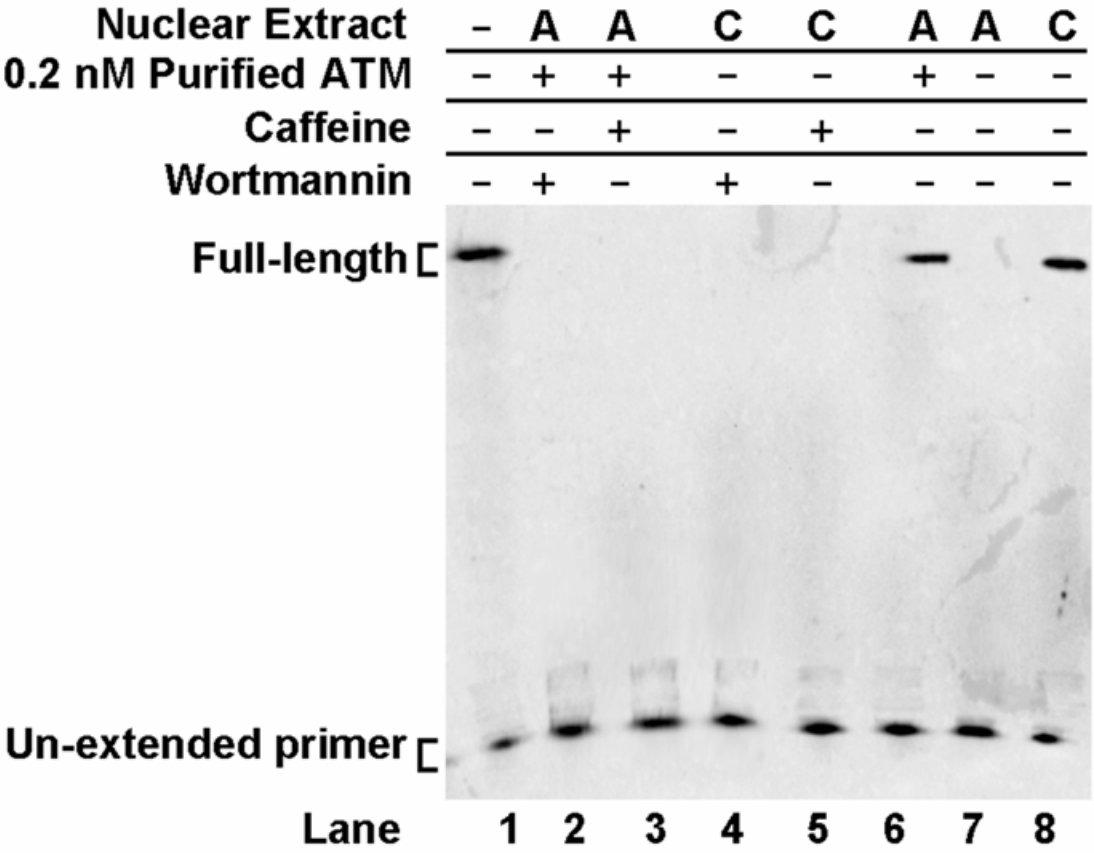
Nuclear Extract – A A C C A A C
0.2 nM Purified ATM – + + – – + – –
Caffeine – – + – + – – –
Wortmannin – + – + – – – –
Full-length
Un-extended primer
Lane 1 2 3 4 5 6 7 8

Fig. 7

(A)

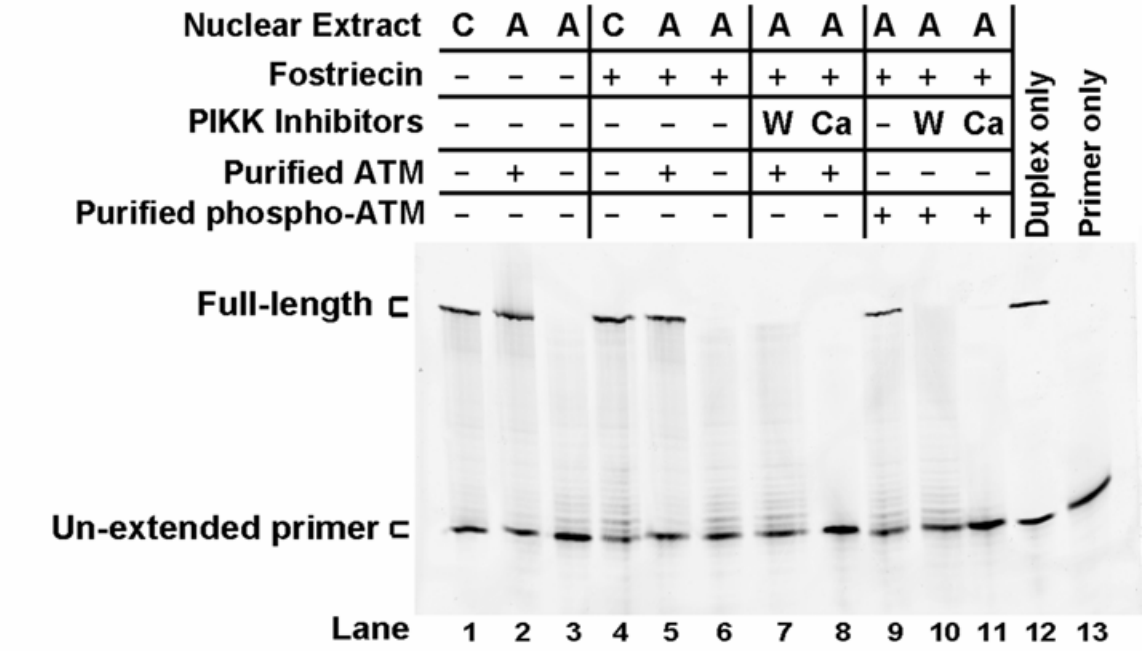
Nuclear Extract C A A C A A A A A A A
Fostriecin – – – + + + + + + + +
PIKK Inhibitors – – – – – – W Ca – W Ca
Purified ATM – + – – + – + + – – –
Purified phospho-ATM – – – – – – – – + + +
Duplex only
Primer only
Full-length
Un-extended primer
Lane 1 2 3 4 5 6 7 8 9 10 11 12 13

(B)

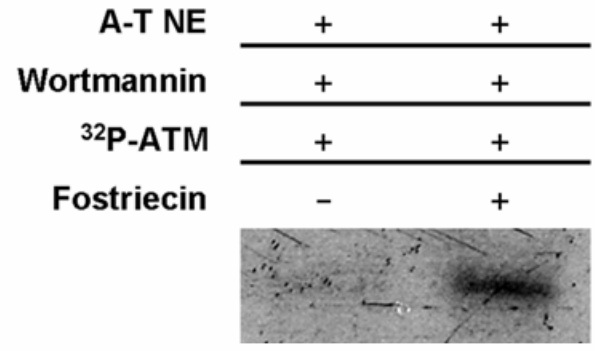
A-T NE + +
Wortmannin + +
32P-ATM + +
Fostriecin – +

Fig. 8

APPENDIX B: ATM REGULATES MRE11-DEPENDENT DNA END-DEGRADATION AND MICROHOMOLOGY-MEDIATED END JOINING

ATM Regulates Mre11-Dependent DNA End-Degradation and Microhomology-Mediated End Joining

Elias A. Rahal[a], Leigh A. Henricksen[a] and Kathleen Dixon[a,b]

[a]*Department of Molecular & Cellular Biology ,University of Arizona, Tucson, AZ 85721, USA.*

[b]*The Arizona Cancer Center, Tucson, AZ 85724, USA.*

* *Corresponding author*: Department of Molecular and Cellular Biology, University of Arizona, Life Sciences South 444A, P.O. Box 210106, Tucson, AZ 85721. Tel.: +1 520 621 7563; fax: +1 520 621 3709.

E-mail address: dixonk@email.arizona.edu (K. Dixon).

Abstract

ATM, the kinase defective in the autosomal recessive syndrome ataxia telangiectasia, is involved in DNA double-strand break-repair and cell-cycle control pathways. We previously reported elevated levels of deletions and error prone double-strand break-repair via microhomology-mediated end joining (MMEJ) in ATM-deficient (A-T) nuclear extracts when compared to controls (ATM+). To assess the involvement of enhanced nuclease activities in A-T extracts we studied the stability of DNA duplex substrates in A-T and control nuclear extracts under DSB repair conditions. We observed a marked increased in DNA end-degradation in A-T nuclear extracts compared to controls. We here report that this repression of degradation by ATM is dependent on its kinase activities. Assessment of DNA substrate stability in extracts from kinase-dead ATM-expressing cells showed elevated degradation levels. This indicated a role for ATM in preventing the degradation of DNA ends, possibly through inhibiting nucleases implicated in MMEJ, such as Mre11. Therefore, we assessed DNA end-stability in Mre11-depleted nuclear extracts and in extracts treated with the Mre11 nuclease inhibitor, Mirin. This resulted in decreased DNA degradation levels in both control and A-T extracts. Knockdown of Mre11 levels also resulted in enhanced DNA end-stability in nuclear extracts. Assessment of MMEJ using an *in vivo* reporter assay system revealed decreased levels of MMEJ repair in Mre11-knockdown cells and in those treated with Mirin. Our results indicate that the Mre11 nuclease plays a role in MMEJ in mammalian cells and that ATM has a regulatory function in the control of error-prone DSB repair and preservation of DNA end-stability at a break.

Key Words: ATM; Mre11; MRN complex; DNA degradation; Double-strand break repair; Microhomology-mediated end joining; PI-3-kinase-like kinases.

1. Introduction

Deficiencies in mediators that participate in genomic maintenance are associated with several disorders characterized by genetic instability, cancer, abnormal development and neurodegeneration (1, 2). Involved proteins frequently have dual tasks as both cell cycle checkpoint and DNA repair mediators. One such example is the ataxia telangiectasia mutated (ATM) protein. A defect in ATM results in ataxia telangiectasia, a human autosomal recessive disorder characterized by neurodegeneration, genetic instability, immunological malfunctions and a propensity for cancer development (3). ATM has an established role in activating checkpoints that halt cell cycle progression in response to a DNA double-strand break (DSB) in mammalian cells (4). However, the functions it may actively engage in during the repair of such a break have remained elusive.

In a previous report we demonstrated that the fidelity of repairing a plasmid harboring a DSB was compromised in nuclear extracts from human ATM-deficient (A-T) cells (5). The mutation frequency was significantly higher in A-T nuclear extracts than in controls. Repaired plasmids harbored deletions spanning the repaired DSB site with rejoining occurring at sequences of microhomology (1-5 nucleotide repeats) flanking the break. This resulted in deletion of the sequences between the two sites of microhomology in addition to the loss of one microhomology site. This type of lesion is the product of repairing a break site via an alternative pathway of DSB repair termed microhomology-mediated end joining (MMEJ). Although the focus of the literature has been on the two major pathways through which a DSB is repaired, non-homologous end-joining (NHEJ) and homologous recombination (HR), it has become evident in recent years that other

"backup" or "alternative" pathways, such as MMEJ, exist (6-11). The mediators implicated in these pathways and their regulation, however, require further elucidation.

Studies in yeast indicate that the Mre11 exonuclease has a major role in MMEJ (12, 13). Moreover, biochemical studies performed with purified recombinant human Mre11 corroborate the ability of this nuclease to mediate MMEJ *in vitro* (14); nevertheless, the role it actually plays in MMEJ repair in mammalian systems has not been clarified. Mre11 is a member of the mammalian MRN (Mre11-Rad50-Nbs1) complex that seems to play a role in recognition and sensing of a DSB. This complex rapidly migrates to DSB sites (15) and recruits ATM. Through interacting with Nbs1, ATM undergoes trans-autophosphorylation and monomerization thus initiating a signaling cascade that results in activating DNA repair and cell cycle control machinery (16). Among ATM's substrates is the MRN complex itself; hence, this complex has functions upstream and downstream of ATM activation (17-19).

An increased frequency of MMEJ in A-T nuclear extracts suggested that ATM suppresses this pathway, perhaps by hindering degradation of DNA ends at a break. Consequently, we examined whether the stability of DNA ends was compromised in A-T nuclear extracts (20). We studied the degradation of short duplex oligonucleotide substrates harboring a single nuclease-susceptible double-stranded end in A-T and control nuclear extracts. Examining the degradation of blunt-ended substrates and of those with various types of overhangs revealed enhanced degradation in A-T nuclear extracts over controls. Furthermore, degradation was enhanced on both strands at the DNA end. Addition of purified ATM to A-T nuclear extracts restored end-stability to levels detected

in control extracts. In the current study we explore the function of ATM's kinase activity in suppressing degradation at DNA ends and the role played by the Mre11 nuclease in this degradation. Moreover, we show that Mre11 partakes in MMEJ in mammalian cells under regulation by ATM.

2. Materials and methods

2.1 Cell culture and preparation of nuclear extracts

AT5BIVA, a SV40-transformed A-T fibroblast cell line, was obtained from the Coriell Cell Repository (Coriell Institute of Medical Research, Camden, NJ). The SV40-transformed human lung fibroblast cell line, WI38VA13, was obtained from ATCC (American Type Culture Collection, Manassas, VA) and was used as a control cell line for AT5BIVA. Maintenance of cell cultures and preparation of nuclear extracts were performed as previously described (20).

2.2 Transient kinase dead (KD)-ATM expression

The KD-ATM expression plasmid was a generous gift from M. Kastan. Cells grown on 150mm plates in antibiotic-free DMEM supplemented with 10% FBS were allowed to reach a confluency of 60%. The medium was replaced with antibiotic and serum-free DMEM and then transfected with the KD-ATM plasmid or a pEGFP-C3 transfection control. Lipofectin (Sigma, St. Louis, MO) was used as a transfection reagent according to manufacturer protocols. After an overnight incubation with the transfection medium at 37°C in 5% CO2, the medium was replaced with DMEM containing 10% FBS and cells were then incubated for 48 hrs to allow expression. Growth medium was then replaced with DMEM containing 10% FBS and supplemented with 1.5 mg/ml Geneticin to select for KD-ATM expressing cells. After 48 hrs, cells were washed and harvested for preparing nuclear extracts as previously described (20).

2.3 Assessment of kinase dead (KD)-ATM expression

To verify the expression of KD-ATM, ATM was immunoprecipitated from nuclear extracts and the precipitates tested in a kinase assay as previously described (21) with some modification. To immunoprecipitate ATM, rProtein G agarose beads (Invitrogen Corporation, Carlsbad, CA) were preblocked overnight in IP buffer (50mM Tris Cl pH 7.5, 300mM NaCl, 10% Glycerol, 1% Triton-X, 1mM PMSF, 1mM DTT) containing 3% BSA and supplemented with Complete, Mini, EDTA-free Protease Inhibitor Cocktail (Roche Diagnostics GmbH, Mannheim, Germany) used according to manufacturer recommendations. Nuclear lysates were pre-cleared by incubation with the pre-blocked rProtein G agarose beads to eliminate kinases that bind non-specifically to the beads. Per 50 μg of nuclear extract, 20 μl of pre-blocked beads were drained from the pre-blocking buffer and added to the extracts. Reactions were tumbled at 4°C for 30 min, centrifuged at 5000 rpm for 1 min, and the beads were then discarded. The process was then repeated and the extracts were pre-cleared three times. Per 50 μg of extract that went through the pre-clearing procedure, 2.5 μg of mouse anti-ATM (Sigma, St. Louis, MO) was added and the reactions were tumbled overnight at 4°C. Then, 20 μl of pre-blocked beads were added and the reactions were tumbled at 4°C for 3 hrs. Beads were then collected by centrifugation at 5000 rpm for 1 min, washed three times with IP buffer, once with Tris/LiCl buffer (100mM Tris Cl pH 7.5, 0.5 M LiCl) and twice with kinase buffer (10 mM HEPES pH7.5, 50mM NaCl, 10mM $MgCl_2$, 10mM $MnCl_2$, 5μM ATP). To perform the kinase assay, following the final wash, beads were resuspended in 20 μl of kinase

buffer in the presence of 1μg PHAS-I (Stratagene, La Jolla, CA) and 3.33 pmol of [γ-^{32}P] ATP. Reactions were then run on 12% denaturing-polyacrylamide gels which were later dried and exposed to a storage phosphor screen (GE Healthcare, Princeton, NJ) for autoradiography and phosphoimage analysis. Exposed screen was scanned with a Typhoon 9410 Variable Mode Imager (GE Healthcare, Princeton, NJ) and analyzed using ImageQuant v5.2 software (Molecular Dynamics, Amersham Biosciences, Princeton, NJ).

2.4 Mre11 Immunodepletion

To prepare Mre11-immunodepleted nuclear extracts a ratio of 50:1 (w/w) of nuclear extract to rabbit anti-Mre11 (Abcam, Inc., Cambridge, MA) was mixed by tumbling at 4°C overnight. Then, 30 μl of protein G magnetic beads (New England Biolabs, Ipswich, MA) per 50 μg of extract originally used were added to the protein-antibody complexes and mixed by tumbling for 3 hrs at 4°C. The magnetic beads were removed from the extracts by separation on a magnetic rack and the immunodepleted supernatants were collected.

2.5 Knockdown of Mre11 Expression

To knockdown Mre11, cells at a confluency of 50% were transduced with lentiviral particles encoding shRNA for Mre11 in DMEM containing Polybrene (Sigma, St. Louis, MO) at a concentration of 8μg/ml. Two shRNA sequences from the MISSION^{TM} TRC

shRNA Target Set NM_005591 (Sigma, St. Louis, MO) were used. The two plasmids used had Sigma reference numbers TRCN0000039868, referred to as Mre11 sh3 in the text, and TRCN0000039872, referred to as Mre11 sh4. Cells were incubated with the virus particles overnight, medium was replaced with DMEM containing 10% FBS and the cells were tested for expression or employed in subsequent experiments 48 hours later.

2.6 Western Immunoblotting

Samples (20 μg) were incubated at 100°C for 5 min in Laemmli sample buffer and then electrophoresed on12% denaturing-polyacrylamide gels. Proteins were transferred to Trans-Blot Medium nitrocellulose membranes (Bio-Rad Laboratories, Hercules, CA), probed and then visualized with the SuperSignal West Dura Extended Duration Substrate (Pierce Biotechnology, Inc., Milwaukee, WI). The FluorChem system (Alpha Innotech Corporation, San Leandro, CA) was used for gel documentation. The Mre11 (1:70,000) primary antibody was obtained from Abcam, Inc. (Cambridge, MA). The GFP (1:1000) primary antibody was obtained from Santa Cruz Biotechnology, Inc (Santa Cruz, CA). The G6PD (1:10,000) primary antibody was purchased from GeneTex, Inc. (Irvine, CA).

2.7 Duplex oligonucleotide substrates

Duplex DNA substrates were generated and employed in the DNA end-processing assay to assess degradation in the nuclear extracts tested. To examine 3’ recessed strand degradation a 71nt Template strand harboring a Cy3 moiety at its 5’ end was hybridized

to a 76nt Top Strand. The 5' end of the 71nt Template and the 3' end of the 76nt Top Strand were protected from nuclease mediated degradation by phosphorothioate bonds linking the last six bases at those ends. To examine 5' end-degradation, a 50nt Top Strand harboring a Cy3sp moiety at its 3' end was hybridized to a 45nt Template. The 3' end of the 50nt Top Strand and the 5' end of the 45nt Template were protected from nuclease mediated degradation by phosphorothioate bonds linking the last six bases at those ends. Hybridization reaction conditions to generate the duplex substrates have been previously described (20).

2.8 DNA end-processing assay

Assessment of duplex substrate degradation was performed as previously described (20) with some modification. Reactions (25 µl) containing 25 µg of nuclear extract in reaction buffer (65.5 mM Tris-Cl pH 7.5, 10 mM $MgSO_4$, 10mM $MnSO_4$, 91 nM EDTA, 9.1% glycerol, 1mM ATP) and 45 pmoles of a DNA duplex were assembled on ice and then incubated at 30°C for various lengths of time, as described per experiment in the text. Reaction buffer was supplemented with Complete, Mini, EDTA-free Protease Inhibitor Cocktail (Roche Diagnostics GmbH, Mannheim, Germany) used according to the manufacturer's instructions. Where indicated, extracts in reaction buffer were pre-treated for 5 min with Mirin at a concentration of 1 mM prior to addition of the duplex substrates and commencing the end-processing assay. End-processing reactions were stopped by adding 5ul per reaction of a mixture of 2% SDS, 50mM EDTA, and 1mg/ml Proteinase K followed by incubation at 37°C for 15 min.

2.9 Product analysis

Products from the DNA end-processing assay were separated on 12% acrylamide/7 M urea sequencing gels (Sequagel Sequencing System reagents, National Diagnostics, Atlanta, GA). Gels were imaged with a Typhoon 9410 Variable Mode Imager and product intensities determined using ImageQuant v5.2 software. Product intensities were corrected for background and then converted into percent intensities where percent intensity = (product intensity/ total lane intensity) x 100.

2.10 Assessment of microhomology-mediated end joining **in vivo**

To examine MMEJ *in vivo*, the pMMEJ plasmid was constructed. This plasmid was derived from the pEGFP-C3 plasmid by PCR mutagenesis using QuikChange II site-directed mutageesis kit (Stratagene, La Jolla, CA) and employing the mutagenesis primer pair of the following sequences: 5'CAT GGT GAG CAA GGG CGA GTT ACG CTA GGG ATA ACA GGG TAA TAT AGG GGC GAG GAG CTG TTC ACC GGG GTG3' and 5'CAC CCC GGT GAA CAG CTC CTC GCC CCT ATA TTA CCC TGT TAT CCC TAG CGT AAC TCG CCC TTG CTC ACC ATG3'. This resulted in an insertion of 35 bases at nucleotide position 628 of the pEGFP-C3 plasmid within the ORF of the wtEGFP gene. This insertion created an I-*Sce*I megaendonuclease recognition site flanked by two 5 bp microhomologies. The sequence of the insert is underlined in the mutagenesis primer pair. The repair of a linearized pMMEJ plasmid by MMEJ results in reconstitution of the wtEGFP gene and consequently allows expression of EGFP. The pMMEJ plasmid was linearized with I-*Sce*I (New England Biolabs, Ipswich, MA) and

then gel-purified using the Zymoclean gel DNA recovery kit (Zymo Research Corp., Orange, CA).

Cells were grown in 6-well plates in antibiotic-free DMEM supplemented with 10% FBS and allowed to reach a confluency of 60%. The medium was then replaced with antibiotic and serum-free DMEM. Linearized pMMEJ was transfected along with the mCherry transfection control plasmid at a ratio of 4:1 into the cells of interest using the Lipofectin (Sigma, St. Louis, MO) transfection reagent according to manufacturer instructions. Circular pMMEJ was used as control where indicated. Cells were incubated overnight with the transfection medium at 37°C in 5% CO2, the medium was then replaced with DMEM containing 10% FBS and cells were incubated for another 48 hrs. Assessment of EGFP and mCherry expression was conducted using the BD LSR II (BD Biosciences, Franklin Lakes, NJ) cytometer and data was analyzed with the FACSDiva v6.1.1 software. The pMMEJ was transfected in excess of the mCherry plasmid; consequently, cells expressing EGFP only were disregarded. The percentage of EGFP expression, and consequently that of MMEJ, was calculated using the following formula: %EGFP expression= (number of cells expressing both EGFP and mCherry / number of cells expressing mCherry) x 100. Where indicated in the text, cells were treated with 25 mM Mirin overnight prior to transfection and then this concentration of the Mre11 nuclease inhibitor was maintained in the growth medium after transfection. Alternatively, Mre11 was knocked down, as described above, prior to transfection with the MMEJ assessment plasmids.

3. Results

3.1 Increased DNA end-degradation in extracts from kinase-dead (KD)-ATM expressing cells

We demonstrated in a previous report that ATM suppresses degradation at DNA ends (20). This function of ATM was ATP dependent and was inhibited by the PI3-kinase-like kinase (PIKK) inhibitors caffeine and wortmannin. The addition of pre-phosphorylated ATM to an ATM-deficient nuclear extract did not succeed in restoring DNA end-stability to levels observed in control extracts (wtATM+). These pieces of evidence taken together suggested that the kinase activity of ATM itself may be required for suppression of DNA end-degradation. To test this possibility we expressed kinase-dead (KD)-ATM in both A-T and control (wtATM+) fibroblasts. In this form of ATM two key catalytic amino acid residues in the kinase active site are substituted (Asp^{2870}→Ala, Asn^{2875}→Lys) hence rendering the kinase inactive (21).

The kinase status of ATM in the KD-ATM expressing cells was assessed by testing the ability of immunoprecipitated ATM from their respective nuclear extracts to phosphorylate PHAS-I (Fig.1A). Nuclear extracts were prepared and ATM was then immunoprecipitated using mouse anti-ATM that was later bound to rProtein G agarose beads. The beads from the immunoprecipitation reactions were incubated with PHAS-I and [γ-^{32}P]ATP. As previously reported (21, 22), the expression of KD-ATM in control (wtATM+) cells imparts a dominant negative effect on these cells; we observed an 80% reduction in phosphorylation of the PHAS-I substrate in nuclear extracts from KD-ATM expressing control cells compared to their non-expressing counterparts (compare Lane 1

to Lane 2 in Fig. 1A). As expected, the expression of KD-ATM in A-T cells did not affect the incapability of extracts from these cells to phosphorylate PHAS-I. Residual phosphorylation of PHAS-I in nuclear extracts from A-T cells and cells expressing KD-ATM can be attributed to a kinase that non-specifically binds to the employed rProtein G agarose beads.

Nuclear extracts prepared from KD-ATM expressing cells and their respective controls were tested for their ability to sustain DNA end-stability (Fig. 1B). We employed our previously-described DNA end-processing assay (20) to measure degradation of DNA ends in the various extracts. Briefly, a duplex DNA substrate protected from nuclease-mediated degradation by phosphorothioate linkages on one end and harboring nuclease-susceptible 5' overhang (Top Strand) and 3' recessed (Template) strands was incubated with the extracts for 15min. The 3' recessed strand was labeled at its nuclease-resistant 5' end with a Cy3 fluorescent marker thus permitting the monitoring of degradation of this strand on a sequencing-grade gel. As we previously reported (20), a sharp decline in the level of full-length strand was observed in the A-T nuclear extracts. We detected a 90% decrease in full-length product in A-T nuclear extracts when compared to controls (compare Lane 4 to Lane 2 in Fig.1B). On the other hand, expression of KD-ATM in the controls led to a 60% decrease in detection of full-length product and an increase in the levels of degradation products (compare Lane 2 to Lane 3 in Fig.1B). No marked differences were observed between extracts from A-T cells and A-T cells expressing KD-ATM. This increase in degradation in extracts from control cells

expressing KD-ATM indicates that ATM engages via its kinase activity in suppressing the degradation of DNA ends.

3.2 Decreased levels of DNA degradation in Mre11-immunodepleted nuclear extracts

The dependence of DNA stability on the kinase activity of ATM suggested that this PIKK regulates the activities of nucleases participating in end-degradation by phosphorylating downstream mediators. One candidate nuclease that may be regulated by ATM is the MRN nuclease complex. This complex is composed of the Mre11 nuclease, the Rad50 ATPase/adenylate kinase and Nbs1, a component that mediates interactions with multiple proteins including ATM (23). Nbs1 is phosphorylated by ATM in response to DNA damage (17, 18) and ATM-dependent phosphorylations of Mre11 (24) and Rad50 (25) have also been described.

To investigate the role of Mre11 in the elevated degradation levels observed in our A-T extracts, we immunodepleted Mre11 from A-T and control nuclear extracts using rabbit anti-Mre11 bound to protein G magnetic beads. Immunodepletion efficiencies were then assessed by probing for Mre11 on a western immunoblot (Fig.2). An 80-90% decrease in Mre11 levels was detectable in extracts immunodepleted with an Mre11 antibody when compared to non-depleted extracts (compare Lanes 1 and 3 to Lanes 2 and 4 in Fig.2).

Immunodepleted extracts were then utilized in an end-processing assay similar to the one described in the previous section. However, a time-course was implemented in

the assessment of DNA degradation (Fig.3A). A slight increase in detection of full-length products at the various time-points tested was noted in the control extracts after Mre11 immunodepletion. In stark contrast, immunodepletion of Mre11 from A-T nuclear extracts resulted in a notable increase in full-length products (Fig.3B). The maximal difference was noted after 15 minutes of incubating the DNA substrate in the nuclear extracts (compare Lane 15 to Lane 17 in Fig3A). At that time point, a 6-fold increase in full-length products was seen in Mre11-immunodepleted A-T nuclear extracts when compared to non-depleted A-T extracts. At that time point, a 12% increase in full-length product level was detected in depleted control extracts compared to respective non-depleted ones (compare Lane 14 to Lane 16 in Fig.3A). This indicates that the uncontrolled degradation process seen to decrease upon Mre11-immunodepletion in A-T extracts is more tightly regulated in the control extracts. This, consequently, limits the margin of enhancing full-length product detection in control extracts.

3.3 Reduced levels of DNA degradation in nuclear extracts treated with Mirin, the Mre11 nuclease inhibitor

A potential pitfall of immunodepleting Mre11 is that along with the nuclease we may have immunoprecipitated other mediators directly responsible for the detected degradation and that interact with Mre11. Thus, to overcome this possibility, we used the Mre11 nuclease inhibitor Z-5-(4-hydroxybenzylidene)-2-imino-1,3-thiazolidin-4-one, more commonly know as Mirin (26). This inhibitor has been shown to suppress DNA degradation by purified Mre11 *in vitro* and to inhibit cellular pathways mediated by the

nuclease *in vivo* (27). Nuclear extracts from A-T and control cells were pre-incubated with Mirin prior to employing them in an end-processing assay.

Mirin-treated extracts were first tested for the degradation of the 3' recessed strand in a short oligonucleotide duplex as delineated above (Fig.4A). Degradation was examined at various time- points. As observed with the Mre11-immunodepletion experiments, improving full-length product detection, and therefore decreasing DNA 3' end-degradation, was limited in Mirin-treated control extracts (Fig.4B). Maximal increase in remaining full-length products in the Mirin-treated controls was by 20% over non-treated control extracts after 15 minutes of incubating the DNA duplex substrates with the extracts (compare Lane 10 to Lane 12 in Fig.3A). At the same time point, in Mirin-treated A-T nuclear extracts the level of full-length product retained after the degradation reaction was 3.5-fold that in non-treated A-T nuclear extracts (compare Lane 11 to Lane 13 in Fig.3A). The difference seen between Mirin-treated A-T and control extracts stresses again the tighter regulation of aberrant nuclease function when ATM is present. Enhancing full-length product detection in A-T extracts after pre-incubation with the Mre11nuclease inhibitor was less than that observed after Mre11-immunodepletion. This may indicate that accessory nucleases that participate in DNA degradation co-immunoprecipitate with Mre11 in the depletion reactions.

To assess 5' end-degradation in Mirin-treated nuclear extracts, the Top Strand was labeled at its nuclease-resistant 3' end with a Cy3sp fluorescent marker and incorporated into a duplex DNA substrate. Degradation was monitored at various time-points after incubation of the duplex substrate with Mirin-treated and non-treated extracts

(Fig.5A). The level of full-length product detected (Fig.5B) was slightly higher in the Mirin-treated control extracts than in non-treated controls with an increase by 14% at the 15 min time point (compare Lane 10 to Lane 12 in Fig.5A). On the other hand, the level of Top Strand full-length product retained in A-T nuclear extracts treated with the Mre11 nuclease inhibitor was 2.5-fold that in non-treated A-T nuclear extracts (compare Lane 11 to Lane 13 in Fig.5A). Mre11 preferentially acts as a 3' to 5' exonuclease on 3' recessed strands. It also has endonuclease functions on single-stranded loops (28). Consequently, the decrease in 5' end degradation upon treating nuclear extracts with Mirin may be indicative of inhibition of a direct Mre11 activity on that strand or an indirect inhibition of an accessory nuclease that acts on that end. One possibility is that mediator-facilitated single-stranded loop structures form on that strand thus allowing direct endonuclease degradation by Mre11. The other possibility is that by inhibiting Mre11 with Mirin, the degradation of the 3' end was hindered thus slowing down the kinetics of 5' end-degradation by another nuclease.

3.4 Decreased DNA degradation in Mre11-knocked down nuclear extracts

Levels of Mre11 were knocked down by transducing A-T and control fibroblast cells with lentiviral particles encoding shRNA for Mre11. Knockdown efficiency was tested by probing for Mre11 on a western immunoblot (Fig.6). Nuclease levels were decreased by around 80% (compare Lanes 1, 2, 5, 6 to Lanes 3, 4, 7, 8 in Fig.6). Nuclear extracts from knocked down cells were prepared and tested for DNA end-degradation as described in previous sections.

The degradation levels of both the Template (Fig.7A) and the Top Strand (Fig.7B) were assessed. Levels of full-length products after incubation with nuclear extracts from Mre11-knocked down control fibroblasts for 15 min were increased by 20% over their non-knocked down counterparts (compare Lanes 1 and 2 to Lanes 4 and 5 in both Fig.7A and Fig.7B). Knocking down Mre11 in A-T fibroblasts resulted in a 5-6 fold rescue of full-length product detection for both strands of the duplex DNA substrate (compare Lanes 6 and 7 to Lanes 8 and 9 in both Fig.7A and Fig.7B). Residual Mre11 is potentially responsible for our inability to fully-rescue full-length product detection. Levels of full-length Template in Mre11-knockdown A-T nuclear extracts were around 10% less than respective levels in non-knockdown control extracts (compare Lanes 2 and 3 to Lanes 8 and 9 in Fig.7A). On the other hand, levels of full-length Top Strand in Mre11-knockdown A-T nuclear extracts were around 30% less than respective levels in non-knockdown control extracts (compare Lanes 2 and 3 to Lanes 8 and 9 in Fig.7B). Worth noting is that the increase in levels of full-length product detection after Mre11 knockdown was similar to that obtained after Mre11 immunodepletion but higher than nuclease inhibition with Mirin. This may indicate that the physical presence of Mre11 is required by accessory nucleases that participate in the reaction and whose kinetics are slowed down by inhibition of Mre11's nuclease activity with Mirin.

3.5 Suppression of in vivo *MMEJ after Mirin-treatment or knocking down Mre11*

To assess MMEJ *in vivo*, the pMMEJ plasmid was used (Fig.8A). This plasmid harbors an insertion of 35 bases within the ORF of a wtEGFP gene. This insertion creates an I-

*Sce*I megaendonuclease recognition site flanked by two 5 bp microhomologies. The repair of an I-*Sce*I linearized pMMEJ plasmid by MMEJ results in reconstitution of the wtEGFP gene and consequently allows expression of EGFP. Control and A-T fibroblasts were transfected with linearized pMMEJ and mCherry plasmids, repair was allowed and fluorescent protein expression was analyzed by flow cytometry as described in the methods section. Repair through MMEJ, as indicated by %EGFP expression levels (Fig.8B), was 2.5 folds higher in A-T cell than in controls. This is in accordance with our formerly reported observations when monitoring *in vitro* MMEJ in nuclear extracts (5). Treatment of control fibroblasts with Mirin resulted in a 20% decrease in MMEJ levels and similar results were obtained with Mre11 knockdown. On the other hand, treatment of A-T cells with Mirin or knocking down Mre11 in that background resulted in a 3-fold decrease in MMEJ, down to levels seen in control fibroblasts. Residual MMEJ levels may be due to incomplete inhibition of Mre11 or an Mre11-independent MMEJ pathway. Results from flow cytometry were corroborated with detection of EGFP expression in tested cells on a western immunoblot (Fig.9).

4. Discussion

Neurodegeneration is a prominent feature of the multi-system disorder syndrome ataxia telangiectasia (A-T) (3) . This facet of the disease, unlike its other symptoms, cannot be easily explained by the cell-cycle and repair deficiencies associated with an ATM malfunction. In the present study we show that ATM suppresses an error-prone pathway of DNA double-strand break repair referred to as microhomology-mediated end joining (MMEJ). This pathway results in deletions and rejoining at short regions of homology that surround the break site. This lapse in repair fidelity may be at the basis of the pathobiological mechanisms leading to neuronal degeneration in A-T. Neurocytes are post-mitotic and a deficiency in repair fidelity poses a serious risk that is probably graver in non-dividing cells. On the other hand, the misregulation of aberrant repair discussed herein likely contributes to the genetic instability and propensity for leukemias and lymphomas observed in A-T.

Repair events via MMEJ have been associated with disease processes resulting in chromosomal translocations and tumor-formation (29-33) . We here demonstrate that DNA degradation and consequent microhomology-directed break rejoining involved in this pathway are highly dependent on Mre11 and in particular on its nuclease function. Both Mre11 knockdown and immunodepletion resulted in a decreased level of DNA substrate degradation. This was prominent in ATM-deficient nuclear extracts, which we had previously shown to have a marked elevation in nuclease activity and in MMEJ. Treating these extracts with Mirin, an inhibitor of Mre11 nuclease activity (27), also resulted in decreased substrate degradation, however, not to the extent seen with Mre11

knock down or immunodepletion. This may indicate the participation of one or more accessory nucleases that require the physical presence of Mre11 at the DNA end but whose kinetics are less so dependent on Mre11 nuclease function.

Using an *in vivo* reporter assay system we observed a decrease in MMEJ levels after Mre11 knockdown and after treating cells with Mirin. This is the first direct demonstration of Mre11 involvement as a nuclease in MMEJ *in vivo* in a mammalian system. Previous reports have indicated that purified Mre11 degrades DNA *in vitro* up to regions of microhomology, where it stalls (14). Moreover, recent biochemical evidence from crystal structure analysis implied that Mre11 may be capable of carrying out MMEJ (34). Other mediators have also been associated with this aberrant repair pathway and these include the BLM helicase (35), PARP-1, XRCC1, DNA ligase III (36), the FEN1 endonuclease, DNA polymerase ε (37) and the Exo1 exonuclease (38). Whether these mediators are involved in the Mre11-depedent pathway we report here is under investigation. Given the complexity of DSB repair in mammalian cells it is not unlikely that more than one pathway leads to the formation of MMEJ products.

The regulation of MMEJ and suppression of erroneous repair are other aspects of this pathway that require further exploration. We have previously shown that an ATM deficiency leads to an increase in MMEJ *in vitro* (5). We here recapitulate this observation *in vivo* and demonstrate that Mre11 is the target of this regulation. This increase in MMEJ is not the result of an incapability to rejoin DNA ends in the absence of appropriate ATM function based on the observation that nuclear extracts from both A-T and control cells are equally efficient in rejoining DNA ends (5). The kinase activity of

ATM was necessary for repression of DNA degradation by Mre11. Thus, inhibition of degradation and MMEJ by ATM is probably through phosphorylation of the nuclease complex. ATM has been shown to phosphorylate Nbs1 in response to DNA damage (17, 18) and ATM-dependent phosphorylations of Mre11 (24) and Rad50 (25) have been reported. Worth noting is that examination of MMEJ in yeast has revealed roles for Mre11 and Tel1, the yeast ATM homologue, in promoting MMEJ (12, 13). This discrepancy in ATM and Tel1 functions is probably an indication of the divergence of these two proteins and of the roles they assume. It may also be another demonstration of pathway differences between yeast and mammalian systems. The yeast Dnl4 (DNA ligase 4), for example is required for MMEJ, whereas its mammalian homologue, LIG4, was shown to be dispensable for the pathway (39-42).

Therefore, we conclude that a DSB leads to activation of ATM via the MRN complex. ATM will then regulate, through its kinase activities, the degradation and rejoining of DNA ends. It in particular suppresses erroneous MMEJ repair of the DSB by inhibiting homology-directed DNA degradation mediated by the Mre11 nuclease (Fig.10).

REFERENCES

[1] Peterson CL and Cote J. Cellular machineries for chromosomal DNA repair, Genes Dev. 18 (2004) 602-616.

[2] van Gent DC, Hoeijmakers JHKanaar R. Chromosomal stability and the DNA double-stranded break connection, Nat Rev Genet. 2 (2001) 196-206.

[3] Taylor AM and Byrd PJ. Molecular pathology of ataxia telangiectasia, J Clin Pathol. 58 (2005) 1009-1015.

[4] Lavin MF and Kozlov S. ATM activation and DNA damage response, Cell Cycle. 6 (2007) 931-942.

[5] Li Y, Carty MP, Oakley GG, Seidman MM, Medvedovic MDixon K. Expression of ATM in ataxia telangiectasia fibroblasts rescues defects in DNA double-strand break repair in nuclear extracts, Environ Mol Mutagen. 37 (2001) 128-140.

[6] DiBiase SJ, Zeng ZC, Chen R, Hyslop T, Curran WJ, Jr.Iliakis G. DNA-dependent protein kinase stimulates an independently active, nonhomologous, end-joining apparatus, Cancer Res. 60 (2000) 1245-1253.

[7] Feldmann E, Schmiemann V, Goedecke W, Reichenberger SPfeiffer P. DNA double-strand break repair in cell-free extracts from Ku80-deficient cells: implications for Ku serving as an alignment factor in non-homologous DNA end joining, Nucleic Acids Res. 28 (2000) 2585-2596.

[8] Guirouilh-Barbat J, Huck S, Bertrand P, Pirzio L, Desmaze C, Sabatier LLopez BS. Impact of the KU80 pathway on NHEJ-induced genome rearrangements in mammalian cells, Mol Cell. 14 (2004) 611-623.

[9] Liang F and Jasin M. Ku80-deficient cells exhibit excess degradation of extrachromosomal DNA, J Biol Chem. 271 (1996) 14405-14411.

[10] Wu W, Wang M, Wu W, Singh SK, Mussfeldt TIliakis G. Repair of radiation induced DNA double strand breaks by backup NHEJ is enhanced in G_2, DNA Repair (Amst). 7 (2008) 329-338.

[11] Zhu C, Mills KD, Ferguson DO, Lee C, Manis J, Fleming J, Gao Y, Morton CCAlt FW. Unrepaired DNA breaks in p53-deficient cells lead to oncogenic gene amplification subsequent to translocations, Cell. 109 (2002) 811-821.

[12] Ma JL, Kim EM, Haber JELee SE. Yeast Mre11 and Rad1 proteins define a Ku-independent mechanism to repair double-strand breaks lacking overlapping end sequences, Mol Cell Biol. 23 (2003) 8820-8828.

[13] Lee K and Lee SE. Saccharomyces cerevisiae Sae2- and Tel1-dependent single-strand DNA formation at DNA break promotes microhomology-mediated end joining, Genetics. 176 (2007) 2003-2014.

[14] Paull TT and Gellert M. A mechanistic basis for Mre11-directed DNA joining at microhomologies, Proc Natl Acad Sci U S A. 97 (2000) 6409-6414.

[15] Nelms BE, Maser RS, MacKay JF, Lagally MGPetrini JH. In situ visualization of DNA double-strand break repair in human fibroblasts, Science. 280 (1998) 590-592.

[16] You Z, Chahwan C, Bailis J, Hunter TRussell P. ATM activation and its recruitment to damaged DNA require binding to the C terminus of Nbs1, Mol Cell Biol. 25 (2005) 5363-5379.

[17] Wu X, Ranganathan V, Weisman DS, Heine WF, Ciccone DN, O'Neill TB, Crick KE, Pierce KA, Lane WS, Rathbun G, Livingston DMWeaver DT. ATM phosphorylation of Nijmegen breakage syndrome protein is required in a DNA damage response, Nature. 405 (2000) 477-482.

[18] Lim DS, Kim ST, Xu B, Maser RS, Lin J, Petrini JHKastan MB. ATM phosphorylates p95/nbs1 in an S-phase checkpoint pathway, Nature. 404 (2000) 613-617.

[19] Kim JE, Minter-Dykhouse KChen J. Signaling networks controlled by the MRN complex and MDC1 during early DNA damage responses, Mol Carcinog. 45 (2006) 403-408.

[20] Rahal EA, Henricksen LA, Li Y, Turchi JJ, Pawelczak KSDixon K. ATM mediates repression of DNA end-degradation in an ATP-dependent manner, DNA Repair (Amst). 7 (2008) 464-475.

[21] Canman CE, Lim DS, Cimprich KA, Taya Y, Tamai K, Sakaguchi K, Appella E, Kastan MBSiliciano JD. Activation of the ATM kinase by ionizing radiation and phosphorylation of p53, Science. 281 (1998) 1677-1679.

[22] Lee JH and Paull TT. Direct activation of the ATM protein kinase by the Mre11/Rad50/Nbs1 complex, Science. 304 (2004) 93-96.

[23] van den Bosch M, Bree RTLowndes NF. The MRN complex: coordinating and mediating the response to broken chromosomes, EMBO Rep. 4 (2003) 844-849.

[24] Yuan SS, Chang HL, Hou MF, Chan TF, Kao YH, Wu YCSu JH. Neocarzinostatin induces Mre11 phosphorylation and focus formation through an ATM- and NBS1-dependent mechanism, Toxicology. 177 (2002) 123-130.

[25] Linding R, Jensen LJ, Ostheimer GJ, van Vugt MA, Jorgensen C, Miron IM, Diella F, Colwill K, Taylor L, Elder K, Metalnikov P, Nguyen V, Pasculescu A, Jin J, Park JG, Samson LD, Woodgett JR, Russell RB, Bork P, Yaffe MBPawson T. Systematic discovery of in vivo phosphorylation networks, Cell. 129 (2007) 1415-1426.

[26] Garner KM, Pletnev AAEastman A. Corrected structure of mirin, a small-molecule inhibitor of the Mre11-Rad50-Nbs1 complex, Nat Chem Biol. 5 (2009) 129-130; author reply 130.

[27] Dupre A, Boyer-Chatenet L, Sattler RM, Modi AP, Lee JH, Nicolette ML, Kopelovich L, Jasin M, Baer R, Paull TTGautier J. A forward chemical genetic screen reveals an inhibitor of the Mre11-Rad50-Nbs1 complex, Nat Chem Biol. 4 (2008) 119-125.

[28] Paull TT and Gellert M. The 3' to 5' exonuclease activity of Mre 11 facilitates repair of DNA double-strand breaks, Mol Cell. 1 (1998) 969-979.

[29] Bentley J, Diggle CP, Harnden P, Knowles MAKiltie AE. DNA double strand break repair in human bladder cancer is error prone and involves microhomology-associated end-joining, Nucleic Acids Res. 32 (2004) 5249-5259.

[30] Shin KH, Kang MK, Kim RH, Kameta A, Baluda MAPark NH. Abnormal DNA end-joining activity in human head and neck cancer, Int J Mol Med. 17 (2006) 917-924.

[31] Weinstock DM, Elliott BJasin M. A model of oncogenic rearrangements: differences between chromosomal translocation mechanisms and simple double-strand break repair, Blood. 107 (2006) 777-780.

[32] Windhofer F, Krause S, Hader C, Schulz WAFlorl AR. Distinctive differences in DNA double-strand break repair between normal urothelial and urothelial carcinoma cells, Mutat Res. 638 (2008) 56-65.

[33] Yoshimoto M, Joshua AM, Chilton-Macneill S, Bayani J, Selvarajah S, Evans AJ, Zielenska MSquire JA. Three-color FISH analysis of TMPRSS2/ERG fusions in prostate cancer indicates that genomic microdeletion of chromosome 21 is associated with rearrangement, Neoplasia. 8 (2006) 465-469.

[34] Williams RS, Moncalian G, Williams JS, Yamada Y, Limbo O, Shin DS, Groocock LM, Cahill D, Hitomi C, Guenther G, Moiani D, Carney JP, Russell PTainer JA. Mre11 dimers coordinate DNA end bridging and nuclease processing in double-strand-break repair, Cell. 135 (2008) 97-109.

[35] Langland G, Elliott J, Li Y, Creaney J, Dixon KGroden J. The BLM helicase is necessary for normal DNA double-strand break repair, Cancer Res. 62 (2002) 2766-2770.

[36] Audebert M, Salles BCalsou P. Involvement of poly(ADP-ribose) polymerase-1 and XRCC1/DNA ligase III in an alternative route for DNA double-strand breaks rejoining, J Biol Chem. 279 (2004) 55117-55126.

[37] Gottlich B, Reichenberger S, Feldmann EPfeiffer P. Rejoining of DNA double-strand breaks *in vitro* by single-strand annealing, Eur J Biochem. 258 (1998) 387-395.

[38] Decottignies A. Microhomology-mediated end joining in fission yeast is repressed by pku70 and relies on genes involved in homologous recombination, Genetics. 176 (2007) 1403-1415.

[39] Guirouilh-Barbat J, Rass E, Plo I, Bertrand PLopez BS. Defects in XRCC4 and KU80 differentially affect the joining of distal nonhomologous ends, Proc Natl Acad Sci U S A. 104 (2007) 20902-20907.

[40] Corneo B, Wendland RL, Deriano L, Cui X, Klein IA, Wong SY, Arnal S, Holub AJ, Weller GR, Pancake BA, Shah S, Brandt VL, Meek KRoth DB. Rag mutations reveal robust alternative end joining, Nature. 449 (2007) 483-486.

[41] Yan CT, Boboila C, Souza EK, Franco S, Hickernell TR, Murphy M, Gumaste S, Geyer M, Zarrin AA, Manis JP, Rajewsky KAlt FW. IgH class switching and translocations use a robust non-classical end-joining pathway, Nature. 449 (2007) 478-482.

[42] Soulas-Sprauel P, Le Guyader G, Rivera-Munoz P, Abramowski V, Olivier-Martin C, Goujet-Zalc C, Charneau Pde Villartay JP. Role for DNA repair factor XRCC4 in immunoglobulin class switch recombination, J Exp Med. 204 (2007) 1717-1727.

Table 1: Oligonucleotides used to assess DNA degradation.

Name	Length (nt)	Sequence
Top Strand	76	5′ACCCAGAGCTCGGTACCCGGGGATCCTCTAGAGTCGACCTGCAGGCATGCAAGCTTGGCACTGGCCGTCG**TTTTAC**
Cy3 Template	71	3′CTCGAGCCATGGGCCCCTAGGAGATCTCAGCTGGACGTCCGTACGTTCGAACCGTGACCGGCAGC**AAAATG**/Cy3
Cy3Sp Top Strand	50	5′ACCCAAGTCGACCTGCAGGCATGCAAGCTTGGCACTGGCCGTCG**TTTTAC**/Cy3Sp
Template	45	3′TCAGCTGGACGTCCGTACGTTCGAACCGTGACCGGCAGC**AAAATG**

Underlined nucleotides are unpaired in the final substrate. Bold nucleotides are linked by phosphorothioate linkages.

Fig. 1- Enhanced DNA degradation after expression of kinase dead (KD)-ATM. (A) Verification of KD-ATM expression by assessing ^{32}P incorporation into PHAS-I. Nuclear extracts from the ATM+ control fibroblast (CF) cell line WI-38VA13, ATM-deficient (AT) cell line AT5BIVA and corresponding cells transfected with the KD-ATM expression plasmid were prepared. ATM was immunoprecipitated from these extracts and the precipitates were employed in a kinase assay in the presence of PHAS-I as a substrate and [γ-^{32}P]ATP. A reaction containing PHAS-I and [γ-^{32}P]ATP in the absence of a nuclear extract (Lane 3) was included as control. Reactions were subjected to SDS-PAGE and the gel was exposed to a storage phosphor screen which was then scanned. (B) 5'Cy3-labeled Template degradation products following gel separation. A duplex DNA substrate with a 5'Cy3-labeled Template was incubated with nuclear extracts from WI-38VA13 (CF), AT5BIVA (AT) and respective cell lines expressing KD-ATM. A reaction with duplex only (Lane 1) in the absence of nuclear extract was included as control.

Fig. 2- Western immunoblot for Mre11 in immunodepleted nuclear extracts. Following Mre11 immunodepletion from WI-38VA13 (CF) and AT5BIVA (AT) nuclear extracts, supernatants were subjected to SDS-PAGE, transferred to a membrane and then probed for Mre11. RPA2 was assayed for as a loading control.

Fig. 3- Decreased DNA degradation in nuclear extracts after Mre11 immunodepletion. (A) 5'Cy3-labeled Template degradation products following gel separation. A duplex

DNA substrate with a 5'Cy3-labeled Template was incubated with nuclear extracts from WI-38VA13 (CF), AT5BIVA (AT) and respective nuclear extracts that were Mre11-immunodepleted. Degradation was allowed to proceed for 3, 5, 10 or 15 min. A reaction with duplex only (Lane 1) in the absence of nuclear extract was included as control and incubated for 15 min. (B) Plot for % intensities of Full-length products. Full products in 3(A) were quantified and expressed as percent intensity (% intensity = (product intensity/total intensity) x 100).

Fig. 4- Reduced levels of Template degradation in Mirin-treated nuclear extracts. (A) 5'Cy3-labeled Template degradation products following gel separation. A duplex DNA substrate with a 5'Cy3-labeled Template was incubated with nuclear extracts from WI-38VA13 (CF), AT5BIVA (AT) and respective nuclear extracts treated with 1mM Mirin. Degradation was allowed to proceed for 5, 10 or 15 min. A reaction with duplex only (Lane 1) in the absence of nuclear extract was included as control and incubated for 15 min. (B) Plot for % intensities of Full-length products. Full products in 4(A) were quantified and expressed as percent intensity (% intensity = (product intensity/total intensity) x 100).

Fig. 5- Reduced levels of Top Strand degradation in Mirin-treated nuclear extracts. (A) 3'Cy3sp-labeled Top Strand degradation products following gel separation. A duplex DNA substrate with a 3'Cy3sp-labeled Top Strand was incubated with nuclear extracts from WI-38VA13 (CF), AT5BIVA (AT) and respective nuclear extracts treated with

1mM Mirin. Degradation was allowed to proceed for 5, 10 or 15 min. A reaction with duplex only (Lane 1) in the absence of nuclear extract was included as control and incubated for 15 min. (B) Plot for % intensities of Full-length products. Full products in 5(A) were quantified and expressed as percent intensity (% intensity = (product intensity/total intensity) x 100).

Fig. 6- Western immunoblot for Mre11 in nuclear extracts after Mre11 knockdown. Nuclear extracts from WI-38VA13 (CF) and AT5BIVA (AT) were prepared. Extracts were also prepared from respective cells in which Mre11 was knocked down by transduction with lentivirus encoding Mre11 shRNA (Mre11 sh3 and Mre11 sh4). The extracts were subjected to SDS-PAGE, transferred to a membrane and then probed for Mre11. Nuclear extracts from cells plated in virus-free transduction medium (Lanes 1 and 5) or transduced with an empty vector (Lanes 2 and 6) were included as controls. G6PD was probed for as a loading control.

Fig. 7- Reduced levels of DNA degradation in nuclear extracts after Mre11 knockdown. (A) 5'Cy3-labeled Template degradation products following gel separation. A duplex DNA substrate with a 5'Cy3-labeled Template was incubated with nuclear extracts from WI-38VA13 (CF) and AT5BIVA (AT) cells. The duplex was also incubated with respective nuclear extracts from cells in which Mre11 was knocked down by transduction with lentivirus encoding Mre11 shRNA (Mre11 sh3 and Mre11 sh4). Nuclear extracts from cells plated in virus-free transduction medium (Lanes 2 and 6) or transduced with an

empty vector (Lanes 3 and 7) were included as controls. A reaction with duplex only (Lane 1) in the absence of nuclear extract was included as control. (B) 3'Cy3sp-labeled Top Strand degradation products following gel separation. A duplex DNA substrate with a 3'Cy3sp-labeled Top Strand was incubated with nuclear extracts from WI-38VA13 (CF) and AT5BIVA (AT) cells. The duplex was also incubated with respective nuclear extracts from cells in which Mre11 was knocked down by transduction with lentivirus encoding Mre11 shRNA (Mre11 sh3 and Mre11 sh4). Nuclear extracts from cells plated in virus-free transduction medium (Lanes 2 and 6) or transduced with an empty vector (Lanes 3 and 7) were included as controls. A reaction with duplex only (Lane 1) in the absence of nuclear extract was included as control.

Fig. 8- Suppression of *in vivo* MMEJ after Mirin-treatment or knocking down Mre11. (A) Schematic representation of the pMMEJ plasmid used to assess *in vivo* MMEJ repair. The pMMEJ plasmid was derived from the pEGFP-C3 plasmid by an insertion of 35 bp within the ORF of the wtEGFP gene. This creates an I-*Sce*I megaendonuclease recognition site flanked by two 5 bp microhomologies. The repair of a linearized pMMEJ plasmid by MMEJ reconstitutes the wtEGFP gene and allows expression of EGFP. (B) WI-38VA13 (CF) and AT5BIVA (AT) cells were transfected with either linear or circular pMMEJ and with a mCherry transfection control plasmid. Repair was allowed and cells were analyzed for fluorescent protein expression by flow cytometry. Cells treated with 25mM Mirin or in which Mre11 was knocked down by transduction with lentivirus encoding Mre11 shRNA (Mre11 sh3 and Mre11 sh4) were also analyzed. Cells

transduced with empty vector or virus-free transduction medium were included as controls. Repair through MMEJ is represented by %EGFP expression (%EGFP expression= (number of cells expressing both EGFP and mCherry / number of cells expressing mCherry) x 100.

Fig. 9- Western immunoblot for Mre11 and EGFP after MMEJ repair in Mirin-treated or Mre11-knockdown cells. WI-38VA13 (CF) and AT5BIVA (AT) cells were transfected with either linear or circular pMMEJ. Repair was allowed and cell extracts were then prepared. Cells treated with 25mM Mirin or in which Mre11 was knocked down by transduction with lentivirus encoding Mre11 shRNA (Mre11 sh3 and Mre11 sh4) were also analyzed. Cells transduced with empty vector (Lanes 2 and 9) or virus-free transduction medium (Lanes 4 and 10) were included as controls. Transfection with linear pEGFP-c3 was used as an EGFP expression control (Lanes 1 and 7). Cell extracts were subjected to SDS-PAGE, transferred to a membrane and then probed for Mre11 and EGFP. G6PD was assayed for as a loading control.

Fig. 10- Model delineating the role of ATM in suppression of erroneous DSB repair via microhomology-mediated end joining. ATM is activated upon the formation of a DSB. Then, its kinase activity maintains end-stability at a break through suppression of Mre11-dependent microhomology-directed DNA degradation and subsequent end joining.

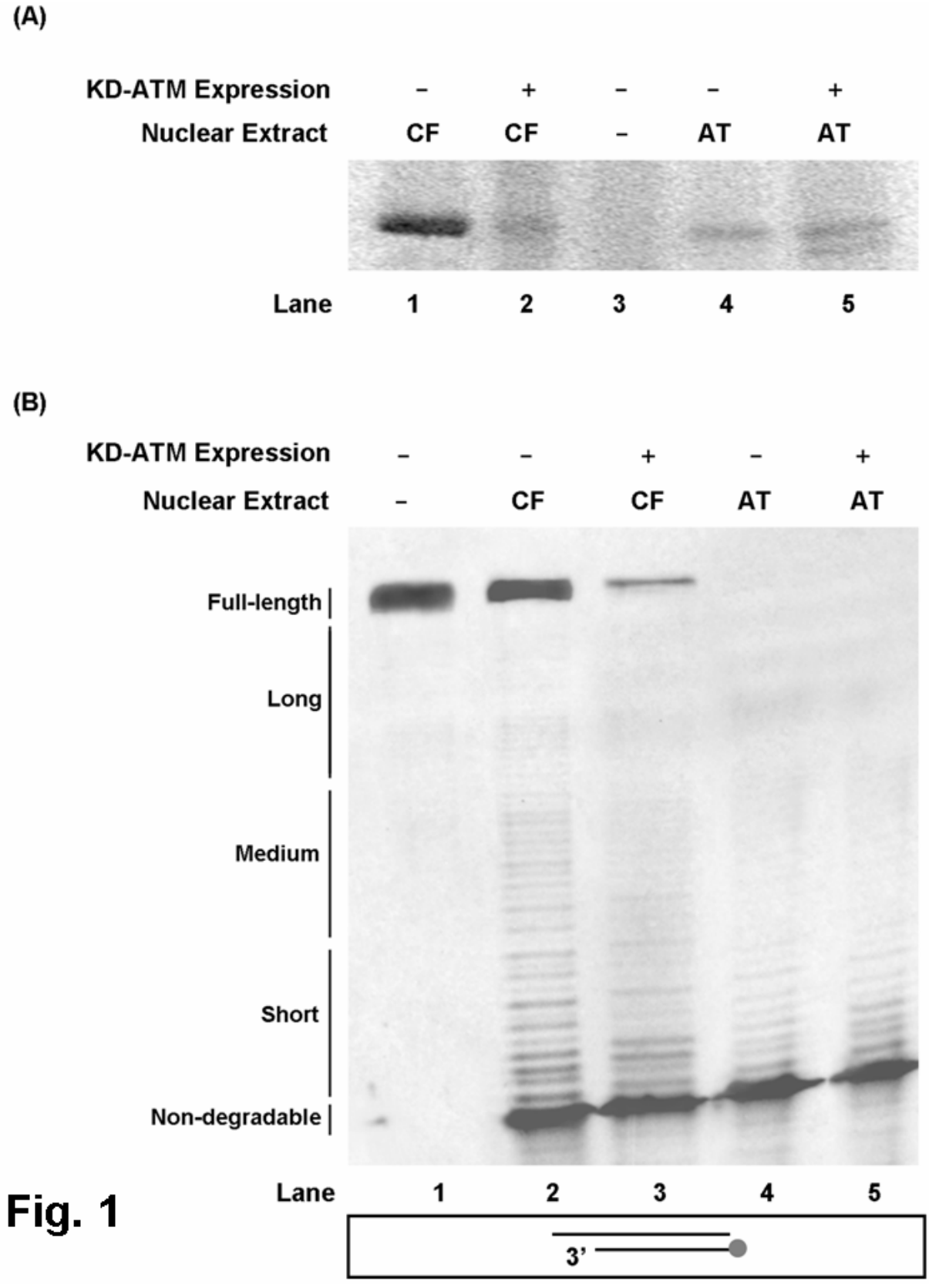
(A)
KD-ATM Expression
Nuclear Extract
CF
AT
Lane
1
2
3
4
5
(B)
KD-ATM Expression
Nuclear Extract
Full-length
Long
Medium
Short
Non-degradable
Lane
3'

Fig. 1

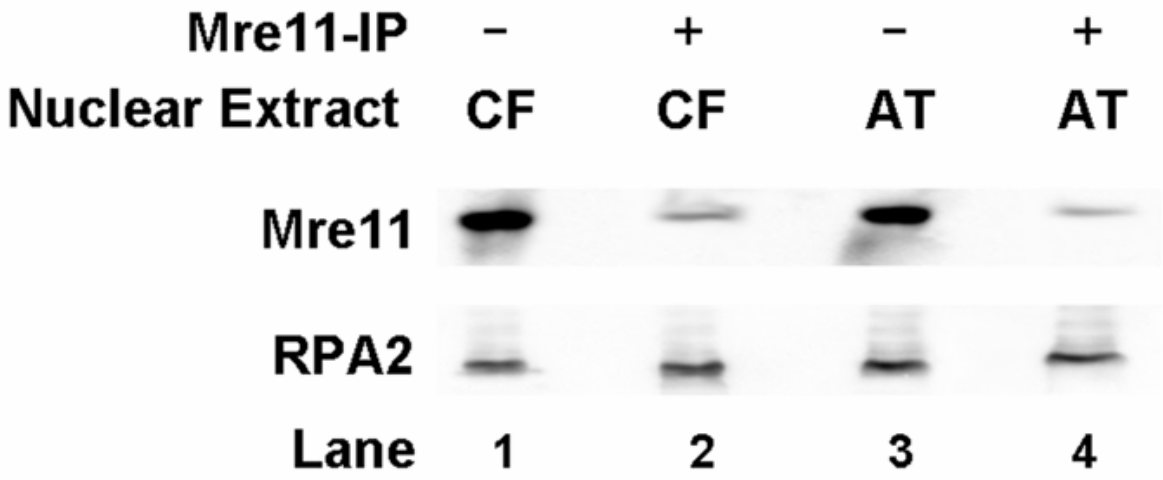

Fig. 2

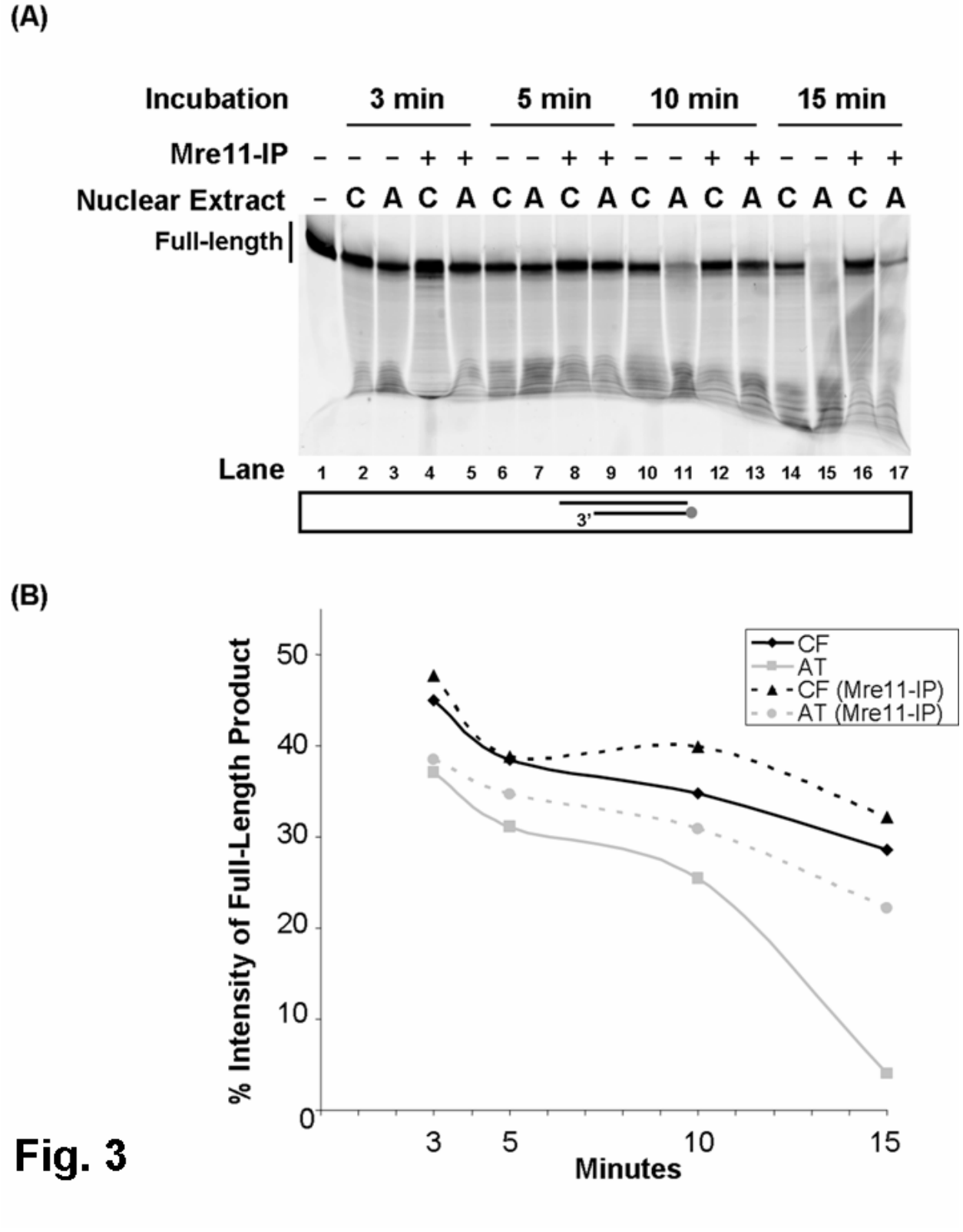
(A)
Incubation
3 min
5 min
10 min
15 min
Mre11-IP
Nuclear Extract
Full-length
Lane
1 2 3 4 5 6 7 8 9 10 11 12 13 14 15 16 17
3'
(B)
% Intensity of Full-Length Product
Minutes
CF
AT
CF (Mre11-IP)
AT (Mre11-IP)

Fig. 3

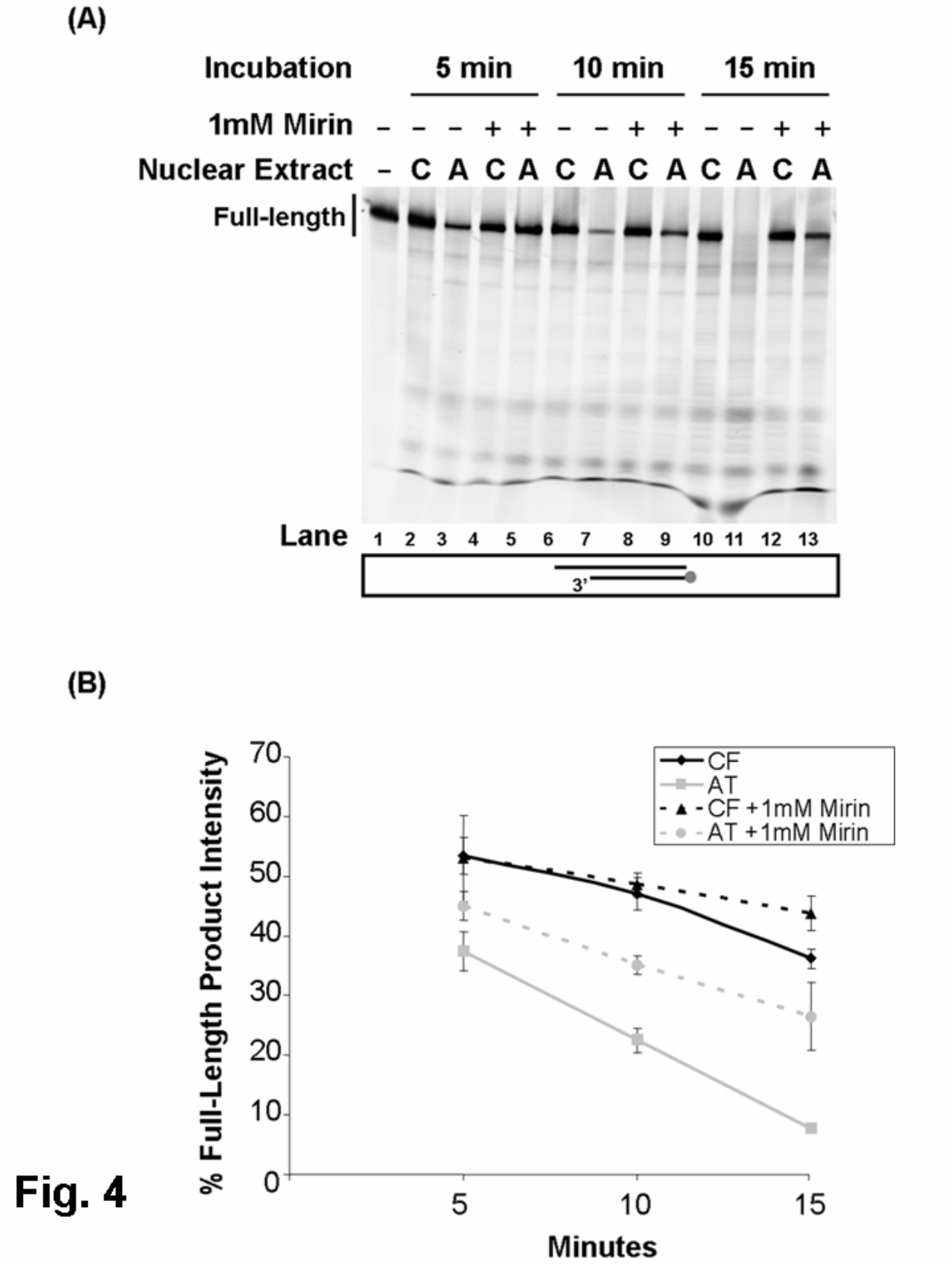
(A)
Incubation
5 min
10 min
15 min
1mM Mirin
Nuclear Extract
Full-length
Lane
1 2 3 4 5 6 7 8 9 10 11 12 13
3'
(B)
% Full-Length Product Intensity
70
60
50
40
30
20
10
0
5
10
15
Minutes
CF
AT
CF +1mM Mirin
AT +1mM Mirin

Fig. 4

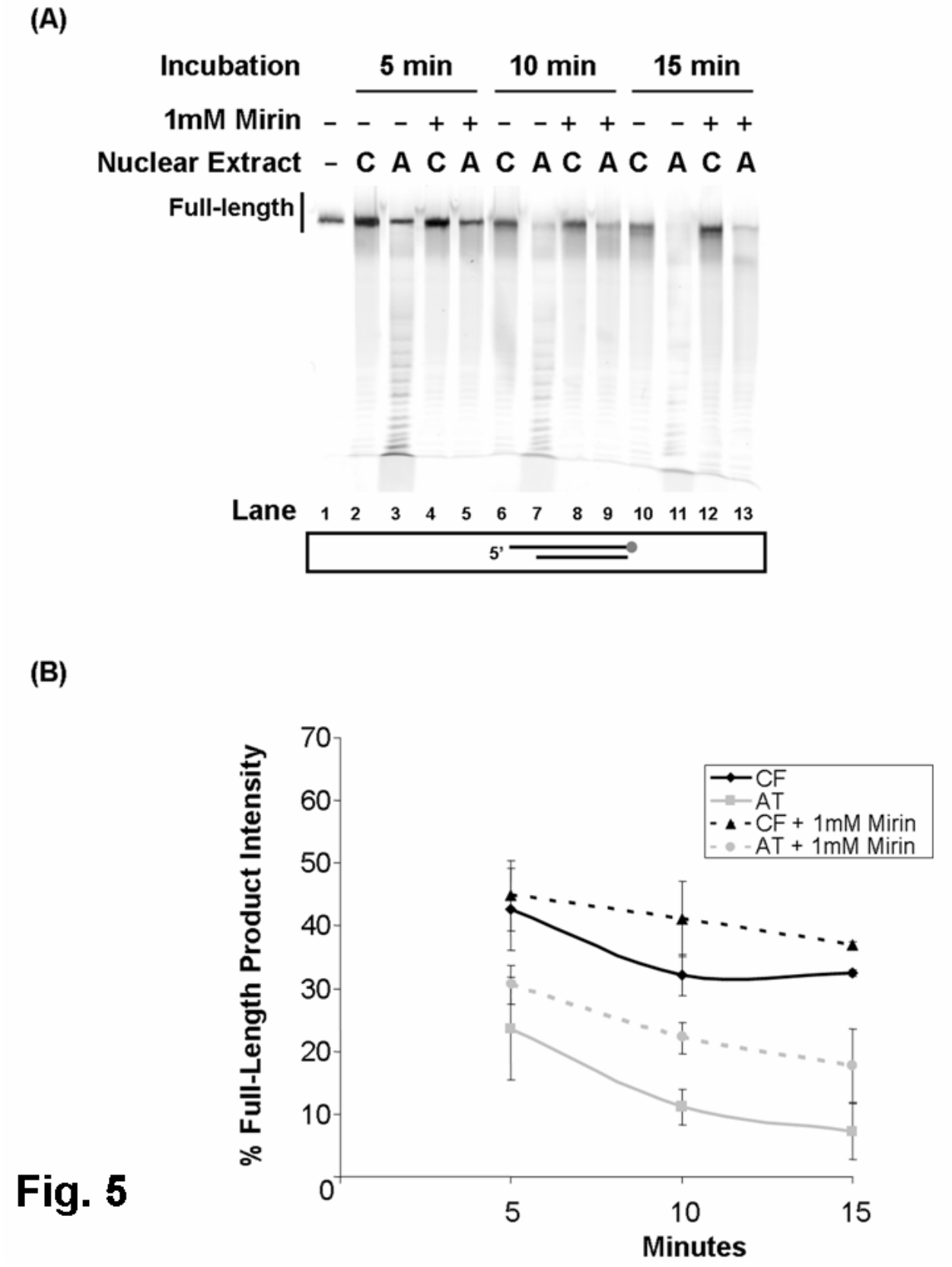
(A)
Incubation
5 min
10 min
15 min
1mM Mirin
Nuclear Extract
Full-length
Lane
1 2 3 4 5 6 7 8 9 10 11 12 13
5'
(B)
% Full-Length Product Intensity
70
60
50
40
30
20
10
0
5
10
15
Minutes
CF
AT
CF + 1mM Mirin
AT + 1mM Mirin

Fig. 5

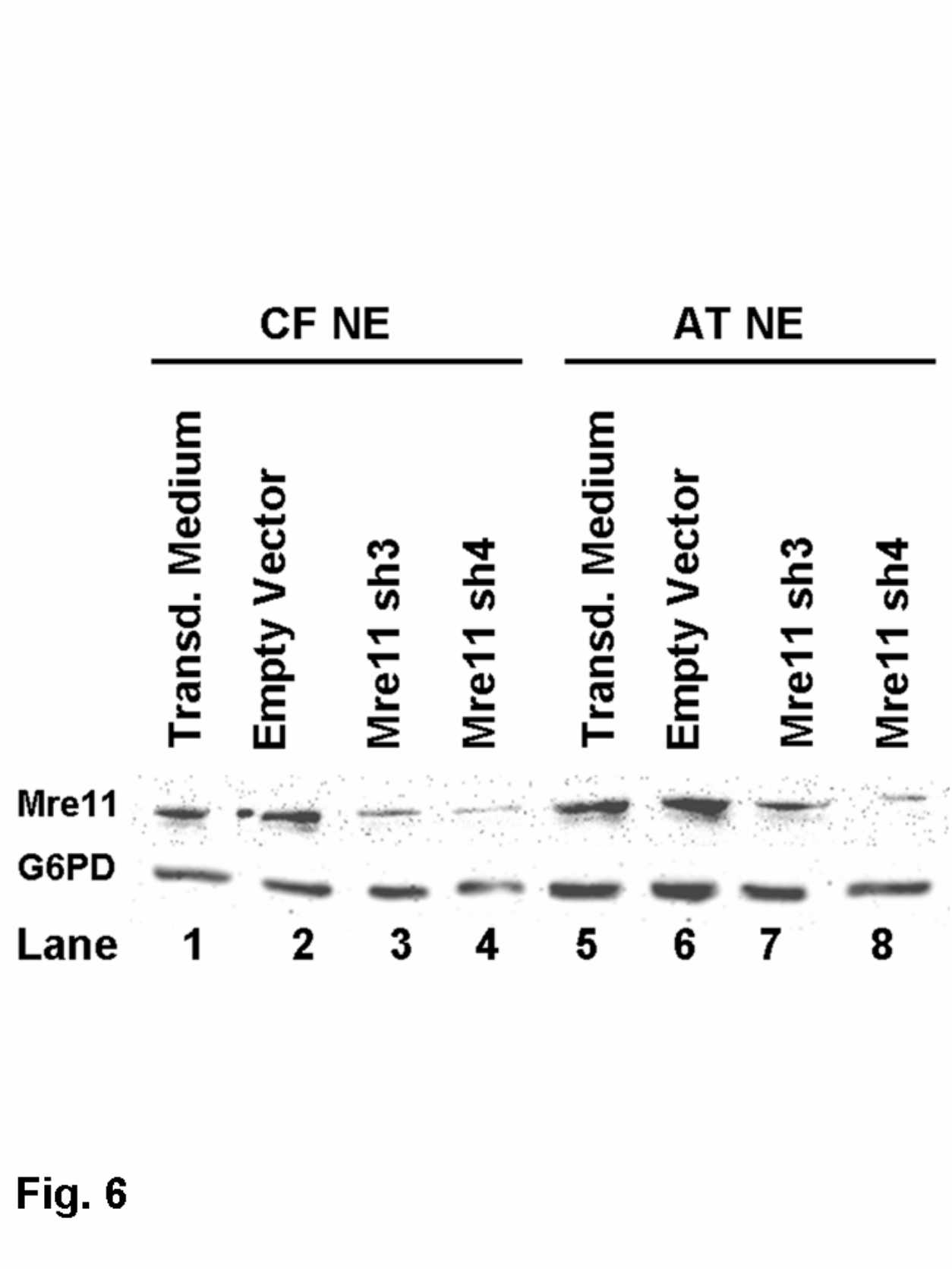
CF NE
AT NE
Transd. Medium
Empty Vector
Mre11 sh3
Mre11 sh4
Transd. Medium
Empty Vector
Mre11 sh3
Mre11 sh4
Mre11
G6PD
Lane
1
2
3
4
5
6
7
8

Fig. 6

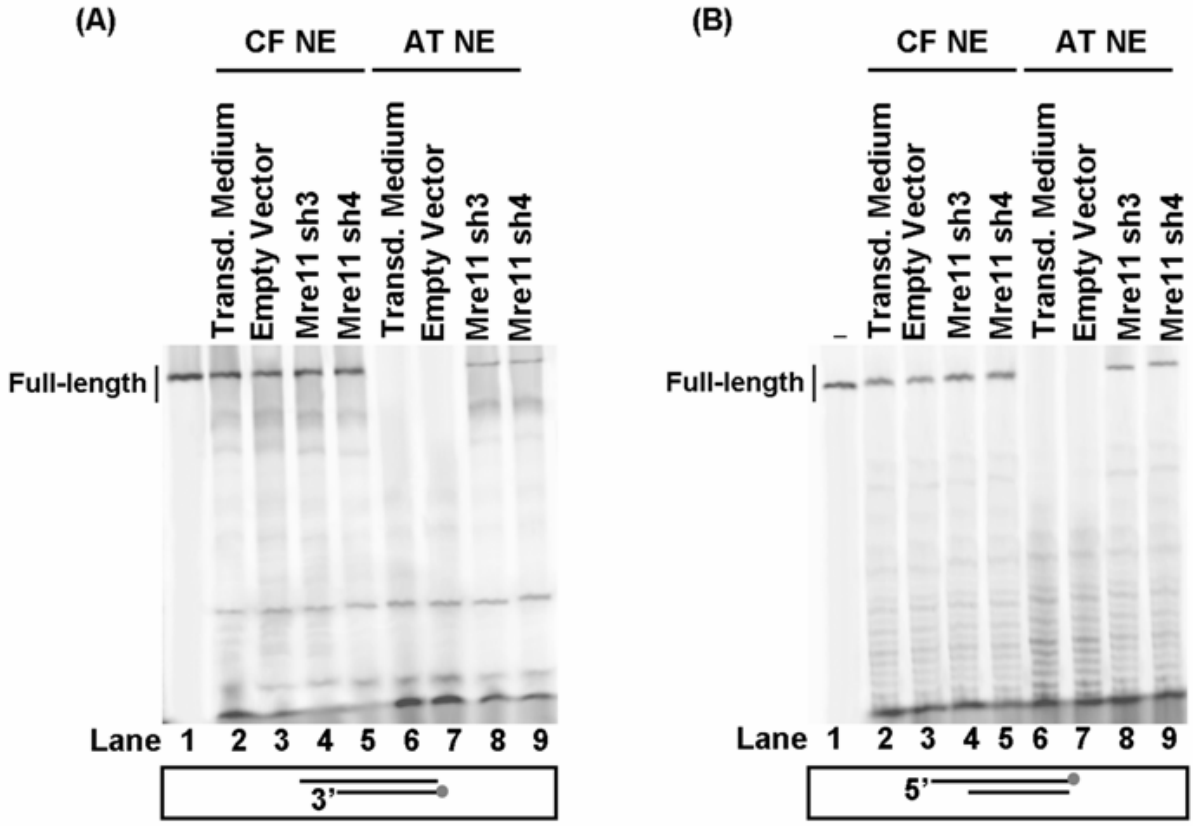
(A)
CF NE
AT NE
Transd. Medium
Empty Vector
Mre11 sh3
Mre11 sh4
Transd. Medium
Empty Vector
Mre11 sh3
Mre11 sh4
Full-length
Lane 1 2 3 4 5 6 7 8 9
3'
(B)
CF NE
AT NE
Transd. Medium
Empty Vector
Mre11 sh3
Mre11 sh4
Transd. Medium
Empty Vector
Mre11 sh3
Mre11 sh4
Full-length
Lane 1 2 3 4 5 6 7 8 9
5'

Fig. 7

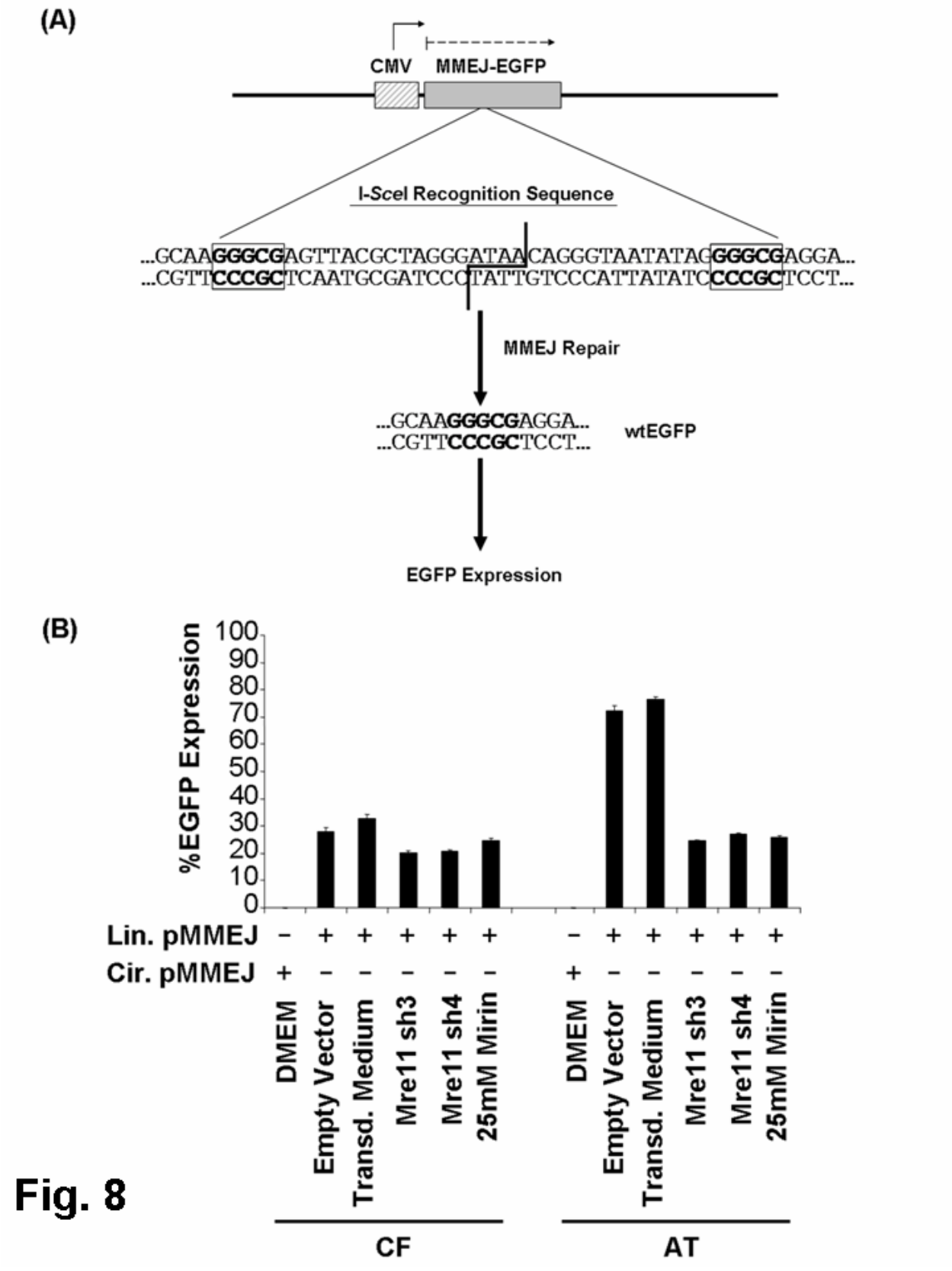
(A)
CMV
MMEJ-EGFP
I-SceI Recognition Sequence
...GCAAGGGCGAGTTACGCTAGGGATAACAGGGTAATATAGGGGCGAGGA...
...CGTTCCCGCTCAATGCGATCCCTATTGTCCCATTATATCCCCGCTCCT...
MMEJ Repair
...GCAAGGGCGAGGA...
...CGTTCCCGCTCCT...
wtEGFP
EGFP Expression
(B)
%EGFP Expression
100
90
80
70
60
50
40
30
20
10
0
Lin. pMMEJ
Cir. pMMEJ
DMEM
Empty Vector
Transd. Medium
Mre11 sh3
Mre11 sh4
25mM Mirin
CF
AT

Fig. 8

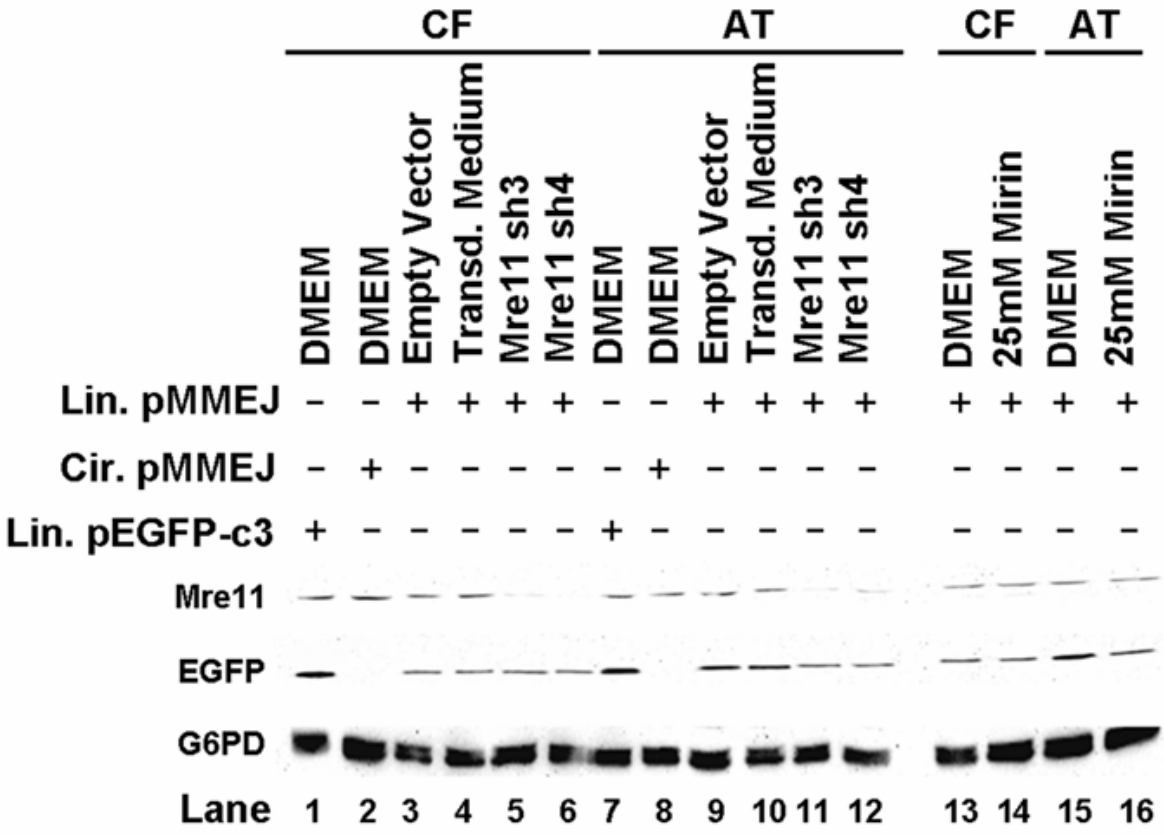
CF
AT
CF
AT
DMEM
DMEM
Empty Vector
Transd. Medium
Mre11 sh3
Mre11 sh4
DMEM
DMEM
Empty Vector
Transd. Medium
Mre11 sh3
Mre11 sh4
DMEM
25mM Mirin
DMEM
25mM Mirin
Lin. pMMEJ
Cir. pMMEJ
Lin. pEGFP-c3
Mre11
EGFP
G6PD
Lane
1 2 3 4 5 6 7 8 9 10 11 12 13 14 15 16

Fig. 9

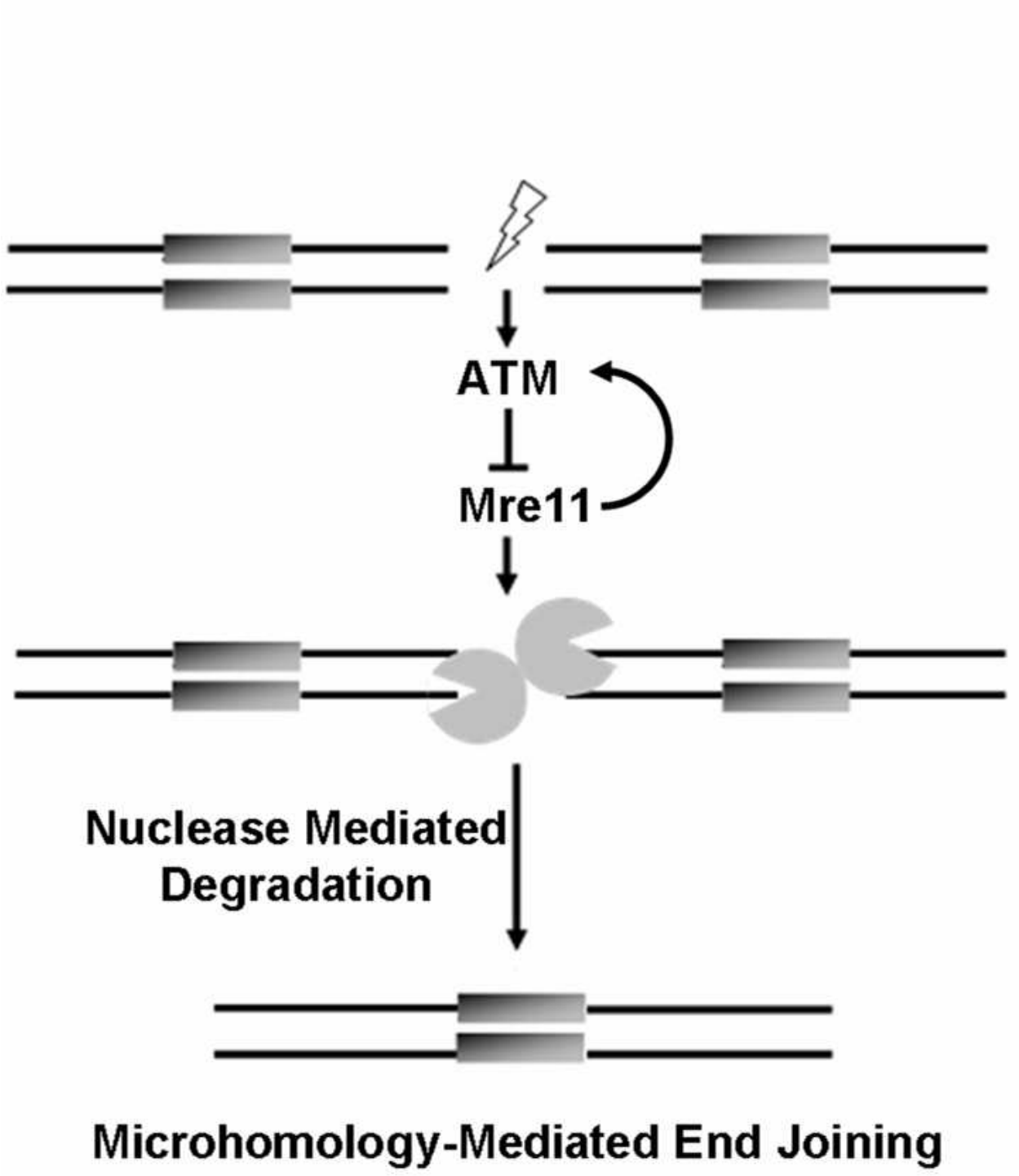
ATM
Mre11
Nuclease Mediated
Degradation
Microhomology-Mediated End Joining

Fig. 10